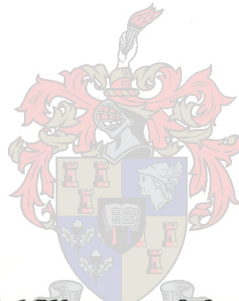


Gel-Particles for Ink-Jet Paper Coating Applications

by

Carmen Cornelia Kriel



***Thesis presented in partial fulfillment of the requirements for the degree
of Master of Science (Polymer Science)***

at the

University of Stellenbosch

Supervisor: Prof. Ron Sanderson

December 2004

Declaration

I, the undersigned, hereby declare that the work contained in this thesis is my own original work and that I have not previously in its entirety or in part submitted it at any university for a degree.

Signature

Date

Abstract

An unsaturated, linear, aliphatic polyamide was synthesized from 1,6-hexanediamine and fumaric acid by means of a phosphorylation polycondensation reaction, and successfully crosslinked with a vinyl monomer during an inverse suspension polymerization reaction. The two vinyl monomers that were used were 2-hydroxyethyl methacrylate (HEMA) and 4-vinyl pyridine. The linear polyamide was characterized by means of nuclear magnetic resonance (NMR) and electrospray mass spectrometry (ESMS), while the crosslinked product was characterized by light scattering and scanning electron microscopy (SEM), as well as cryo-SEM. The average particle diameters of the crosslinked product were found to be in the range of 100 to 300 nm.

One of the synthesized crosslinked products was used in coating formulations on starch-coated paper. The paper samples were evaluated and compared on the basis of printing quality, colour density and colour uniformity of a printed image, as well as the wet-rub resistance of the coating. A formulation containing 0,1% of the HEMA crosslinked polyamide product was found to give the best performance of the printed image in terms of printing quality, colour density and colour uniformity. Wet-rub resistance was found to improve with increasing concentration of the crosslinked polyamide product.

Opsomming

'n Onversadigde, lineêre, alifatiese poli-amied is berei vanaf die monomere 1,6-heksaandiamien en fumaarsuur deur middel van 'n fosforilasie-polikondensasie reaksie, waarna die produk suksesvol gekruisbind is tydens 'n inverse-suspensie polimerisasie-reaksie. Twee vinielmonomere, naamlik 2-hidroksi-etiel-metakrilaat (HEMA) en 4-viniel-piridien, is gebruik. Die lineêre poli-amied is deur middel van kern magnetiese resonansie (KMR) en elektronsproei-massaspektrometrie (ESMS) gekarakteriseer, en die kruisgebinde produk deur middel van ligverstrooiing, skandeer-elektronmikroskopie (SEM), en lae-temperatuur SEM. Daar is bevind dat die gemiddelde partikeldeursnee van die kruisgebinde produk tussen 100 en 300 nm was.

Een van die bereide, kruisgebinde produkte (wat met HEMA gekruisgebind is) is gebruik in bedekkingsformules op stysel-bedekte papier. Die papiermonsters is ge-evalueer en vergelyk ten opsigte van drukkwaliteit en die diepte en egaligheid van die kleur van 'n gedrukte beeld, asook die natskuurweerstand van die deklaag. Daar is bevind dat 'n formulering wat 0.1% van die kruisgebinde poli-amied produk bevat die beste vertoning lewer in terme van drukkwaliteit, kleur diepte en egaligheid van kleur. Daar is verder bevind dat die natskuurweerstand van die deklaag verbeter het wanneer die konsentrasie van die kruisgebinde poli-amied produk in die formulering verhoog is.

Acknowledgements

God the Father, God the Son, and God the Holy Spirit, without whom this thesis could certainly not have been possible, and this degree not obtained! Thank you Lord for the prayers that were answered and the original ideas You inspired – but most of all thank you for the strength to persevere. I love You with all my heart.

Prof. R.D. Sanderson, my study leader, for the chance he gave me to do something different and individual, and giving me the opportunity to finish it. Thank you Doc for the constant encouragement and your eternal optimism!

Valeska Cloete, head of the Paper Coatings Group at the Department of Chemistry and Polymer Science, University of Stellenbosch. Thank you for the discussions on everything, the present thesis included. Your support has meant a lot to me. I thank you and all the others in the group for the fun we've had; you are all fantastic people and I'm glad I got to know you guys!

My parents, Keith and Irma Kriel, for their permanent belief that I can do anything! I love you both very much and I think you have laboured with me on this more than anyone else.

Durandt Swart, for his constant and never-ending belief and faith. Dankie liefie dat jy so geweldig ondersteunend was. Jy is regtig soos die koel windjie wat waai op die warmste dag, of die sonstraaltjie wat deurkom as dit al twee weke lank reën! BBLVJ.

Dr Margie Hurndall, for her input and valuable advice during the writing and editing stages.

Everyone at the Department of Chemistry and Polymer Science at the University of Stellenbosch for their support and input, especially Dr. James McCleary and the Free Radical Group.

Dr A. Venter of the Electrospray Mass Spectrometry laboratory at the University of Stellenbosch for the electrospray mass spectrometry (ESMS) work performed.

Jean Kensie and Elsa Joubert at the Nuclear Magnetic Resonance laboratory at the University of Stellenbosch for the NMR samples that they ran, especially the overnight and weekend work that they did.

Miranda Waldron at the Electron Microscope Unit of the University of Cape Town, for the scanning electron microscopy (SEM) and the cryo-SEM work performed.

Table of contents

List of abbreviations	xii
List of figures	xiii
List of tables	xvi
List of reaction schemes	xviii
Chapter 1: Introduction and Objectives	1
1.1 Introduction	1
1.2 Ink-jet paper	1
1.3 Aims	2
1.4 Objectives	3
1.5 The 2,6-Polyamide	4
1.6 Layout of the thesis	5
Chapter 2: Ink-jet Paper	6
2.1 Introduction	6
2.2 Ink	6
2.3 Printing quality	7
2.3.1 Optical density	9
2.3.2 Resolution	9
2.3.3 Print through	11
2.3.4 Rub-off	11
2.4 Coating components	11
2.4.1 Binders	12
2.4.2 Pigments	13
2.4.2.1 Silica	13

2.4.2.2 Precipitated Calcium Carbonate	14
2.4.3 Patent literature relating to improvement of ink-jet paper	14
2.5 Conclusion	16
Chapter 3: Polyamides: Properties and Synthesis	18
3.1 Introduction	18
3.2 Properties	19
3.3 Synthesis	20
3.3.1 Linear polyamides	20
3.3.1.1 Phosphorylation	21
3.3.1.2 Stoichiometry	22
3.3.1.3 Reaction solvent	24
3.3.2 Crosslinked particles	25
3.3.2.1 Crosslinking by means of free-radical chain addition reaction	25
3.3.2.2 Inverse suspension polymerization	27
3.3.2.3 Choice of vinyl monomers	29
3.4 Conclusion	29
Chapter 4: Experimental	30
4.1 Materials used	30
4.2 Synthesis	31
4.2.1 Preparation of linear polyamides	31
4.2.2 Preparation of the crosslinked particles	33
4.3 Characterization	35
4.3.1 NMR	35
4.3.2 ESMS	35

4.3.3 Light scattering	36
4.3.4 SEM	36
4.4 Coating of paper samples	37
4.4.1 Preparation of formulations	37
4.4.2 Coating of base paper	37
4.5 Printing of paper samples	38
4.5.1 Wet-rub test	39
Chapter 5: Results and Discussion	40
5.1 Linear polyamides	40
5.1.1 Solvent	41
5.1.2 Stoichiometry	43
5.2 Crosslinked polyamides particles	45
5.2.1 Results of synthesis	45
5.2.2 Crosslinking	45
5.2.2.1 Crosslinking of N50	46
5.2.2.2 Crosslinking of N100	48
5.2.2.3 Crosslinking of N200	52
5.2.2.4 Summary	54
5.2.3 Particle formation	54
5.2.3.1 Light scattering	55
5.2.3.2 SEM	56
5.2.3.1 N50-H	56
5.2.3.2 N100-H	58
5.2.3.3 N100-VP	58
5.2.3.4 N200-H	60

5.2.3.3 Summary	60
5.2.4 Paper coated with crosslinked polyamide particles	61
5.2.4.1 Printing quality, colour density and colour uniformity	61
5.2.4.2 Wet-rub test	62
5.2.4.3 Summary	63
Chapter 6: Method considered for the quantitative determination of printing quality	64
6.1 Introduction	64
6.2 Geographical Imaging Systems technology	64
6.3 Paper application	65
6.4 Method	65
6.5 Experimental work	67
6.6 Results	68
6.6.1 Ink-boundary between magenta and yellow ink colours	68
6.6.2 Comparison with visual observation	69
6.7 Disadvantages	70
6.8 Conclusion	70
Chapter 7: Conclusions and Recommendations	71
7.1 Conclusions of this study	71
7.2 Recommendations for future work	72

Chapter 8: References	74
Appendix 1: ^{13}C NMR spectra of polymer products	79
Appendix 2: ESMS spectra of polymer samples produced	90

List of abbreviations

δ	Chemical shift
Da	Dalton
ESMS	Electrospray Ionization Mass Spectrometry
GIS	Geographical Imaging Systems
HEMA	2-Hydroxyethyl methacrylate
HLB	Hydrophilic lipophilic balance
kDa	Kilodalton
KPS	Potassium persulfate
LiCl	Lithium chloride
MeOH	Methanol
N_{AA}	Number of unreacted AA molecules present in reaction after a specific time period
N_{AA0}	Original number of AA molecules present in reaction
nm	Nanometer
NMP	N-methyl pyrrolidone
NMR	Nuclear magnetic resonance
p	Probability of finding a reacted group
PCC	Precipitated calcium carbonate
Proglyme	Dipropylene glycol dimethyl ether
PVOH	Polyvinyl alcohol
r	Stoichiometric ratio of the functional groups present
SEM	Scanning electron microscopy
TPP	Triphenyl phosphite
μm	Micrometer
w/o	Water-in-oil
\tilde{x}_n	Number-average chain lengths / Average degree of polymerization

List of figures

Chapter 1

- 1.1 The 2,6- polyamide, identified as a potentially suitable polymeric material for use as a hydrophilic, organic polymer with cationic end-group functionality.

Chapter 2

- 2.1 Typical composition of aqueous ink-jet ink.
- 2.2 Offset lithographic printing technique.
- 2.3.a Generation of ink droplets by thermal means.
- 2.3.b Generation of ink droplets by mechanical (piezo-electrical) means.
- 2.4.a Pigment with uniform, small particle size.
- 2.4.b Pigment with broad particle size distribution.

Chapter 3

- 3.1 The repeating amide group in a polyamide.
- 3.2 Hydrogen bonding between adjacent amide groups.
- 3.3 Thermally induced splitting of KPS.
- 3.4 Schematic diagram of proposed water-in-oil emulsion system used during crosslinking of linear polyamide.
- 3.5 2-Hydroxyethyl methacrylate (HEMA)
- 3.6 4-Vinyl pyridine

Chapter 4

- 4.1 Test pattern printed on coated paper samples.

Chapter 5

- 5.1 Different electronegative environments present within the polyamide, with equivalent areas indicated.
- 5.2.a ^{13}C NMR Spectrum of N50 for the δ -range 30 – 75 ppm.
- 5.2.b ^{13}C NMR Spectrum of N50-H for the δ -range 30 – 75 ppm.
- 5.3.a ^{13}C NMR Spectrum of N100 for the δ -range 30 – 70 ppm.
- 5.3.b ^{13}C NMR Spectrum of N100-H for the δ -range 30 – 70 ppm.
- 5.4 ESMS spectrum of sample N200, showing the absence of molecular weight species between 76 kDa and 166 kDa.
- 5.5 SEM photographs of dry, crosslinked polyamide samples a) N50-H, b) N100-H, c) N100-VP, d) N200-H.
- 5.6.a SEM view of frozen polyamide sample N50-H containing water.
- 5.6.b SEM view of polyamide sample N50-H after sublimation of water has occurred.
- 5.7 SEM photograph of N100-H showing the particles, as well as the micrometer sized conglomerates made up of clusters of nano-sized particles.
- 5.8 SEM photograph of N100-VP showing conglomerates consisting of nano-sized particles.
- 5.9 SEM photograph of N200-H, showing the measured sizes of particles.
- 5.10 Image printed on a paper sample partially coated with Formulation 2.

Chapter 6

- 6.1 Graph of the “value” column containing the values assigned to the cells of the boundary area between two colours in a printed image, as printed on a standard paper sample.
- 6.2 Magenta/ yellow ink colour boundaries for different coated paper samples that were analyzed.

List of tables

Chapter 2

- 2.1 Summary of some patents submitted for ink-jet recording media.
- 2.2 Patents submitted for particles intended for ink-jet paper coating applications.

Chapter 3

- 3.1 Degrees of polymerization and corresponding weights and molar ratios of monomers.

Chapter 4

- 4.1 Variables that were present during the synthesis of the various linear polyamide samples.
- 4.2 Ingredients that were varied in the coating formulations that were prepared for the coating of starch-sized paper, given as parts per hundred.

Chapter 5

- 5.1 Details of the products of the linear polyamide synthesis reactions.
- 5.2 Carbon shift ranges predicted for the functional groups and methylene carbons with NMR prediction software.
- 5.3 δ -Ranges where groups of peaks were found in ^{13}C spectra of N50 and P50.
- 5.4 Degrees of polymerization desired and corresponding required molar ratios of monomers, with resulting molecular weight.
- 5.5 Molecular weights determined for polymer samples by ESMS technique.
- 5.6 Results of crosslinking reactions performed on samples N50, N100, and N200.

- 5.7 The three molecular weight species present, with highest concentrations, for sample N50 and its crosslinked products, samples N50-H and N50-VP, as determined by ESMS.
- 5.8 Relative concentrations of double bond peak at δ 129 ppm and amide peaks at δ 181 ppm.
- 5.9 The three molecular weight species present, with highest concentrations, for sample N100 and its crosslinked products, samples N100-H and N100-VP, as determined by ESMS.
- 5.10 Concentrations of double bond peaks relative to amide peaks for samples N100, N100-H, and N100-VP.
- 5.11 The three molecular weight species present with highest concentrations, for sample N200 and its crosslinked products, samples N200-H and N200-VP, as determined by ESMS.
- 5.12 Concentrations of double bond peaks relative to amide peaks for samples N200, N200-H, and N200-VP.
- 5.13 Particle diameters and percentage of particles of each particular diameter, as found for each of the successfully crosslinked polyamide samples.
- 5.14 Ingredients of Formulation 2, as given in parts per hundred.

Chapter 6

- 6.1 Coating formulations prepared during development of GIS method.

List of reaction schemes

Chapter 3

- 3.1 Triphenyl phosphite-lithium chloride induced phosphorylation reaction.

Chapter 4

- 4.1 The preparation of a linear polyamide from 1,6-hexanediamine and fumaric acid, using a phosphorylation polycondensation technique.
- 4.2 Crosslinking reaction between polyamide chains and a vinyl monomer, such as 4-VP or HEMA.

Chapter 1:

Introduction and Objectives

1.1 Introduction

Ink-jet paper is currently a very important consumer product, especially due to recent developments in digital imaging photography.

The availability of digital imaging technology to the layman has led to desktop ink-jet and laser printers playing an increasingly important role, hence the demand for suitable printing paper has increased tremendously. Ink-jet paper has thus come to play a significant role in the world paper market.

Unfortunately, the affordable ink-jet paper currently available has poor resolution compared to photographic prints. Comparable photo-quality paper is available, but it is so expensive that it is excluded from common, everyday use in the average-income home, and only finds specialized application in printing and marketing businesses. It remains cheaper for home-users to have digital photographs printed at specialized printing shops.

The quality of a print is dependant on the ink, paper, and printer combination, and any, or all, of these factors may be investigated in efforts to improve the end result. Of these factors, it is the surface properties of the paper, imparted by the coating on the base paper, that is the most crucial¹.

It has been suggested that a good performance, low-cost ink-jet paper product should be developed for the ink-jet paper market to fill the gap between the expensive, good quality paper products and the inexpensive, low quality paper products¹.

1.2 Ink-jet paper

All paper intended for ink-jet use is coated with an ink-receptive layer made up of fillers, binders, and other additives. It is the fillers that have an effect on the resolution and quality of the printed image.

The most common, affordable ink-jet paper products are produced by using ground calcium carbonate as mineral filler¹, while most of the expensive, photo-quality paper products contain a silica filler, also of mineral origin. This expensive silica filler results in the superior whiteness and print resolution² of the photo-quality papers, but is also the reason for the superior price of these ink-jet paper products.

The binder does not play a significant role in the resolution or quality of the printed image, and is added to bind the inorganic mineral filler to the cellulosic paper surface. It does, however, increase the price of the coating without adding to the quality of the end product. It would be a large advantage if the binder could be replaced with a less expensive alternative.

1.3 Aims

The overall aim of this project was to investigate the possibility of preparing a suitable synthetic polymer product, which could be used to:

- replace part, or all, of the silica filler currently used, and thereby decrease the cost of expensive photo-quality printing paper, or
- replace the polyvinyl alcohol (PVOH) binder in the coating to lower costs and to reduce the number of components in the coatings.

The aim thus describes a synthetic polymer product with characteristics of both binders and fillers.

In selecting a suitable polymer material, the following characteristics that are required of fillers, and binders, for ink-jet paper coating applications, therefore had to be considered:

- Quick absorption of the ink carrier fluid (usually water in ink-jet inks) to prevent ink spreading, and decrease the drying time of the ink
- An affinity for the anionic dyes and pigments in the printing inks, thus preventing the inks bleeding into one another, and also improving drying times of the inks.

- A smooth and well covered printing surface, which will result in uniform colour density appearance, by discouraging ink bleeding that occurs due to gravitational effects, and preventing ink wicking that occurs along exposed fibers.
- Excellent binding properties between the cellulosic fibers and the pigments.

These attributes can be achieved by selecting a material with the following chemical and physical characteristics:

- A hydrophilic structure, leading to quick absorption of the carrier fluid due to chemical forces, such as hydrogen bonding
- A large surface area with cationic bonding sites, to which the anionic dyes and pigments can chemically bond, and which can thus lead to the particles acting as glue between the cellulosic paper surface and the inorganic mineral pigments.

1.4 Objectives

The physical and chemical requirements mentioned above thus led to the division of the research into the following specific objectives:

- 1) Identification of a suitable hydrophilic, organic polymer with cationic functionality;
- 2) Synthesis of a linear pre-polymer of the above type, and characterization of the product in terms of molecular weight and functionality;
- 3) Crosslinking of the pre-polymer into hydrophilic particles, and determination of the particle size of the crosslinked product when dispersed in water;
- 4) Replacing the PVOH binder and/or the silica pigment in ink-jet paper coatings with the synthesized crosslinked particles, and printing of the subsequently coated paper with a desktop ink-jet printer;
- 5) Comparison of the printed paper samples with respect to printing quality, colour density and colour uniformity.

1.6 Layout of the thesis

Ink-jet inks, ink-jet paper coatings, the binders, and the pigments currently in use in the industry, with special emphasis on the necessary characteristics for excellent print quality and resolution, are discussed in Chapter 2.

Chapter 3 provides a theoretical background to the synthesis of the linear, unsaturated 2,6-polyamide pre-polymer, by means of phosphorylation polymerization, as well as the crosslinking of the synthesized polyamide with a vinyl monomer during inverse suspension polymerization.

Chapter 4 contains experimental results; procedures of the reactions that were carried out to prepare the linear polyamide and the crosslinked product, as well as the mixing of the coating formulations and subsequent coating of paper samples are described. The characterization of the synthesized 2,6-polyamides and crosslinked products, in terms of molecular weight, structure, and swollen particle size, are described, along with the wet-rub test performed on the coated paper samples. The printing quality, colour density, and colour uniformity of the printed paper samples are also discussed.

The results of the reactions, characterizations, and tests performed are discussed in Chapter 5. Consideration is also given to the suitability of the synthesized products for use in ink-jet coating applications.

In Chapter 6 the development of a possible method for quantitative determinations of printing quality is considered.

Finally, in Chapter 7 conclusions are made, specifically referring to the original aims of the project. Recommendations for future work are included.

Chapter 2: Ink-jet paper

2.1 Introduction

Ink-jet paper is specialized paper intended for use in electronic, non-impact printing technologies such as ink-jet and laser printing. The base paper is treated with a coating depositing an ink receptive layer, usually a combination of inorganic pigment, resin, and various additives.

2.2 Ink

Printing ink for conventional printing methods is a mixture of resin, carrier fluid, additives, and dyes or pigments. The resin bonds the ink to the substrate surface and acts as a dispersing agent; the carrier fluid is the medium through which the pigment or dye is carried to the substrate; the additives change the rheological properties of the ink, improving flow and viscosity and thus aiding the printing process. The dyes and pigments supply the colour.

Ink-jet inks, however, have a slightly different composition^{2,4}. The vast majority of these inks are water based² and made up of organic dyes, higher boiling alcohols, and water as the main carrier. The composition of a typical ink-jet ink is illustrated in Figure 2.1.

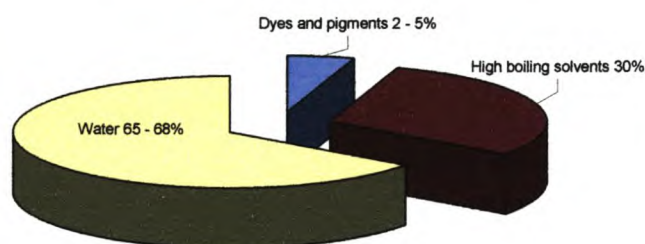


Figure 2.1: Typical composition of aqueous ink-jet ink.

Ink-jet inks need to remain mobile due to the demands of ink-jet printers, and thus the inks are formulated without using resins. Resin-containing ink formulations become

highly viscous when very small amounts of carrier fluid evaporate, thus clogging nozzles and necessitating high printer maintenance. The absence of the resins, however, demands that the dyes must have an affinity for the paper surface, and thus most ink-jet dyes are organic acids with anionic charges, easily attracted and bonded onto the cationic binders of the paper (normally polyethylimine).

2.3 Printing Quality

Ink-jet printing is a non-impact printing technique, far removed from the conventional printing techniques, such as lithography, which are used for the industrial printing of magazines, newspapers, and books.

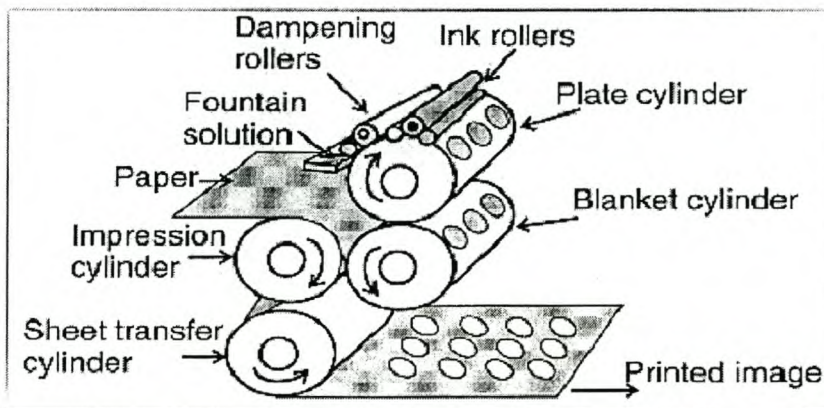


Figure 2.2: Offset lithographic printing technique.

The technology applied in ink-jet printing is vastly different. With conventional techniques, ink is applied on the paper web by contact, usually with a system of one or more rollers, as is illustrated in the diagram of offset lithographic printing in Figure 2.2.

With ink-jet technology, micro-sized ink droplets are generated and ejected onto the paper surface. Figure 2.3⁵ shows the two means whereby ink droplets are ejected:

- a) thermal.
- b) mechanical (piezo-electrical).

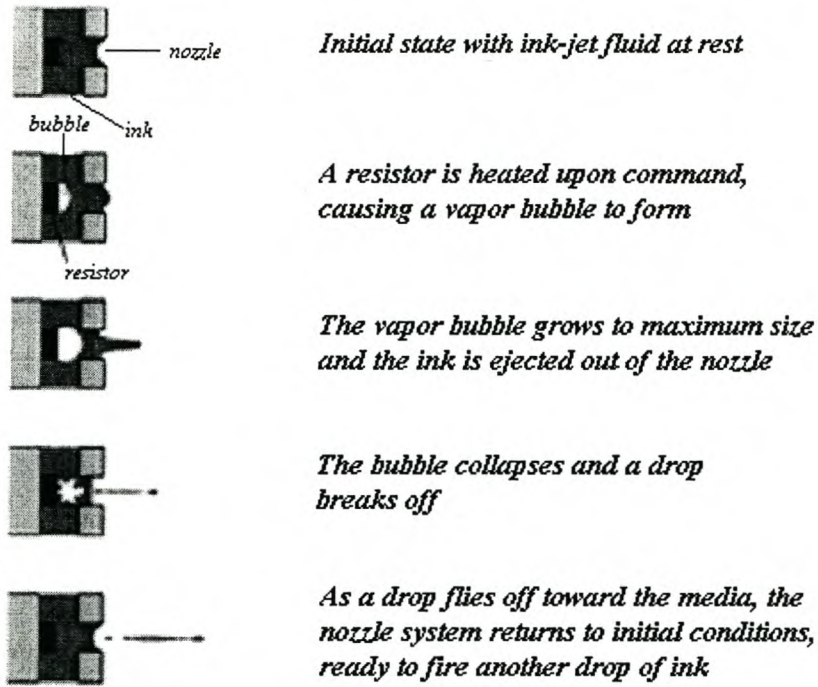


Figure 2.3.a) Generation of ink droplets by thermal means⁵.

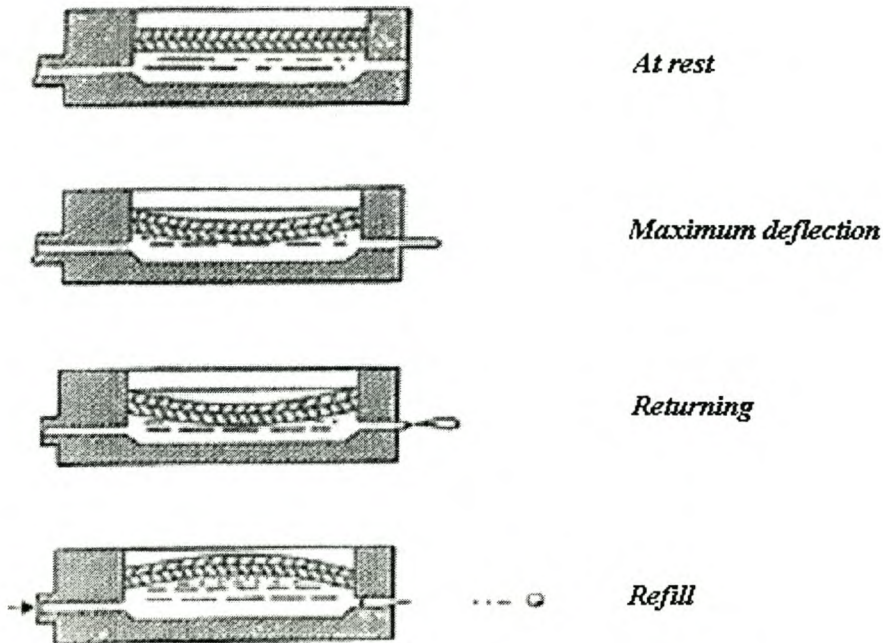


Figure 2.3.b) Generation of ink droplets by mechanical (piezo-electrical) means⁵.

Due to these different technologies, the requirements of ink-jet printing paper are very different from paper intended for conventional printing techniques. However, these requirements are still closely related to the specifications for a high resolution and quality print, which, for ink-jet printing, can be summarized in terms of^{2,4}:

- Optical density
- Resolution of ink boundaries
- Ink print-through
- Resistance to rub-off when wetted.

2.3.1 Optical density

Optical density is a measure of the intensity of the colour of the printed image. A high optical density results in bright, true colours that greatly improve the appearance of an ink-jet image.

Optical density is directly related to the density of the absorbed dyes and pigments on the paper surface, and thus a surface on which the dyes are well fixed will lead to an increase in dye density, and therefore optical density. The anionic dyes are especially attracted by cationic surfaces, and in some paper products cationic additives are added to the coatings to improve dye adsorption and fastness⁶.

A good ink-jet paper product will therefore optimally have cationic functionality to fix the dyes and pigments.

2.3.2 Resolution

Resolution refers to the size of the ink droplets on the paper surface and the sharpness and clarity of the droplet boundaries. Ideally, after initial contact of the ink droplet on the paper surface, the droplets should remain small and circular², the boundaries sharply delineated, and only merging to the extent that a uniform colour is achieved from adjoining droplets⁴.

The size and shape of the ink droplets are most affected by the drying time of the ink. Factors such as paper stock composition, paper sizing, paper filler, and coating composition all affect the drying time of ink on a specific paper surface.

The wetting delay time^{2,7} is a convenient method by which different papers may be compared. The wetting delay is the time the ink droplet sits on the substrate surface before absorption of the carrier fluid begins. A decrease in wetting delay time will lead to quicker absorption and thus a decrease in ink drying time, and thus an improvement in the printing resolution of a paper product.

Wetting delay time is affected by two factors, namely surface roughness, and the affinity of the binder and pigment system for the ink carrier fluid. According to Lyne and Aspler in their publication "*Paper for Ink-jet Printing*", published in the TAPPI Journal in 1985², wetting delay time can be minimized by coating a substrate with a "high-porosity, high-surface-area material that wets virtually instantaneously with water". Silica is such a material, and is used extensively in ink-jet paper coating applications. This mineral filler is discussed in more detail later in this chapter (section 2.4.2.1).

Lyne and Aspler² also contend that "the coating material should be homogeneous down to a scale of a few microns" to minimize bleeding and roughness of the droplet. This may be achieved by:

- the use of a pigment with very small, uniform particle size, able to pack closely;
- the use of a pigment with a broad particle size distribution, where the smaller particles fill the void spaces formed between the larger particles.

In both cases the result will be smooth and uniform surfaces, as illustrated diagrammatically in Figure 2.4.

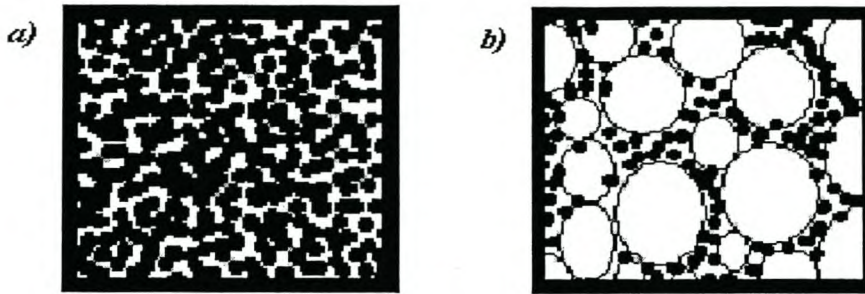


Figure 2.4: a) Pigment with uniform, small particle size; b) Pigment with broad particle size distribution.

2.3.3 Print-through^{4,8}

Print-through of a paper substrate occurs when the printed image strikes through to the back of the paper. This occurs when the dyes and pigments are carried too far into the paper substrate by the ink carrier fluid, thus becoming visible at the back.

Fast ink drying times and increased ink-fastness can prevent this from happening. A paper base which is hydrophobic will also prevent print-through, because the ink carrier fluid will not travel readily through the base paper and will remain within the coating.

2.3.4 Rub-off^{4,8}

A printed image should, ideally, not be affected when rewetted and rubbed. The dyes, although initially water soluble, should be fixed on the paper surface and become insoluble after drying. The pigments and dyes should also have such great affinity for the surface that they cannot be removed by rubbing or smearing, and must chemically bond to the surface. This is just as important for the initial coating, and makes the use of strong binders imperative.

2.4 Coating components

There are three basic groups of components in ink-jet paper coatings:

- Binders
- Pigments
- Rheology additives.

Of these, only the rheology additives do not actually have an effect on the printability of paper. They are added specifically to aid the application of the coating on the substrate by changing the rheological properties of the coating, and are therefore not included in this discussion.

2.4.1 Binders

The binder is the glue which attaches the filler to the cellulosic fibers of the paper surface. This mechanical means is necessary, because the fillers have no affinity for the cellulosic paper surface, and would otherwise easily be rubbed off the surface after the applied coating has dried.

Two hundred years ago the first coatings contained animal glue as binder, but nowadays this natural product has been replaced with others such as starch, and synthetic products such as PVOH, styrene-butadiene, and acrylics⁹.

PVOH is the preferred binder in ink-jet paper coating applications. This is due to its hydrophilicity and binding strength, which is almost four times that of starch, the other most commonly used binder for ink-jet coating applications.^{8,10} The hydrophilicity aids in the quick absorption of the ink carrier fluid, it leads to decreased wetting delay time, and to the subsequent quick drying of the ink. The binding strength of PVOH is not only important for the reason discussed above, but also assists greatly in the rub-off resistance of printed images.

These two favourable characteristics of PVOH, namely binding strength and hydrophilicity, are determined by both the molecular weight and degree of hydrolysis of the polymer. Low (31 - 50 kDa) or medium (85 - 124 kDa) molecular weight PVOH grades have greater binding strength, while a higher degree of hydrolysis leads to an increase in the hydrophilicity of the polymer. The ideal grades for ink-jet coating applications are therefore those of low or medium molecular weight, with 98,0 - 98,8% hydrolysis (considered as fully hydrolyzed)¹⁰.

Other advantages of PVOH include its ability to improve and aid the brightness of high brightness ink-jet paper products, as well as its environmental friendliness, and its easy recycle-ability.

2.4.2 Pigments

The pigment is the component in an ink-jet coating added specifically to affect and improve the quality and resolution of printed images. As discussed earlier in this chapter (section 2.3), there are specific factors that affect the quality of printed images, and a suitable pigment must have characteristics that influence these factors positively.

Although there are literally hundreds of different grades and shades of pigment available to the coatings formulator, all different with regards to pore volume and structure, particle size, hydrophilicity, charge, and even mode of production, there are basically two mineral fillers that are currently used in ink-jet coating applications. These are silica and precipitated calcium carbonate.

2.4.2.1 Silica

The best paper currently available for ink-jet applications contains silica as the main pigment component^{1,2}, specifically amorphous grades such as fumed and precipitated silica.

Amorphous grades are porous and hydrophilic, and have a very high affinity for water, which is usually the main ink carrier fluid component⁴. The carrier fluid is absorbed into the pores, and higher pore volume will lead to faster absorption. Silica coatings therefore give almost negligible wetting delay time, which promotes fast ink setting, and increased sharpness of ink drop boundaries⁶.

Amorphous grades also have large surface areas on which the ink dyes and pigments can fix, leading to further improvements in ink setting time.

Silicas are usually used in combination with a strong binder such as PVOH, because the porosities of the pigment particles cause inherent weaknesses in coating formulations⁶.

Silicas are very expensive pigments due to their high production costs⁸. They also have unfavourable effects on rheology, by increasing the viscosity of coating formulations. They are unsuitable for conventional printing applications because they have poor surface strength and cannot withstand the tack forces in these processes.

2.4.2.2 Precipitated Calcium Carbonate

Precipitated calcium carbonate (PCC) offers a low cost¹ pigment alternative to silica in ink-jet coating applications, because of high control over the manufacturing parameters, but it does not give the same performance in printing quality and resolution due to comparatively lower surface areas⁸.

PCC is often used as a co-pigment with silica to reduce costs in ink-jet coating applications⁸.

According to Donigian et al.; in their publication "*Ink-jet dye fixation and coating pigments*", published in 1999⁴, PCC works according to a different mechanism in ink-jet paper coatings to that of silica. They contend that PCC has a greater affinity for the dyes in the ink than for the ink carrier fluid, and thus works by allowing the fluid to be transported quickly to the base paper from where it may evaporate, while anchoring the ink dye. This is opposite to the silica mechanism of dye absorption, in which the silica particles show great affinity for the carrier fluid and absorb the fluid quickly into the internal porous structure of the pigments, as discussed in the previous section.

Coatings with PCC therefore offer better rub-off and print-through resistance by improved fixing of the dye, but may cause increased wetting delay times.

2.4.3 Patent literature relating to improvement of ink-jet paper

In efforts to improve the resolution and print quality of ink-jet paper, the use of various pigment-binder combinations have been suggested and patented.

Table 2.1: Summary of some patents submitted for ink-jet recording media.

Non-microporous film type ink-jet media					
Single layer	Ref #	Multi layer			Ref #
DE-A 4322178	11	EP-A 0634287			12
EP-A 0806299	13	JP 08282088			14
JP 2276670	15	JP 2000-108501			16
JP 5024336	17	JP 2003-48639			18
Advantages					
		Base layer on support absorbs ink carrier fluid			
		Top ink receptive layer improves gloss and ink density			
Disadvantages					
		Increased costs			
		Slows down manufacturing process			
Microporous film type ink-jet media					
Single layer	Ref #	Multiple layer	Ref #	Thin layer	Ref #
US-A 5605750	19	US-A 5605750	19	WO-A 9619346	20
WO-A 9907558	21	US-A 6020058	22	BE-A 1012087	23
EP-A 0995611	24	WO 02/053391	25	EP-A 0283200	26
US-A 4861644	27			US-A 4350655	28
US-A 4833172	29				
Advantages					
High absorption speed for carrier fluids			Lower costs		
Disadvantages					
High cost			Hydrophobic, ink does not dry		
Coating thickness too thick for usual application (>150 μm)					

Patent WO 02/053391²⁵ contains an excellent review of the patent applications submitted for ink-jet recording media within the last 15 years, and the various different approaches to the improvement of resolution and printing quality that have been investigated. A summary of this patent study has been given in Table 2.1, with a comparison of the major advantages and disadvantages of each approach. Other relevant patents found in literature have also been included.

There are also patents for the production of porous inorganic coating pigments, such as porous calcium carbonate³⁰ and silicate³¹, specifically intended for ink-jet use.

As mentioned previously in section 2.4.2, the pigments available on the world market for ink-jet printing applications are mostly inorganic minerals. There are, however, a number of recent patents on polymeric core-shell particles developed specifically for the coating industry³²⁻³⁶. In these patents, the outer shell is a polymer, and the inner core is either inorganic fillers such as silica, or a soft polymeric substance. Table 2.2 lists a number of these patents.

Although there have been a number of patents describing the synthetic polymeric particles and microspheres, none of these products are intended for paper coating applications. Their fields of application include chromatography³⁷, as substitute for metals and ceramics³⁸, and the coating of interior substrates³⁹ such as beverage and beer cans.

2.5 Conclusion

If a synthetic polymer is to replace the mineral fillers that are currently used in ink-jet paper coating applications, it will need to have the characteristics of the mineral fillers discussed in this chapter, and improve the requirements for printing quality and resolution that were discussed earlier in this chapter.

Briefly, the polymer particles will need a combination of the following characteristics:

- a small particle size
- a large surface area

- an affinity for the ink carrier fluid (hydrophilicity)
- an affinity for the ink dyes (cationic functionality).

As a replacement for the PVOH binder in the formulation, the polymer will further need to have an affinity for the cellulosic paper fibers and the inorganic mineral pigments, as well as hydrophilicity and it must aid in the brightness of the paper.

Table 2.2: Patents submitted for particles intended for ink-jet paper coating applications.

Polymeric core-shell particles			
	Ref #		Ref #
EP 1132217 A1	32	US 2002155260 A1	36
Disadvantages			
Needs specialized treatment of substrate surface, or undercoating, for adhesion			
Inorganic polymeric core-shell particles			
	Ref #		Ref #
US 2004001925 A1	33	EP 1184195 A1	34
EP 1184194 A2	35		
Disadvantages			
Needs specialized treatment of substrate surface, or undercoating, for adhesion of particles.			
Solvent absorbing layer is needed to absorb ink-carrier fluid.			

Chapter 3: Polyamides - Properties and Synthesis

3.1 Introduction

Polyamides are macromolecules that are made up of amide-containing, repeating units, as illustrated in Figure 3.1.

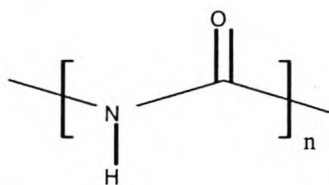


Figure 3.1: The repeating amide group in a polyamide.

Polyamides are considered as belonging to the first generation of polymeric materials, and were introduced during the 1930s when Wallace H. Carothers - then employed by the DuPont Experimental Station in the USA - first synthesized and studied polyamides as a result of his studies of polycondensation reactions.

Initially, polyamides were particularly exciting as a replacement for silk in women's hosiery, due to the strength and chemical resistance of these materials. During World War II their usefulness was further exploited in various different products - from parachute material, to rope and lines.

The first commercially produced polyamide was Nylon 6,6. This polyamide was used in the production of stockings, and this is where the term “nylons” for women’s tights originates.

According to convention, polyamides are classified according to the number of the carbon atoms in the diamine monomer, followed by the diacid monomer, e.g. Nylon 6,6 is a polyamide of hexamethylene diamine and adipoyl chloride - the acid component.

3.2 Properties

Polyamides are materials that show high resistance to chemicals, temperature, and water corrosion, and are inherently very strong.

These characteristics can be explained by the strong hydrogen bonds that are formed between the polar amide groups of adjacent polyamide chains, as illustrated in Figure 3.2. High degrees of crystallization result in very high melting temperatures, as well as resistance to solvents, water, and saponification. Interestingly, polyamides with an even number of carbon atoms between amide groups have higher melting temperatures than their odd numbered counterparts⁴⁰.

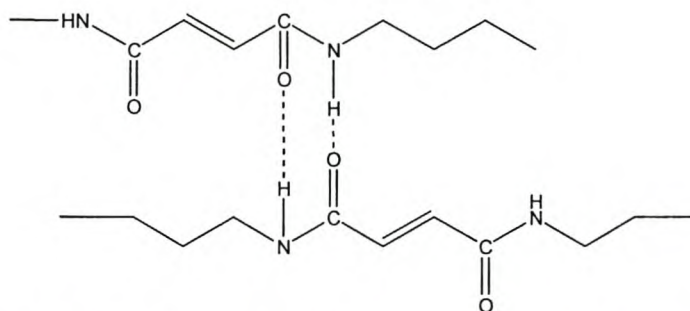


Figure 3.2: Hydrogen bonding between adjacent amide groups.

As discussed in Chapter 2, a polymer that is to replace the mineral fillers and the PVOH binder currently used in ink-jet paper coating applications must have certain characteristics, such as:

- a small particle size
- a large surface area
- an affinity for the ink carrier fluid (hydrophilicity)
- an affinity for the ink dyes (cationic functionality).

Polyamides already inherently possess some of these characteristics, such as hydrophilicity and affinity for both the inorganic pigments and the cellulosic paper fibers due to the nature of the amide groups. Further, the physical characteristics of large surface area and particle size may be obtained by the careful choice of suitable starting materials and polymerization process.

Polyamides produced from aliphatic, unsaturated monomers were considered to be potentially suitable materials to fulfill the above required characteristics. An unsaturated, linear polyamide can be produced, and crosslinked with a vinyl monomer during a free-radical chain addition reaction, performed in an emulsion, to produce particles for which:

- Particle size may be controlled by surfactant concentration and stirring speed
- Surface area will be a combination of particle size and molecular weight.

Crosslinking is necessary to achieve the formation of particles, and to prevent the particles from dissolving in water. Instead, the particles will swell in water, allowing for adequate dispersion, leading to sufficient covering of the base paper surface during coating.

3.3 Syntheses

3.3.1 Linear Polyamides

There are various ways of producing polyamides⁴⁰⁻⁴², the most common of these being a polycondensation reaction between a diamine and a diacid. Other polycondensation reactions that are used to produce polyamides include the reaction of diamines with diacid derivatives, such as acid halides or esters, and amino acid polycondensations. The ring-opening polymerization of lactams is another popular technique.

There are also a variety of different polymerization processes that can be used for these different types of reactions. These processes include interfacial and solution polymerization, solid-phase polymerization, and melt polymerization⁴². The choice of process depends on the state and solubility of the chosen monomers, and will determine the phase of the final product.

Although the melt polycondensation of diamines with diacids is considered to be the easiest and most obvious approach in terms of synthesis, there are a number of inherent disadvantages:

- Temperatures of between 200 and 300 °C are needed to overcome the high activation energy required by the acid groups. Such high temperatures pose

stoichiometric problems due to the volatility of the diamine monomers and the accompanying possibility of evaporation.⁴⁰

- At such high temperatures degradation of many of the starting materials and monomers are possible.⁴³

To overcome the high temperatures otherwise required, acid chloride monomers are often used instead of diacids⁴⁰. The former have considerably lower activation energies than diacid monomers, and polymerization occurs at lower temperatures, but the use of these monomers leads to the formation of hydrogen chloride gas as an unwanted by-product.

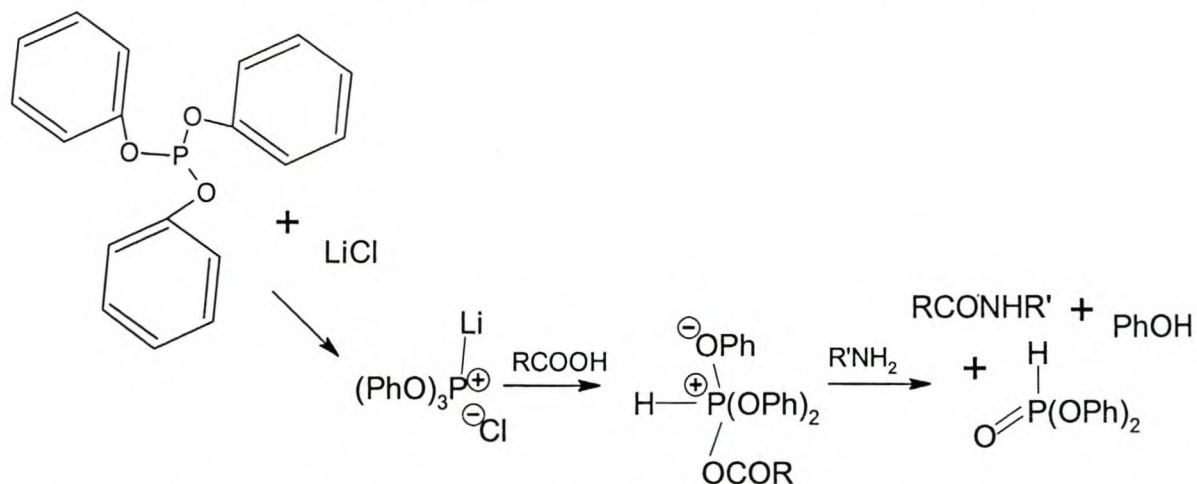
The condensation reaction of polyamides by means of phosphorous compounds offers an alternate process. It involves the use of diacid and diamine monomers, but can be carried out at considerably lower reaction temperatures³.

3.3.1.1 Phosphorylation

The polymerization of polyamides by means of phosphorous containing compounds was first described by Yamazaki and Higashi in their publication “*New Condensation Polymerizations by means of Phosphorus Compounds*”, published in 1981³. The publication describes the solution polycondensation of diamines with diacid monomers at temperatures of 100 °C and below.

One of the proposed reactions involves a phosphite-lithium chloride system, in which diacid and diamine monomers undergo hydrolysis-dehydration in the presence of an aprotic solvent, such as N-methyl-pyrrolidone (NMP). The hydrolysis-dehydration reaction is promoted by triphenyl phosphite and a metal salt, such as LiCl or CaCl₂. The reaction mechanism is shown in Reaction scheme 3.1.

This type of reaction is not confined to specific diamine or diacid monomers, but can be used with aliphatic, aromatic, or unsaturated species. The majority of publications have dealt with the polycondensation of aromatic polyamides⁴³⁻⁴⁸, and some with the polycondensation of aromatic poly(amide-imides)^{49,50}. There have, however, been no publications describing the polycondensation of unsaturated, aliphatic polyamides.

Reaction scheme 3.1: Triphenyl phosphite-lithium chloride induced phosphorylation reaction.

As an objective of this thesis, the synthesis of a polyamide from an unsaturated, aliphatic diacid monomer and an aliphatic diamine monomer was to be investigated. The synthesis of aromatic polyamides by means of a triphenyl phosphite-lithium chloride system in an aprotic solvent, as described in literature^{43,44,47-50}, was used as the template for developing the polymerization methodology that was followed during the reactions.

The monomers chosen for the synthesis of the linear polyamide were fumaric acid and 1,6-hexanediamine, with the diacid taken as the limiting agent. A single unit in the polyamide would thus be made up of one diacid and one diamine molecule, as was illustrated in Figure 1.1 (section 1.5) making the molecular weight of a single unit equal to 184 Da.

3.3.1.2 Stoichiometry

The number-average chain lengths, or degree of polymerization, can have a great effect on the porosity, pore size and solubility characteristics of the linear polyamides. Hence, in this study the effect of different chain lengths, corresponding to specific molecular weights, was investigated.

Wallace H. Carothers, who was previously mentioned as the discoverer of polyamide chemistry, devised the following simple equation which can be used to calculate the

number-average chain lengths in a linear step-growth polymerization, such as a polycondensation reaction, between two difunctional monomers AA and BB:

$$\boxed{\bar{X}_n = \frac{1}{1-p}} \quad (3.1)$$

Where p : Probability of finding a reacted group of either kind.

If it is assumed that AA is the limiting agent, then p becomes the probability of finding a reacted group of monomer AA, thus:

$$\boxed{p = \frac{N_{AA0} - N_{AA}}{N_{AA0}}} \quad (3.2)$$

Where N_{AA0} : Original number of molecules of AA present in reaction.

N_{AA} : Number of unreacted molecules of AA present in reaction after a specific time.

By substituting equation 3.2 into Carothers' equation (3.1), it is possible to arrive at the following equation for the number-average chain lengths:

$$\boxed{\tilde{x}_n = \frac{1+r}{1+r-2rp}} \quad (3.3)$$

Where \tilde{x}_n : Number-average chain lengths, or average degree of polymerization.

p : The probability of finding a reacted group.

$r = \frac{N_{AA0}}{N_{BB0}}$: The stoichiometric ratio of the functional groups present.

If the reaction is assumed to continue until complete conversion is achieved, then $p = 1$, and equation 3.3 becomes:

$$\boxed{\tilde{x}_n = \frac{1+r}{1-r}} \quad (3.4)$$

It is thus possible to determine the stoichiometric ratio (r) of the monomers AA and BB necessary to achieve pre-determined average degrees of polymerization and molecular chain length.

To investigate the effect of the degree of polymerization (or number average chain-length) on porosity and pore size, three different degrees of polymerization were chosen, and equation 3.4 was used to calculate the molar ratios of the monomers required to achieve these values at complete conversion. Table 3.1 shows the molar ratio values, along with the expected molecular weights, for each of the degree of polymerization values chosen. The molecular weights are calculated using the molecular weight of 184 Da per unit.

Table 3.1: Degrees of polymerization and corresponding weights and molar ratios of monomers.

Dp	Molar Ratio		Mw (Da)
	Diacid	Diamine	
50	49	51	9 200
100	99	101	18 400
99200	199	201	36 800

3.3.1.3 Reaction solvent

The aprotic solvent used in the condensation reactions performed by Yamazaki and Higashi³ was N-methyl pyrrolidone (NMP). Unfortunately, this material has been classified as a hazardous air pollutant, which means that the Clean Air Act demands it must be phased out of industrial applications within the next few years. This made it an unsuitable choice for use in this study, the outcome of which could have an industrial application.

As an alternative, dipropylene glycol dimethyl ether, or Progylme, an environmentally friendly, aprotic solvent product of Clariant GmbH, was therefore considered. The supplier of this product claims that it could be used as a substitute for and alternative to

NMP, because of the similarities in solubility and physical characteristics between the two materials. Progylme has not been listed as a hazardous air pollutant, and is claimed to exhibit low toxicity, excellent chemical stability, and outstanding solvency of organic materials⁵¹.

3.3.2 Crosslinked Particles

A linear, unsaturated polyamide may be crosslinked by a free-radical chain addition polymerization involving a vinyl monomer, to form hydrophilic particles that will swell in water. To produce the end product in the form of particles, the reaction can be carried out as an inverse suspension polymerization.

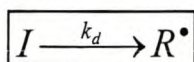
3.3.2.1 Crosslinking by means of free-radical chain addition reaction

The unsaturation in a linear polyamide may easily be utilized in a free-radical chain addition reaction, whereby a vinyl monomer is used to crosslink the polyamide chains.

Typically, in this kind of reaction, the polymer is dissolved either in the monomer or in a suitable solvent, to which is added the vinyl monomer and a free-radical initiator. The steps that occur in this type of polymerization are:

- Initiation
- Propagation
- Transfer
- Termination

During *initiation* there are two important reactions that occur. In the first reaction the initiator molecule is split into radical fragments. This splitting may be thermally induced, as is the case with potassium persulfate (KPS), or it may be light-induced, as is the case with dibenzil.



Where I : initiator molecule

R^\bullet : initiator radical

k_d : rate constant for the initiation reaction.

The thermally induced splitting of KPS is shown in Figure 3.3.

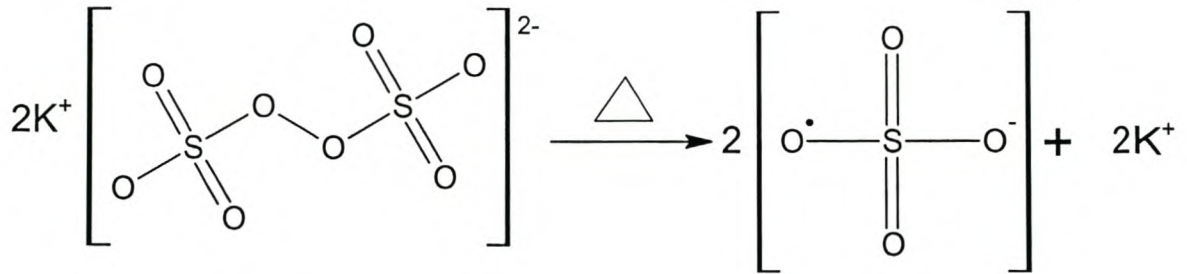
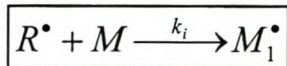


Figure 3.3: Thermally induced splitting of KPS.

In the subsequent reaction a monomer radical is formed by the addition of a monomer molecule to the initiator radical.



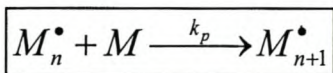
Where R^{\bullet} : initiator radical

M : monomer molecule

M_1^{\bullet} : monomer radical

k_i : rate constant for the initiation reaction

During *propagation*, further monomer molecules are added to the monomer radical, leading to the formation of oligomer radicals and polymer radicals. The successive addition of monomer molecules to these radical structures are repetitive.



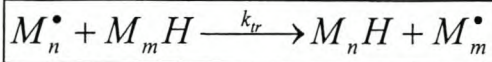
Where M_n^{\bullet} : monomer radical

M : monomer molecule

M_{n+1}^{\bullet} : polymer or oligomer radical

k_p : rate constant for the propagation reaction

Transfer reactions occur when a radical molecule removes a proton from another molecule nearby, and thus becomes saturated, while the second molecule becomes a radical. These types of reactions will not be significant in this system



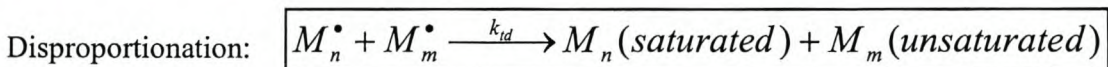
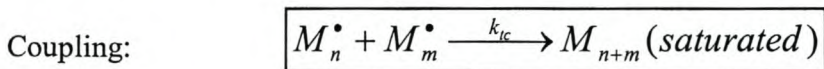
Where M_n^\bullet and M_m^\bullet : polymer radicals

$M_m H$: polymer, monomer, solvent, initiator, or transfer agent

$M_m H$: saturated polymer chain

k_{tr} : rate constant for the transfer reaction

Termination is the process whereby propagation is ended, and may occur by the combination of two radicals, which is known as coupling, or by the transfer of the radical elsewhere on the chain or onto another molecule altogether. This is known as disproportionation.



Where M_n^\bullet and M_m^\bullet : polymer radicals

M_{n+m} , M_n and M_m : polymer molecules

k_{tc} and k_{td} : rate constants for the termination reactions

3.3.2.2 Inverse suspension polymerization

The paper coating application for which the crosslinked polyamide is intended makes use of a powder for easy incorporation into the coatings. Preparation of the polyamide by means of a simple solution crosslinking reaction will therefore not give the required result, because the product will be a solid mass of crosslinked polymer.

In order to produce particles as the end product, it was decided to perform the crosslinking reaction by making use of inverse suspension polymerization. This type of polymerization has been used with success in the preparation of beads of crosslinked copolymers of neutralized maleic anhydride with other monomers⁵², and thermosensitive copolymers of poly(N-isopropyl acrylamide)-co-2-hydroxyethyl methacrylate⁵³.

In this study this entails the dispersion of an aqueous solution, containing the linear polyamide, vinyl monomer, and initiator, in an alkane solvent, known as the oil phase. The dispersed droplets are prevented from coagulation by the presence of a surfactant - a long-chain molecule with both hydrophobic and hydrophilic areas - which surrounds the dispersed droplets. The system is diagrammatically illustrated in Figure 3.4.

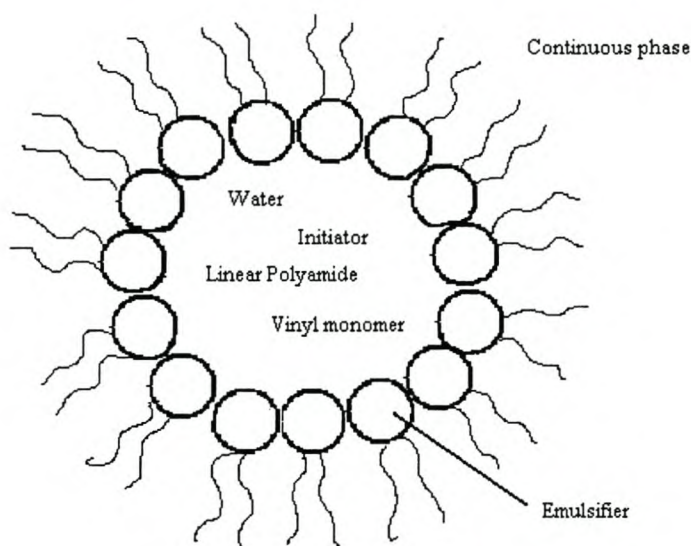


Figure 3.4: Schematic diagram of proposed water-in-oil emulsion system used during crosslinking of linear polyamide.

This kind of system, where an aqueous phase is dispersed in an oil phase, is known as a water-in-oil (w/o), or inverse emulsion.

The selection of a suitable surfactant is very important for the formation of a stable w/o emulsion. The hydrophilic lipophilic balance (HLB) value of a surfactant indicates the mass fraction of the surfactant which projects into the aqueous phase. Water-in-oil emulsions are favoured when the greater fraction of the mass of the surfactant lies within the oil phase, and thus a surfactant with a low HLB value will be needed⁵³.

The range of SPAN[®] surfactants, produced and manufactured by ICI Americas Inc, has low HLB values and is used to form w/o emulsions.

3.3.2.3. Choice of vinyl monomers

Two vinyl monomers were chosen in the crosslinking reactions. These were 2-hydroxyethyl methacrylate (HEMA), shown in Figure 3.5, and 4-vinyl pyridine, shown in Figure 3.6.

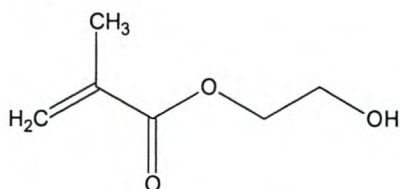


Figure 3.5: 2-Hydroxyethyl methacrylate (HEMA)

HEMA was chosen because of its hydrophilicity, and its ability to undergo hydrogen bonding.

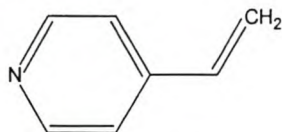


Figure 3.6: 4-Vinyl pyridine

4-Vinyl pyridine was chosen in an effort to impart cationic functionality to the crosslinked product. It was hoped that the cationic functionality would fix the anionic dyes and thus improve the colour density.

3.4 Conclusion

Polyamides have certain chemical characteristics that made them suitable for the scope of this thesis, namely their hydrophilicity.

By choosing the monomers for vinyl functionality it would be possible to crosslink the polyamides with a suitable vinyl monomer, thus preventing them from dissolving in water, and rather leading to swelling, allowing them to maintain their shape. Cationic functionality, or added hydrophilicity, could also be imparted to the end product in this way.

The particles could be produced by inverse suspension polymerization, making it possible to exert control over swellability and swollen particle size.

Chapter 4: Experimental

4.1 Materials used

N-Methyl pyrrolidone (NMP) was vacuum distilled in-house before use and stored under nitrogen atmosphere over 4Å molecular sieves. Methanol (MeOH), Acetone, and N-heptane were of 99.0% purity, or greater. These solvents were used without further purification.

Dipropylene glycol dimethyl ether (Proglyme), an aprotic solvent intended as an environmentally friendly replacement for NMP, was received as a free sample from Clariant GmbH. It was used without further purification.

Potassium persulfate (KPS), 99% pure, and lithium chloride (LiCl) were bought from Acros Organics. The materials were dried at 100 °C in a vacuum oven for 48 hours, and stored in a desiccator before use.

Triphenyl phosphite (TPP), at a purity of greater than 97%, as well as SPAN[®] 40, a registered product of ICI Americas Inc, were bought from Fluka and used as such.

Fumaric acid, of 99% purity, 4-vinylpyridine, at 95% purity, and 2-hydroxyethyl methacrylate (HEMA), GC grade, were bought from Sigma-Aldrich and used as such. HEMA was stored in a fridge below 5 °C, and 4-vinylpyridine in a freezer below -5 °C.

Hexane-1,6-diamine was bought from Fluka as GC grade, and stored in a tightly closed container under an inert atmosphere.

Silica HP39 was bought from Ineos Silicas Ltd.

BYK 333, a slip and mar additive used in the coating formulations, was bought from BYK-Chemie GmbH.

The polyvinyl alcohol used in the coating formulations was Celvol 203, and was bought from Celanese Chemicals (Europe GmbH).

The Laponite used in the coating formulations was the JS grade, and was received as a free sample from Rockwood Additives Ltd.

Freshly distilled analytical grade water was used as needed.

4.2 Synthesis

The polyamide particles were synthesized during a two step process. Firstly, water-soluble, linear, unsaturated aliphatic polyamide chains of low degrees of polymerization were synthesized by means of a phosphorylation condensation technique. Thereafter, the polyamide chains were crosslinked with one of two vinyl monomers, HEMA or 4-vinyl pyridine, during an inverse suspension polymerization, using a free radical reaction, to create particles.

4.2.1 Preparation of the linear polyamides

During the synthesis of the linear polyamide there were two variables that resulted in the formation of different products. These variables were:

- The solvent in which the synthesis was carried out
- The stoichiometric ratio of the monomers in the reaction mixture, which determines degree of polymerization and molecular weight.

Table 4.1 contains the information for each of the different polyamide samples that were synthesized, and tabulates the variables of degree of polymerization, molecular weight, and reaction solvent for each sample.

The laboratory procedure for the synthesis of the linear polyamides is described below.

A 250 ml, three-necked, round-bottom flask was equipped with a reflux condenser with bubbler, a medium-size teflon coated rugby-ball magnetic follower, a nitrogen inlet, and a thermometer. The system was purged with dry nitrogen gas for 20 minutes, before the

addition of LiCl (equal to 4% of the solvent mass), triphenyl phosphite, the diacid monomer (fumaric acid), and 200 ml aprotic solvent (either NMP or Proglyme).

Table 4.1: Variables that were present during the synthesis of the various linear polyamide samples.

Sample name	Degree of polymerization	Molecular weight expected (Da)	Reaction solvent
N50	50	9 200	NMP
N100	100	18 400	NMP
N200	200	36 800	NMP
P50	50	9 200	Proglyme
P100	100	18 400	Proglyme
P200	200	36 800	Proglyme

Stirring was commenced, while the nitrogen gas flow continued, and the reaction mixture was heated to 105 °C in a silicon-oil bath. When the desired temperature had been reached, the diamine monomer (1,6 hexanediamine) was injected into the mixture.

The reaction was allowed to continue for 2 hours with continuous stirring (300 rpm) under a nitrogen atmosphere. The oil bath was removed and the reaction cooled to room temperature under nitrogen gas flow, whilst stirring continued. The mixture was poured into 400 ml MeOH, and stirred slowly for 5 minutes. No precipitate was observed. The crude reaction mixture was a dark, black liquid with a viscosity similar to that of water.

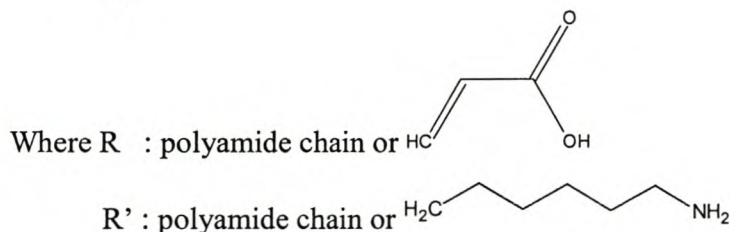
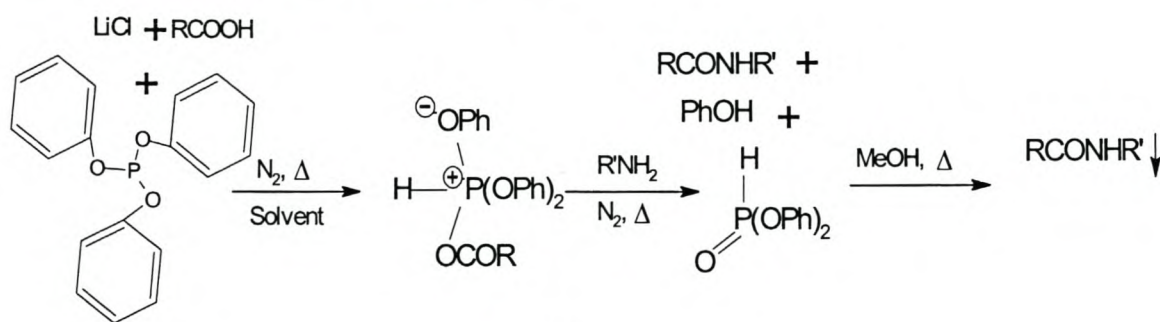
The MeOH was then distilled off. After about 90% of the MeOH had been distilled off a sharp, almost instantaneous increase in temperature of about 20 °C was observed. The remaining mixture was allowed to cool to room temperature, and poured back into MeOH. A precipitate formed.

The precipitated product was allowed to settle for 12 hours, after which the upper, clear MeOH layer was decanted and the product filtered using a sintered glass funnel of porosity 3, and a Venturi vacuum system. The filtered product was refluxed in MeOH for

2 hours, filtered a second time with a sintered glass funnel of porosity 3 and Venturi vacuum, and then dried for 24 hours in a vacuum oven at 100 °C.

Reaction scheme 4.1 shows the preparation of a linear polyamide from 1,6-hexanediamine and fumaric acid, as described above, by means of a phosphorylation condensation reaction.

Reaction scheme 4.1: The preparation of a linear polyamide from 1,6-hexanediamine and fumaric acid, using a phosphorylation polycondensation technique.



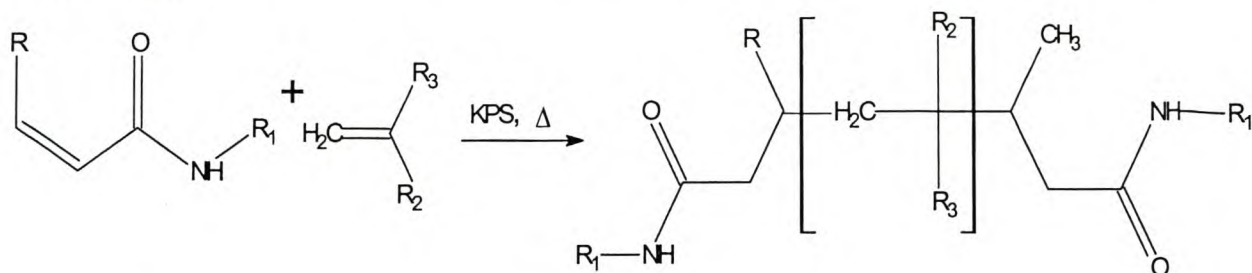
Solvent : NMP or Proglyme

4.2.2 Preparation of the crosslinked particles

The unsaturated, linear polyamide chains produced by means of the phosphorylation reaction described above were used to synthesize particles by the use of a crosslinking reaction involving one of two vinyl monomers, either HEMA or 4-vinyl-pyridine, in an inverse suspension polymerization process.

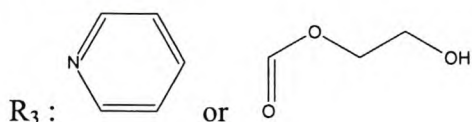
The crosslinking reaction is shown in Reaction scheme 4.2.

Reaction scheme 4.2: Crosslinking reaction between polyamide chains and a vinyl monomer, such as 4-VP or HEMA.



Where R and R₁ : polyamide chains

R₂ : H or CH₃



To an Erlenmeyer flask, fitted with a teflon coated bar-shaped magnetic follower, condenser with glass bubbler, and nitrogen gas inlet, a specific volume of n-heptane as continuous phase and 5% by solvent weight of Span[®] 40, a non-ionic surfactant, were added. The solution was heated under dry nitrogen gas flow, whilst stirring until the surfactant had completely dissolved in the n-heptane. The mixture was then allowed to cool to room temperature.

In a separate glass beaker, 70% of solids weight of linear polyamide, 30% by solids weight vinyl monomer, and 2% KPS were added to de-ionized water to make a 10% solids mixture. This mixture was stirred until all the components were dissolved and the solution was homogeneous.

The water phase was slowly added to the continuous phase by means of a pipette, whilst vigorously stirring at 800 rpm. The stirring speed was later increased to 1200 rpm and the mixture was stirred, under nitrogen gas flow, at room temperature, for 15 minutes.

After the formation of a stable emulsion, the reaction mixture was heated to 90 °C, in a silicon-oil bath. The stirring speed was then decreased and maintained at 400 rpm. The nitrogen gas flow was discontinued. At 90 °C the half-life of the KPS initiator is 1.5

hours and thus the emulsion was left to react for 3 hours to ensure adequate time for the initiator to dissociate.

At the end of the reaction, the oil bath was removed and the mixture allowed to cool to room temperature, and then poured into 150 ml acetone. The precipitated product was filtered with a sintered glass funnel of porosity 3 using a Venturi vacuum system, then refluxed in acetone for 2 hours, filtered a second time with a sintered glass funnel of porosity 3 and a Venturi vacuum system, and then dried in a vacuum oven for 12 hours at 50 °C.

4.3 Characterization

4.3.1 NMR

Both the linear polyamide and the crosslinked particles were characterized for functionality by means of ^{13}C Nuclear Magnetic Resonance (NMR) spectroscopy.

Nuclear Magnetic Resonance spectroscopy was performed on a Varian VXR 300 MHz instrument at 25 °C. The solvent used was deuterated water for all samples, and the spectra were referenced externally to dioxane.

4.3.2 ESMS

Molecular weight determinations were performed by means of Electrospray Ionization Mass Spectrometry (ESMS). This technique was identified as suitable for the application, because water soluble samples are easily analyzed, it is not affected by the morphology of the chains, and gives absolute molecular weight values for polymers with molecular weights of up to 1 000 kDa⁵⁴, although the transform software is only accurate for values of up to 200 kDa.

A Waters Micromass Q-TOF Ultima mass spectrometer was used for mass spectrometry. The samples were ionized with electrospray ionization in the positive mode. A capillary voltage of 3.5 kV, a cone voltage of 100 V, and a source temperature of 150 °C were used. The samples were dissolved in the mobile phase at a concentration of 1

mg/ml. The samples were introduced into the ionization source using, as mobile phase, a 2% acetonitrile solution containing 0.1% formic acid. 10 μ l of each sample was injected into the mobile phase and introduced into the source at a flow rate of 40 μ l/min. A Waters CapLC capillary HPLC pump was used for solvent delivery. The scan rate was 1 s/scan, and the range was 100 to 1999 m/z. Analyses were performed using MassLynx 4.0 software from Waters Micromass. Molecular weights of the multiple charged ions were calculated using the Transform software routine.

Sample preparation was as follows: 1.0 mg/ml aqueous solutions of the polymer samples were prepared, and filtered through a 0.45 micron membrane filter to remove large impurities that could damage the instrumentation.

4.3.3 Light Scattering

Light scattering was performed on a Malvern Zetasizer light scattering instrument, and used to determine particle size and particle size distribution of the crosslinked polyamide samples.

The samples were dissolved in a 1 mmol sodium chloride solution, at sufficient concentrations to achieve the Tindall effect.

4.3.3 Scanning Electron Microscopy (SEM)

Scanning electron microscopy (SEM) and Cryo-SEM were performed by Miranda Walker at the Electron Microscope Unit of the University of Cape Town. The techniques were used to investigate the dry and swollen diameters of the crosslinked polyamide particles. The information gained was used to calculate the swelling ratio's of the gel-particles.

SEM sample preparation involved the drying of 1% sample solutions on SEM stubs, which are then gold sputter coated.

Cryo-SEM involved the freezing of 1% sample solutions in liquid nitrogen, then viewing the frozen material under the microscope. This made it possible to investigate the particles in their swollen state.

4.4 Coating of paper samples

Various formulations for the coating of starch-sized base paper were prepared, containing different percentages of silica and the synthesized, crosslinked polyamide. The paper was then coated with the different formulations.

4.4.1 Preparation of formulations

Table 4.2 shows the ingredients that were varied for each coating formulation. All the formulations contained 27.8 parts of an 18% Laponite JS dispersion, and 0.2 parts of BYK 333. The crosslinked polyamide sample that was used in the coating formulations was N200-H.

The procedure for the preparation of the formulations was always the same: the ingredients were added together and stirred at 300 rpm with an overhead stirrer, until the formulation was homogeneous.

4.4.2 Coating of base paper

Starch-sized base paper was coated with the prepared coating formulations. A 24 μm wire bar was used, on a laboratory draw-down coating machine, at a speed setting of 6. The coating formulation was applied to the coating bar by hand, using a plastic pipette.

Due to the low viscosity of the prepared formulations, a double coating was applied to the paper samples to ensure sufficient coating weight. After coating the paper samples were dried in an oven at 70 °C for 30 seconds, and left overnight to dry completely.

Table 4.2: Ingredients that were varied in the coating formulations that were prepared for the coating of starch-sized paper, given as parts per hundred.

Formulation	Crosslinked polyamide*	Silica HP39	PVOH (10 % solution)	Water
1	0	5.0	50	17
2	0.1	4.9	50	17
3	0.3	4.7	50	17
4	0.9	4.1	50	17
5	1.8	3.2	50	17
6	0	5.0	0	67
7	0.1	4.9	0	67
8	0.3	4.7	0	67
9	0.9	4.1	0	67
10	1.8	3.2	0	67

* Synthesized crosslinked polyamide N200-H, or N200-PV

4.5 Printing of paper samples

The dry, coated paper samples were printed on a Canon desk-top S800 ink-jet printer, with the test pattern that is shown in Figure 4.1.



Figure 4.1: Test pattern printed on coated paper samples.

4.5.1 Wet-rub test

The printed paper samples were tested by means of the wet-rub test. This test involves wetting and rubbing the coated paper surface for 6 seconds with your finger, and then transferring the residue onto a black paper surface. The smear is allowed to dry.

The residue remaining on the black paper gives an indication of the wet-rub resistance of the coating, and the various formulations can thus be compared in terms of wet-rub resistance.

Chapter 5:

Results and Discussion

In this chapter the results of the preparation and characterization of the linear polyamide, as well as the crosslinked polymer particles, are discussed. Included are also the details of the coating formulations that were prepared, and the subsequent coating and printing of starch-sized base paper samples.

5.1 Linear polyamides

The different polymer samples that were prepared are tabulated in Table 5.1, with physical data such as yield percentage, appearance of the samples and water solubility at room temperature.

Table 5.1: Details of the products of the linear polyamide synthesis reactions.

Sample	Water soluble	Physical characteristics	Yield (%)
N50	yes	Light brown powder	100
N100	yes	Light brown powder	70.5
N200	yes	Light brown powder	54.2
P50	slightly	White powder	82.4
P100	yes	White solid	82.5
P50	yes	White solid	76.6

A discussion of the effects of the previously mentioned variables on the products follows below.

5.1.1 Solvent

Two different solvents were used: NMP and Proglyme, as discussed in section 3.3.1.3. The solvent in which the polymerizations were performed was a variable in the experiments, which resulted in the formation of different polymeric products.

Samples N50 and P50 were chosen as examples of the two different products from the two different solvents. They differ only with regards to the solvent that was used during the synthesis reaction, and was used to investigate the effect of the choice of solvent on the structure of the linear polyamide product. For N50 the solvent was NMP and for P50 the solvent was Proglyme. The ^{13}C NMR spectra of the two samples can be seen in Appendix 1.

The structure of a single unit in the expected polyamide product contains 10 carbons, as depicted in Figure 5.1. Due to chemical equivalence, however, only seven different electronegative environments were expected to be present in the NMR spectrum of this polyamide; these are indicated and numbered in Figure 5.1. It was thus expected that seven groups of peaks would similarly be found on the ^{13}C spectrum of a successfully synthesized polyamide.

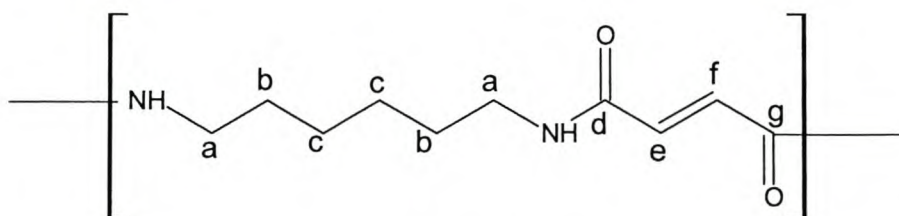


Figure 5.1: Different electronegative environments present within the polyamide, with equivalent areas indicated.

The successfully synthesized polymer should also contain two distinct functionalities, namely the double bond and the amide group. The peaks for these functionalities are located in well separated areas on the ^{13}C spectrum, and would thus be easily identified if they were present. The chemical shift ranges where the peaks of these functionalities were predicted to appear are given in Table 5.2. The predictions were gained from NMR

prediction software. The shift range for the methylene carbons of the polyamide is also indicated.

Table 5.2: Carbon shift ranges predicted for the functional groups and methylene carbons with NMR prediction software.

Environment	Predicted δ -range (ppm)
-NH-CO-	160 – 180
-C=C-	100 – 145
-CH ₂ -	0 – 55

Table 5.3 gives the peaks that were found in the spectra of the samples N50 and P50.

Table 5.3: δ -Ranges where groups of peaks were found in ¹³C spectra of N50 and P50.

N50 δ -range (ppm)	P50 δ -range (ppm)
25 – 42	15 – 16
115 – 129	56 – 58
180 – 182	72 – 76

A comparison of Tables 5.2 and 5.3 showed that N50, produced in NMP, had three groups of peaks that fell exactly within the expected ranges for the functional groups within the polyamide. Sample N50 therefore appeared to be the desired polyamide product.

In the spectrum of sample P50, the sample that was produced in Proglyme, three groups of peaks were identified. Only one of these groups corresponded to the functional groups expected, and this group confirmed the presence of the methylene carbons. The other two groups of peaks did not correspond to the amide and double bond functionalities expected, but corresponded with the ranges expected of amine (δ 25 – δ 70 ppm) and ether functionalities (δ 40 – δ 80 ppm).

Peaks that would indicate the presence of amide and double bond functionalities were found to be missing completely from the spectrum of sample P50. This indicated that the fumaric acid monomer had been excluded from incorporation into the end product.

Sample P50 was thus clearly not the desired polyamide. It was a substance which contained both amine and ether functionality, as evidenced by the NMR spectrum, most probably indicating that the Progylme solvent had reacted with the diamine monomer. The product was not the expected polyamide.

Progylme was thus found to be unsuitable as an aprotic solvent for the phosphorylation polycondensation reaction, and could therefore not be used as a replacement for NMP for the preparation of linear polyamide products by means of phosphorylation reactions.

5.1.2 Stoichiometry

It was intended to produce various polyamides with, various degrees of polymerization, in order to investigate the effect of chain length and molecular weight on porosity, pore size, and solubility.

The synthesis of different molecular weight polymers would depend on the stoichiometric balance between the two different monomers, and thus the ratio between the monomers, necessary to achieve specific desired chain lengths, were calculated, as discussed in section 3.3.1.2. Table 5.4 shows the degrees of polymerization that were chosen for investigation, and gives the molar ratios of the 1,6-hexanediamine to the fumaric acid, calculated for each value.

Molecular weight determinations were performed by means of Electrospray Ionization Mass Spectrometry (ESMS).

For each of the samples, the three molecular weight species with the highest concentrations were identified and listed in Table 5.5, along with the relative peak intensities for each of the species. The intensities indicated the relative concentrations of the different molecular weight chains within each sample. The ESMS spectra of the

samples are shown in Appendix 2. The highest molecular weight species, as listed in Table 5.5, have been labeled on the spectra in Appendix 2.

Table 5.4: Degrees of polymerization desired and corresponding required molar ratios of monomers, with resulting molecular weight.

Dp	Molar Ratio		Mw (Da)
	Diamine	Diacid	
50	49	51	9 200
100	99	101	18 400
200	199	201	36 800

Table 5.5: Molecular weights determined for polymer samples with ESMS technique.

N50		N100		N200	
Molecular weight (kDa)	Peak intensity (%)*	Molecular weight (kDa)	Peak intensity (%)*	Molecular weight (kDa)	Peak intensity (%)*
73.6	100	75.6	100	191.0	100
57.4	79.5	42.3	84.0	166.0	67.6
47.4	71.4	7.6	74.1	31.9	49.4
P50		P100		P200	
Molecular weight (kDa)	Peak intensity (%)*	Molecular weight (kDa)	Peak intensity (%)*	Molecular weight (kDa)	Peak intensity (%)*
165.4	100	113.8	100	158.7	100
154.1	98.1	86.7	95.0	105.6	69.8
153.3	79.0	108.3	89.8	89.4	60.5

* Calculated relative to the intensity of the highest peak

The data in Table 5.5 shows that the stoichiometric control was unsuccessful. The molecular weights of all the polymer samples were considerably higher than those that were predicted and expected.

Fortunately, large differences in molecular weight between the polyamide samples were found, making it possible to still investigate the effects of molecular weight on the swellability of the subsequently crosslinked particles, as discussed in section 3.3.1.2.

Knowledge of the molecular weights of the polyamides was useful in the investigation of the success of the subsequent crosslinking reactions. Increases in molecular weight indicated the presence of crosslinked structures in the polymers, as will be discussed in section 5.2.2.

5.2 Crosslinked polyamide particles

The unsaturated, water soluble, linear polyamides that were produced by means of the phosphorylation reactions in NMP, were consequently crosslinked. These were samples N50, N100, and N200. The crosslinking occurred according to a free radical reaction involving one of two vinyl monomers, either 2-hydroxyethyl methacrylate (HEMA) or 4-vinyl-pyridine.

The crosslinking reactions were carried out as water-in-oil emulsions during inverse suspension polymerization, as discussed in section 3.3.2.2 and section 4.2.2.

5.2.1 Results of synthesis

The results of the crosslinking experiments for the three polyamide samples N50, N100, and N200 are given in Table 5.6.

5.2.2 Crosslinking

The success of the crosslinking reactions was determined by looking at the following factors:

- Molecular weight
- Functional group

- Structural information of the particles.

Molecular weight investigations were performed by ESMS, while ^{13}C NMR was used to investigate functional groups and molecular structure. Particle size determinations were made by light scattering and SEM.

Table 5.6: Results of crosslinking reactions performed on samples N50, N100, and N200.

Crosslinked particle	Polyamide sample	Vinyl monomer	Physical characteristics of	Water soluble	Yield (%)
N50-H	N50	HEMA	Dark cream solid, black patches	Yes	81.2
N50-VP	N50	4-Vinyl Pyridine	Dark cream solid	Yes	66.8
N100-H	N100	HEMA	Cream solid, brown patches	Yes	88.0
N100-VP	N100	4-Vinyl Pyridine	Light cream solid	Yes	63.9
N200-H	N200	HEMA	Cream solid	Yes	74.4
N200-VP	N200	4-Vinyl Pyridine	Dark cream solid	Yes	66.8

5.2.2.1 Crosslinking of N50

Table 5.7 gives the three molecular weight species with the highest concentrations that were found by means of ESMS for samples N50, N50-H, and N50-PV. The ESMS spectra can be seen in Appendix 2.

Sample N50-H had molecular weight species (154.1 kDa), double the size of the highest species found in the linear polyamide (73.6 kDa). This indicated the presence of crosslinked polymer chains, even if these were only the soluble fraction that had passed through the filter. Sample N50-VP, however, did not show any high molecular weight

species. This could, however, have been caused by the filtration during sample preparation, and thus verification by NMR was required.

Table 5.7: The three molecular weight species present, with highest concentrations, for Sample N50 and its crosslinked products, Samples N50-H and N50-VP, as determined by ESMS.

N50		N50-H		N50-VP	
Molecular weight (kDa)	Peak intensity (%)*	Molecular weight (kDa)	Peak intensity (%)*	Molecular weight (kDa)	Peak intensity (%)*
73.6	100	154.1	100	53.0	100
57.4	79.5	42.3	35.8	41.4	91.3
47.4	71.4	41.5	33.3	22.3	89.1

* Calculated relative to the intensity of the highest peak

The ^{13}C NMR spectra of samples N50, N50-H, and N50-VP are shown in Appendix 1. The samples were not filtered during sample preparation, and thus high molecular weight species present would also be detected.

For comparative purposes the relative concentrations of the double bond peaks located at $\delta 130$ and $\delta 121$ ppm, and the amide peaks located at $\delta 181$ - $\delta 180$ ppm, were calculated for each of the three samples, and tabulated in Table 5.8.

Table 5.8: Relative concentrations of Double bond peak at $\delta 129$ ppm and amide peaks at $\delta 181$ ppm.

Sample	Double bond	Amide
N50	0.50	1.00
N50-H	0.37	1.00
N50-VP	0.52	1.00

The relative concentration of the double bonds in the sample crosslinked with HEMA (N50-H) was found to have decreased by almost a third, indicating that crosslinking had occurred.

Furthermore, a number of small peaks appeared in the spectrum of the crosslinked polymer N50-H, and these were not present in the spectrum of the linear polymer N50, as can be seen in Figure 5.2.a and 5.2.b. These peaks corresponded accurately with the positions of the methylene carbons of the methacrylate functionality, as predicted by NMR predictions software. These peaks are predicted to be visible at $\delta 60$ and $\delta 65$ ppm. The presence of the methacrylate methylene carbons were thus confirmed, indicating that crosslinking with HEMA as vinyl monomer had occurred.

Upon comparison of the ^{13}C spectrum of the linear polyamide N50 with that of the product of the reaction between N50 with 4-VP, namely N50-VP, no differences were observed; the spectra were exactly alike. The relative concentrations of the double bonds also remained the same for both samples. Crosslinked polyamide was therefore not present in this sample.

5.2.2.2 Crosslinking of N100

Table 5.9 gives the three molecular weight species with the highest concentrations that were found by means of ESMS for samples N100, N100-H, and N100-PV. The ESMS spectra are shown in Appendix 2.

Both samples N100-H and N100-VP show the presence of molecular weight species (137.6 kDa, 133.6 kDa) that are more than double that of the highest molecular weight (75.6 kDa) found for the linear polyamide N100, thus indicating that both the crosslinking reactions must have resulted in the formation of crosslinked polymer.

The ^{13}C NMR spectra of the three samples are shown in Appendix 1. The samples were not filtered during sample preparation, thus high molecular weight species were still present during analysis.

Figure 5.2.a: ^{13}C NMR Spectra of N50 for the δ -range 30 – 75 ppm

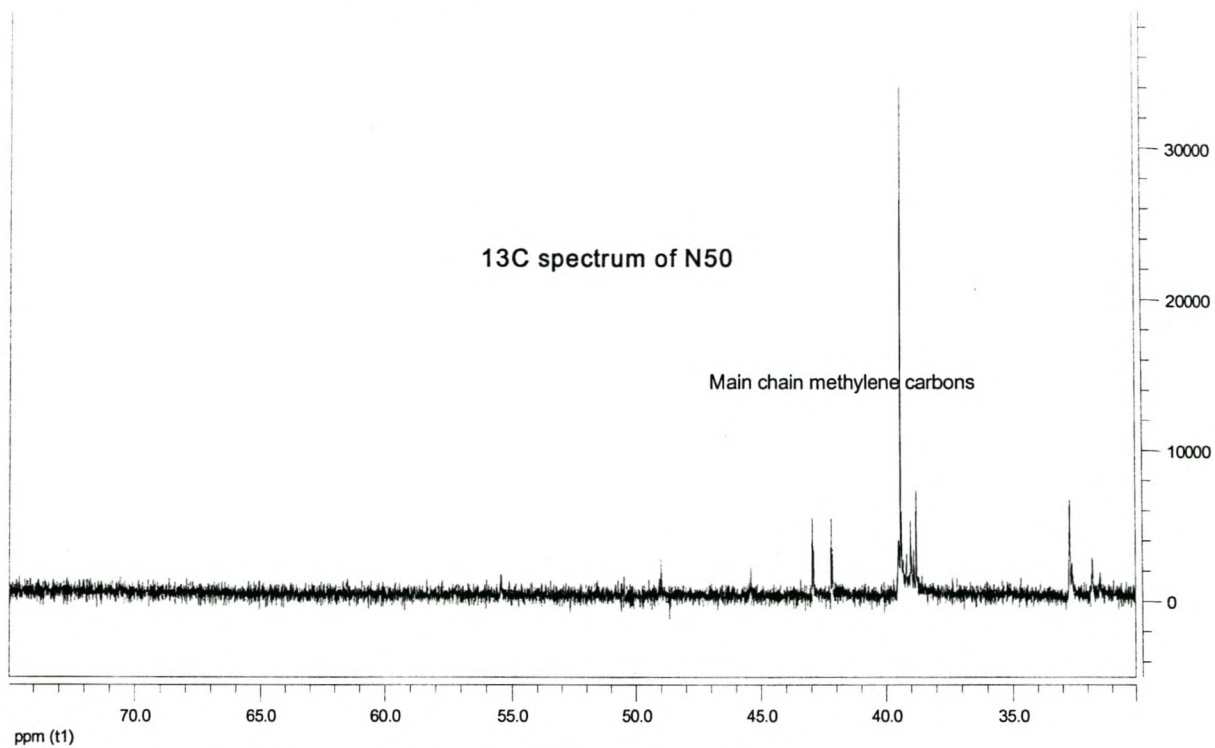


Figure 5.2.b: ^{13}C NMR Spectra of N50-H for the δ -range 30 – 75 ppm

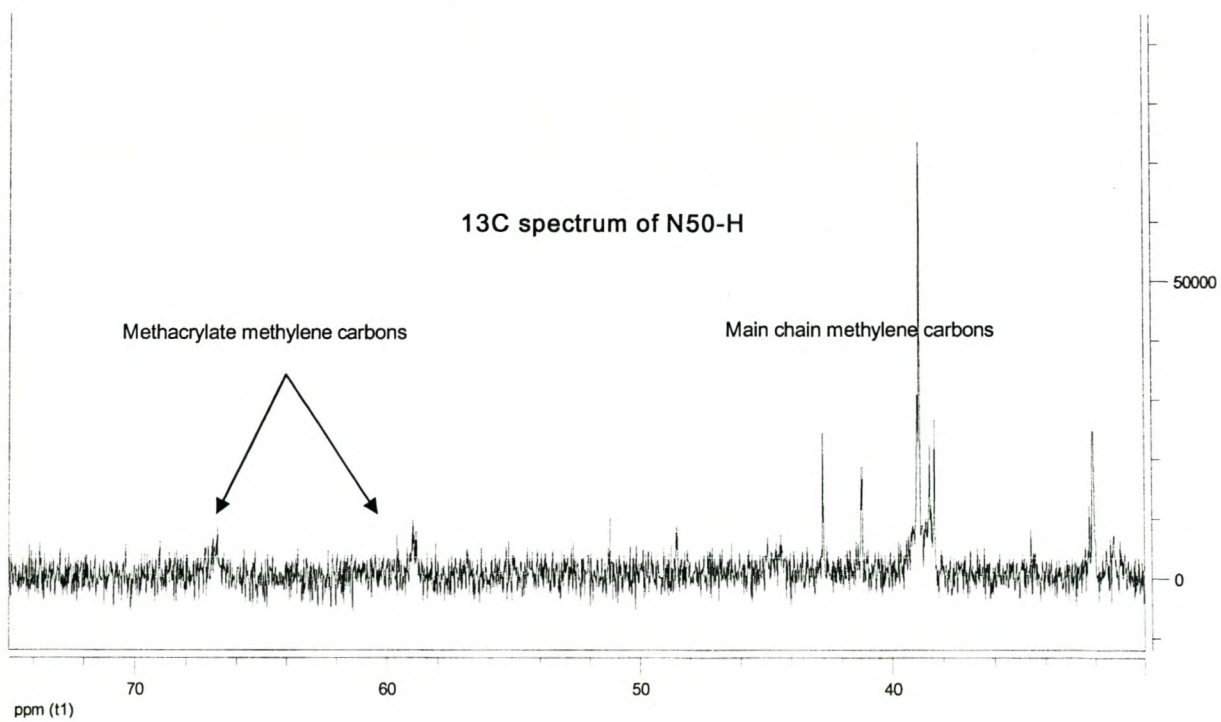


Table 5.9: The three molecular weight species present, with highest concentrations, for Sample N100 and its crosslinked products, Samples N100-H and N100-VP, as determined by ESMS.

N100		N100-H		N100-VP	
Molecular weight (kDa)	Peak intensity (%)*	Molecular weight (kDa)	Peak intensity (%)*	Molecular weight (kDa)	Peak intensity (%)*
75.6	100	137.6	100	133.6	100
42.3	84.0	61.2	39.5	99.3	61.4
7.6	74.1	52.5	35.8	101.4	53.7

* Calculated relative to the intensity of the highest peak

In the ^{13}C spectrum of the supposedly crosslinked sample N200-H the methylene peaks of the methacrylate tails were found at $\delta 67$ and $\delta 59$ ppm, corresponding perfectly to the predicted values, and thus confirming the presence of crosslinked polymer.

In the spectrum of sample N100-H a number of small peaks appeared which corresponded accurately with the predicted positions of the methylene carbons of the methacrylate tail. The magnified spectra are shown in Figure 5.3. A comparison of the double bond concentrations, given in Table 5.10, also showed that the double bond concentration in sample N100-H had decreased. The presence of the methacrylate methylene carbons was thus confirmed, indicating that crosslinking with HEMA as vinyl monomer had most probably occurred.

The spectrum of sample N100-VP showed distinct differences to that of the linear polyamide sample N100. The double bond peaks, located at $\delta 131$ and $\delta 121$ ppm, had decreased in intensity, and in Table 5.10 it can clearly be seen that the double bond concentration of N100-VP had decreased. At the same time, peaks indicating the presence of aromatic carbons of the pyridine ring of 4-VP had appeared at $\delta 148$ and $\delta 125$ ppm. The presence of crosslinked polyamide in the sample was therefore shown.

Figure 5.3.a: ^{13}C NMR Spectrum N100 the δ -range 30 – 70 ppm

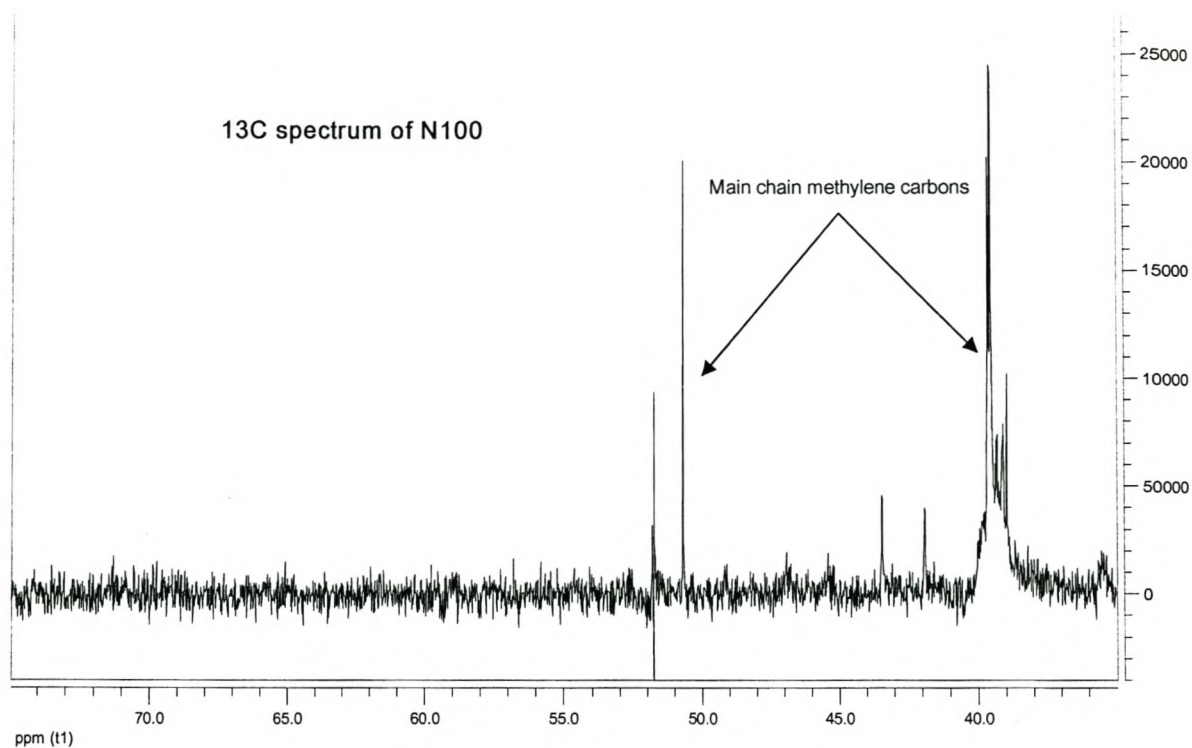


Figure 5.3.b: ^{13}C NMR Spectrum of N100-H for the δ -range 30 – 70 ppm

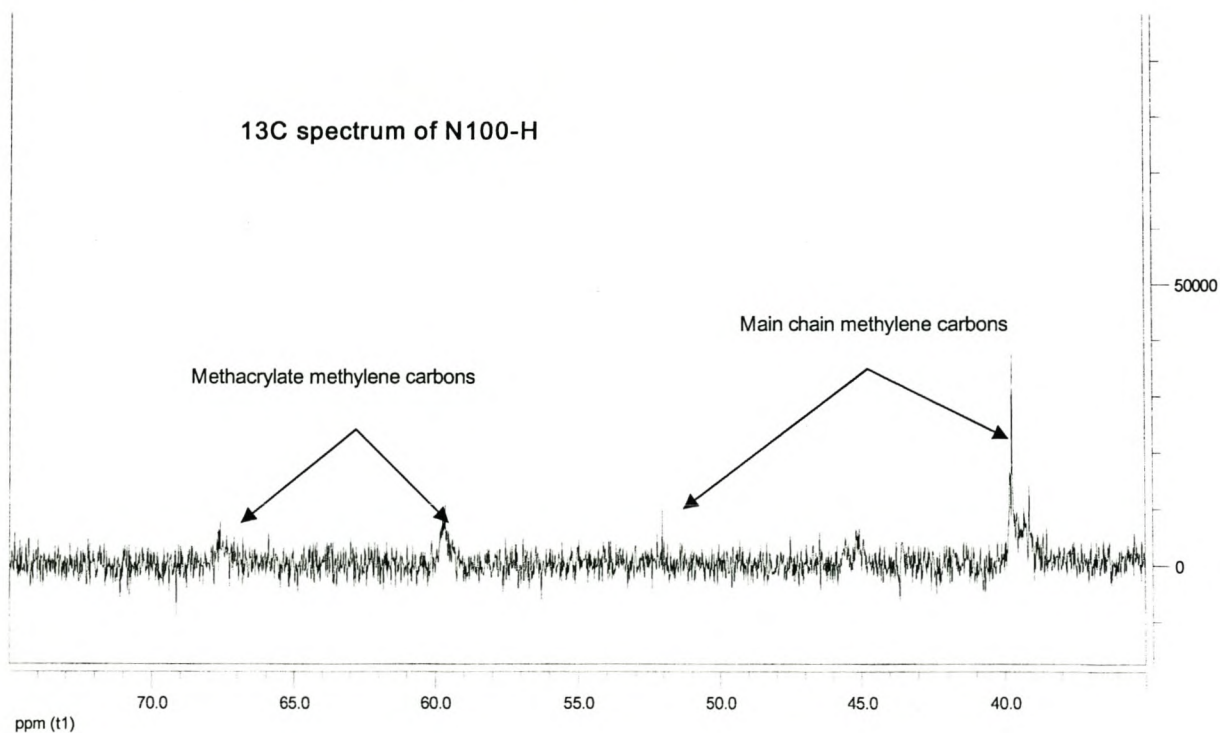


Table 5.10: Concentrations of double bond peaks relative to amide peaks for samples N100, N100-H, and N100-VP

Sample	Double bond	Amide
N100	3.05	1.00
N100-H	2.02	1.00
N100-VP	1.00	1.00

5.2.2.3 Crosslinking of N200

Table 5.11 gives the three molecular weight species with the highest concentrations that were found by means of ESMS for samples N200, N200-H, and N200-PV. The ESMS spectra can be viewed in Appendix 2.

Sample N200-H did not have high molecular weight chains. Due to the very high molecular weight chains present within the linear polyamide sample N200 (see section 5.1.2) the presence of high molecular weight chains was expected if crosslinking had occurred. There was, however, the possibility that these species were not detected, due to the detector which had only been calibrated up to 200 kDa, or because they had been filtered out by the 0.45 micron filter. Thus no conclusions could be drawn from the ESMS spectrum alone.

Table 5.11: The three molecular weight species present, with highest concentrations, for Sample N200 and its crosslinked products, Samples N200-H and N200-VP, as determined by ESMS.

N200		N200-H		N200-VP	
Molecular weight (kDa)	Peak intensity (%)*	Molecular weight (kDa)	Peak intensity (%)*	Molecular weight (kDa)	Peak intensity (%)*
191.0	100	58.3	100	138.5	100
166.0	67.6	43.9	87.7	152.9	76.5
31.9	49.4	48.7	66.7	140.0	74.1

* Calculated relative to the intensity of the highest peak

The ^{13}C NMR spectra of the linear polyamide sample N200 and that of the product from the HEMA crosslinking reaction, sample N200-H, were compared. These samples were not filtered during sample preparation. The spectra are shown in Appendix 1.

A comparison of the double bond concentrations, given in Table 5.12, showed that the double bond concentration in sample N200-H had decreased. In the ^{13}C spectrum of the supposedly crosslinked sample N200-H the methylene peaks of the methacrylate tails were found at $\delta 67$ and $\delta 59$ ppm, corresponding perfectly to the predicted values, and thus confirming the successful crosslinking of the polymer.

Table 5.12: Concentrations of double bond peaks relative to amide peaks for samples N200, N200-H, and N200-VP

Sample	Double bond	Amide
N200	3.00	1.00
N200-H	1.30	1.00
N200-VP	2.60	1.00

From the ESMS spectrum of sample N200, as shown in Figure 5.4, no species of molecular weights between 76 kDa and 166 kDa were originally found to be present in the polyamide, and thus the appearance of species in this region in sample N200-VP indicated the possibility that lower molecular weight chains had undergone crosslinking. The presence of very high molecular weight crosslinked chains could not be confirmed due to the limits of the detector, and because these may have been filtered out during sample preparation.

The relative double bond concentration of the N200-VP sample had been found to have decreased only slightly. This indicated that if crosslinking had occurred, it was only to a small degree. However, when the ^{13}C spectra of the two samples N200 and N200-VP were compared, the spectra were exactly alike and no evidence of crosslinking was found for sample N200-VP.

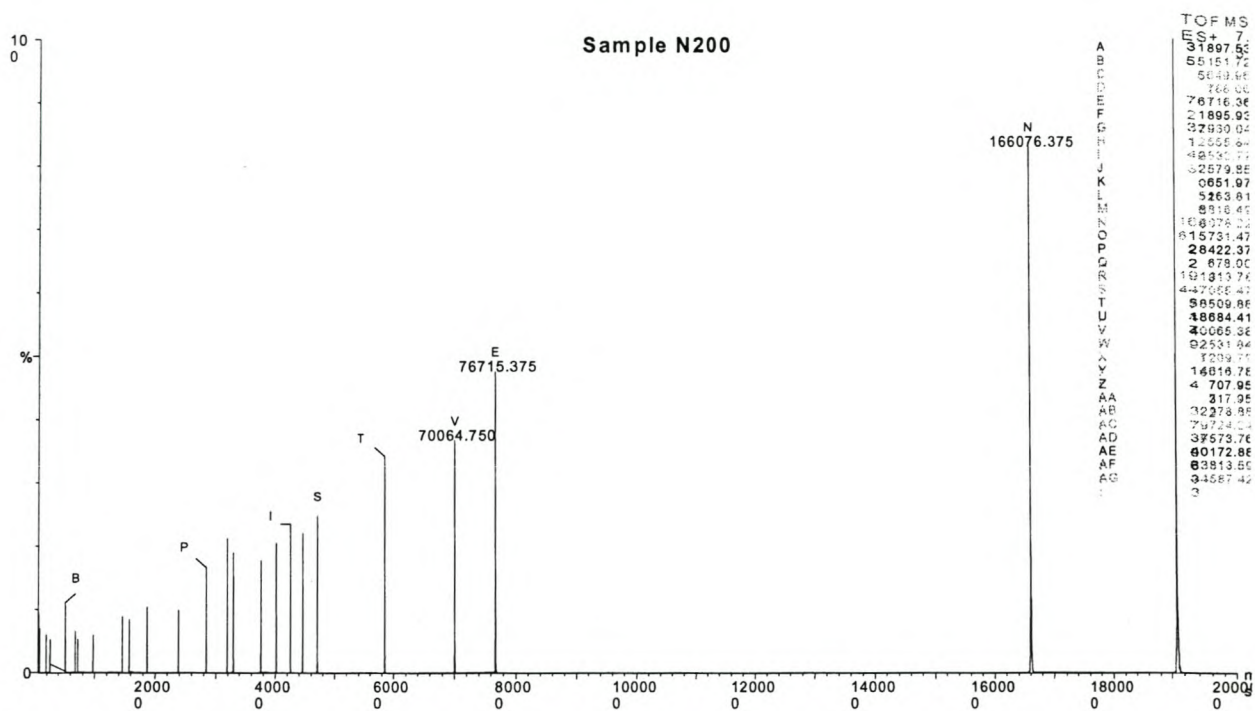


Figure 5.4: ESMS spectrum of sample N200, showing the absence of molecular weight species between 76 kDa and 166 kDa.

5.2.2.4 Summary

Almost all of the crosslinking reactions that were performed were found to have led to the formation of crosslinked polyamide samples when the data from ¹³C NMR and ESMS was taken into account.

The exceptions were the two crosslinking reactions that were attempted between the linear polyamide samples N50 and N200, and the vinyl monomer 4-VP. No conclusive evidence was found to support crosslinking in these reactions, and they were considered as being unsuccessful.

5.2.3 Particle formation

The intended outcome of the crosslinking experiments was the formation of hydrophilic polyamide particles, capable of swelling in water.

Light scattering, SEM, and Cryo-SEM was used to investigate the sizes of the particles and their swelling behaviour in aqueous medium. Particles sizes were determined for the four successfully crosslinked samples, namely N50-H, N100-H, N100-VP, and N200-H.

5.2.3.1. Light scattering

The particle diameters for each sample, as determined by light scattering, are listed in Table 5.13, along with the percentage of particles with similar diameter values. With the exception of sample N100-VP, the diameters of the swollen, crosslinked polyamide samples appear to fall within the nanometer range.

These results were further investigated by SEM and Cryo-SEM.

Table 5.13: Particle diameters and percentage of particles found for each particular diameter, as found for each of the successfully crosslinked polyamide samples.

N50-H		N100-H		N100-VP		N200-H	
Particle diameter (nm)	Percentage particles found	Particle diameter (nm)	Percentage particles found	Particle diameter (nm)	Percentage particles found	Particle diameter (nm)	Percentage particles found
72	13.5	107	18	1143	15.5	326	26
91	36.5	135	42	1439	39	411	50
115	34.5	170	31	1812	32	517	24
145	12.5	214	8	2282	8.5	Other	0
182	2	Other	1	Other	5		
Other	1						

5.2.3.2. SEM

SEM was used to investigate the dry crosslinked polyamide samples. Cryo-SEM was used to investigate the crosslinked polyamide samples when dispersed in water.

None of the images of the dry crosslinked polyamide samples, as shown in Figure 5.5, indicated the presence of any particles, which was in opposition to the findings of the light scattering experiment.

In the light scattering experiments, however, the samples had been dispersed in water, and thus it was Cryo-SEM was used to investigate the behaviour of the crosslinked samples in the dispersed state, to determine if this was different to the dry state. It was found that, for all the crosslinked polyamide samples except N50-H, the material was indeed in the form of particles when dispersed in water.

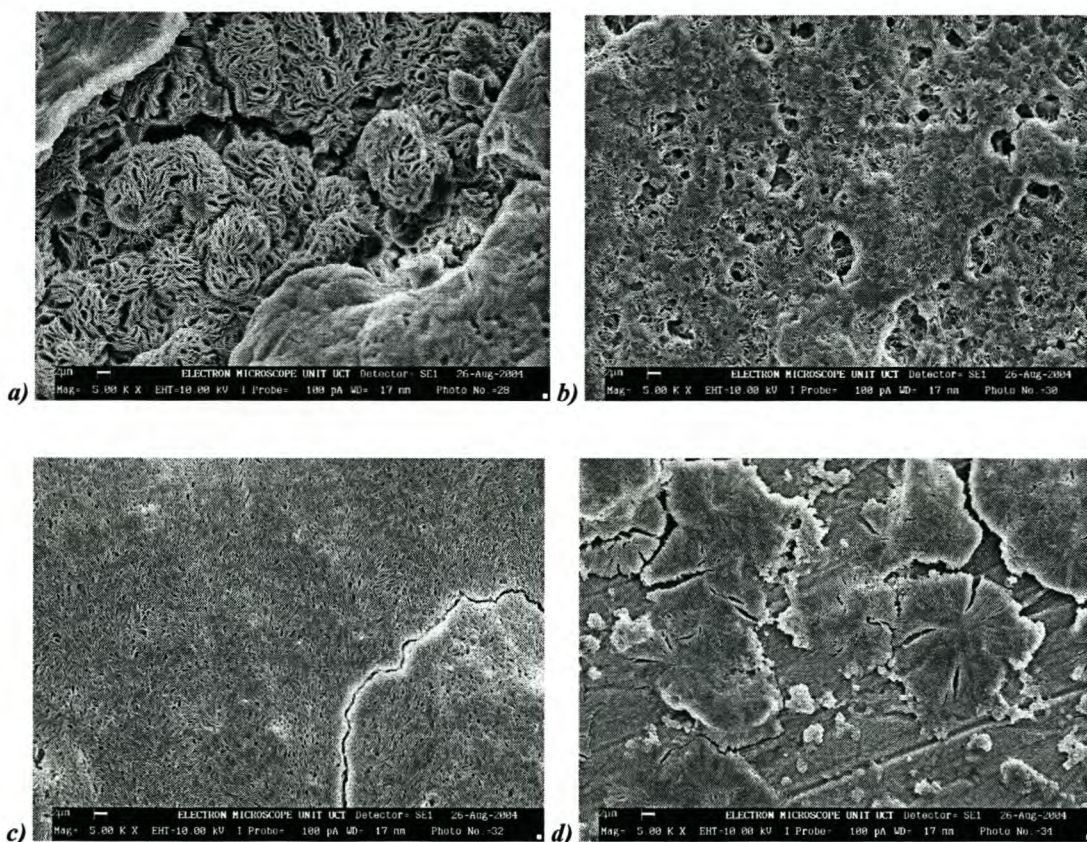


Figure 5.5: SEM photographs of the dry, crosslinked polyamide samples a) N50-H, b) N100-H, c) N100-VP, d) N200-H.

5.2.3.2.1 N50-H

Figure 5.6 are Cryo-SEM photos of sample N50-H. Figure 5.6.a is a view of the swollen sample (still containing frozen water), while Figure 5.6.b shows the sample after water

had sublimed off. It is clear that the sample is not made of particles. Instead, it appears that the sample is made up of long filaments that have intertwined to form a swollen, three-dimensional network. This is similar to the effect that is seen in the SEM photograph of the dry sample (see Figure 5.5.a).

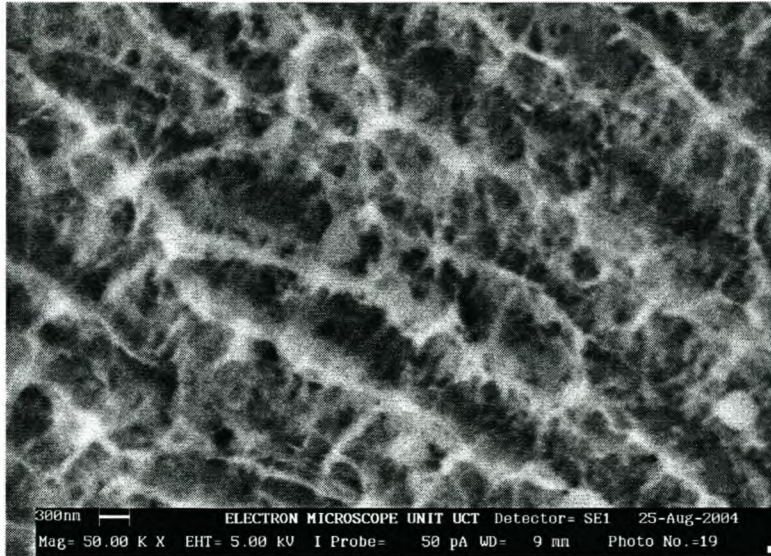


Figure 5.6.a: SEM view of frozen polyamide sample N50-H containing water.



Figure 5.6.b: SEM view of polyamide sample N50-H after sublimation of water has occurred.

After sublimation the network is not visible, and it appears as if the polymer has formed a film with holes in it.

This effect is misleading. The dark spots are, in fact, areas of similar functionality that interact differently with the electron beam of the microscope than the surrounding material, thus leading to the appearance of dark spots.

Cryo-SEM photographs therefore show that the formation of particles was not successful for the sample N50-H.

5.2.3.2.2. N100-H

From the Cryo-SEM photographs of the polyamide sample N100-H it was found that the polymer was definitely in the form of particles.

Light scattering indicated that most particles present were in the range of 100 – 200 nm in diameter, with a small percentage of particles present with diameters between 1 – 2 μm . Cryo-SEM confirmed the presence of the nano-sized particles, but showed that the large micrometer sized particles were in fact conglomerations of unseparated nano-particles. Figure 5.7 is a Cryo-SEM photograph of sample N100-H, still containing water. The conglomerates are clearly visible, as well as the nano-particles that they are made up of.

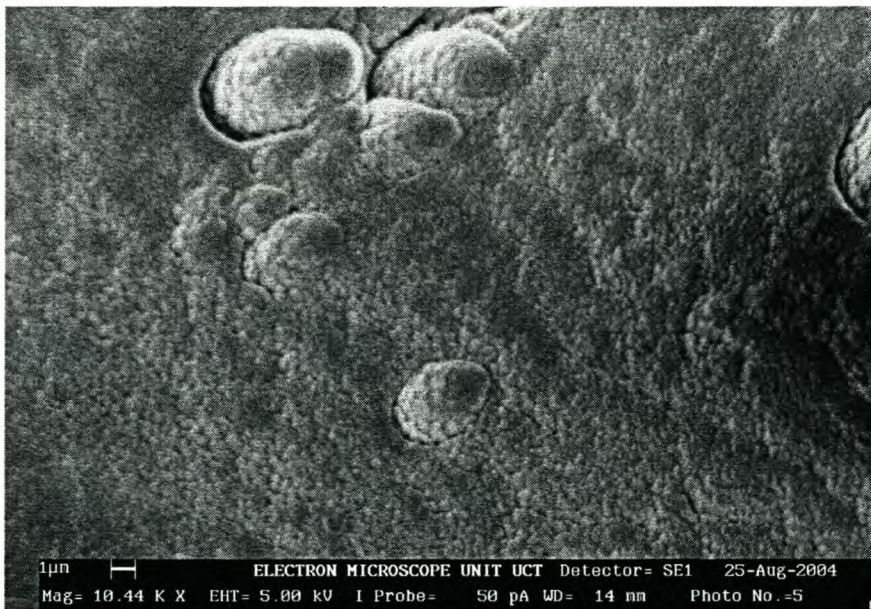


Figure 5.7: SEM photograph of N100-H showing the particles, as well as the micrometer sized conglomerates made up of clusters of nano-sized particles.

5.2.3.2.3. N100-VP

Cryo-SEM confirmed that sample N100-VP consisted of particles.

Light scattering indicated the presence of a large percentage of particles with diameters of 1 to 2 μm . The presence of a small percentage of particles with diameters between 4 and 10 μm were also indicated.

Cryo-SEM, however, showed that the light scattering results were incorrect. The sample was, in fact, made up of nano-sized particles, between 70 and 130 nm in size. The large particles identified by light scattering were conglomerates of unseparated nano-sized particles. Presumably, these particles were too small in comparison with the large conglomerates and were thus not detected by the light scattering instrument.

Figure 5.8 is a Cryo-SEM photograph of sample N100-VP, showing a group of conglomerates of various sizes. It is clear that these conglomerates consist of clusters of nano-sized particles.

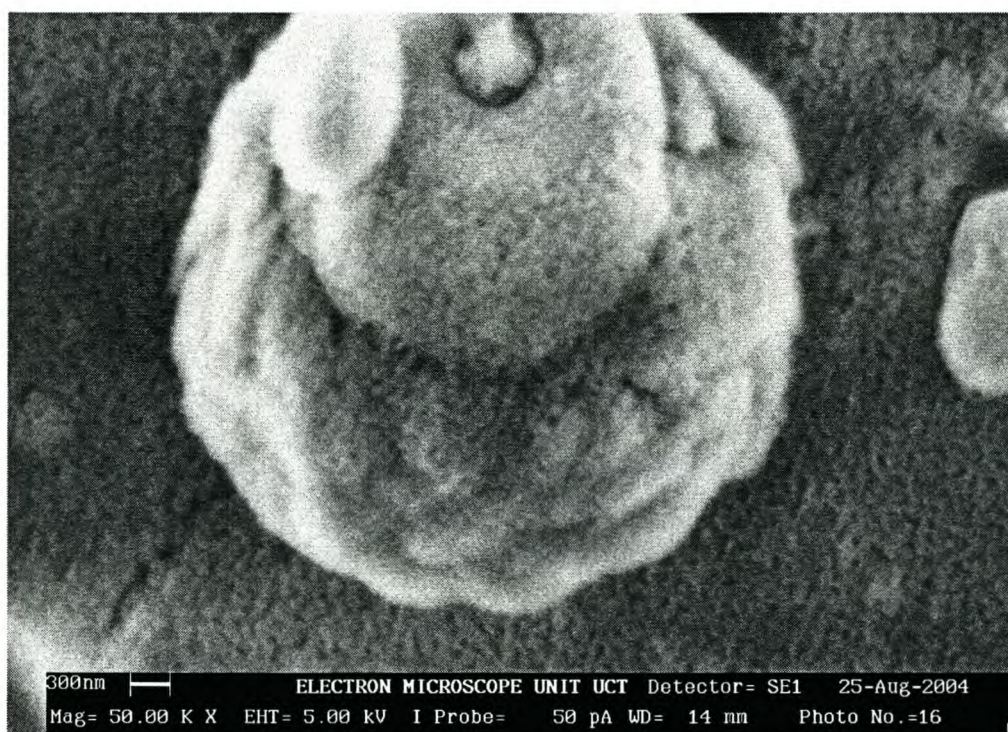


Figure 5.8: SEM photograph of N100-VP showing conglomerates consisting of nano-sized particles.

5.2.3.2.4. N200-H

Cryo-SEM confirmed that sample N200-H consisted of densely packed, nano-sized particles.

The light scattering measurements had indicated the presence of particles with diameters between 200 and 500 nm. The Cryo-SEM results, however, indicated that these measurements were incorrect – the particles were, in fact, found to be 150 nm in diameter on average. Figure 5.9 shows a Cryo-SEM photograph of sample N200-H, with the measured diameters of two of the particles indicated.

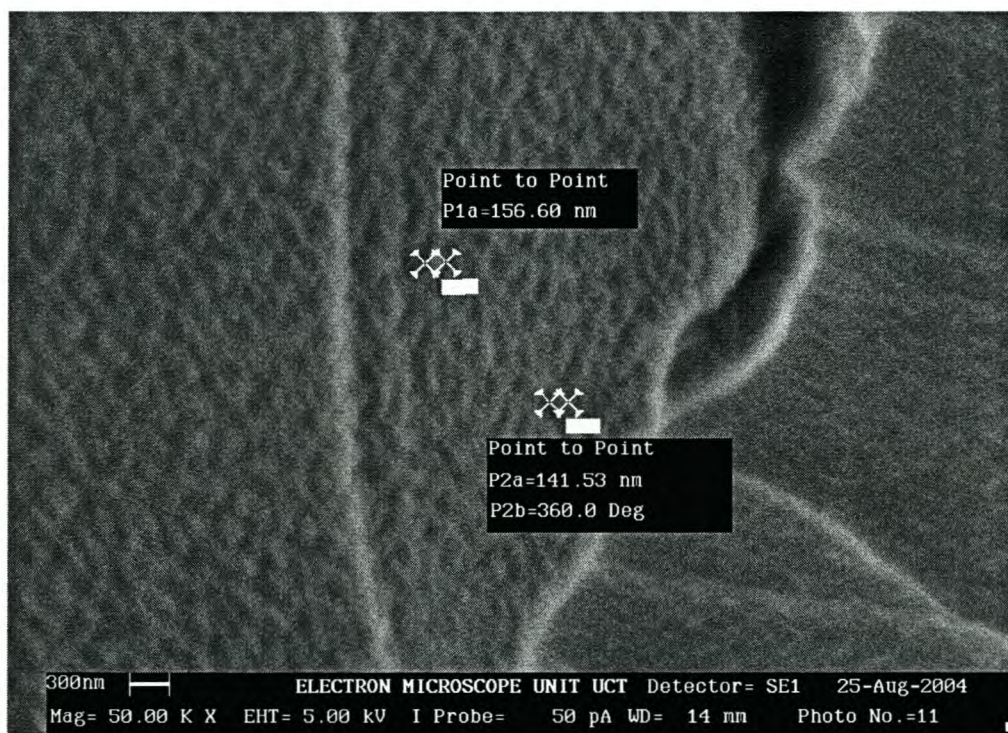


Figure 5.9: SEM photograph of N200-H, showing the measured sizes of particles.

5.2.3.3. Summary

The four successfully crosslinked samples, namely N50-H, N100-H, N100-VP, and N200-H were investigated by SEM and light scattering to determine whether particle formation had occurred during the synthesis.

With the exception of sample N50-H, the crosslinked polyamides were found to form particles when dispersed in water, although the dry samples were not in the form of particles. The emulsion technique used during the crosslinking reactions, as described in section 3.3.2.2, was thus proven to be successful for the formation of particles.

5.2.4 Paper coated with crosslinked polyamide particles

Crosslinked polyamide sample N200-H was chosen for the coating of the paper samples to be used for further testing. This crosslinked polymer showed uniform particle size, and completely dispersed in water without the formation of conglomerates.

The printed paper samples were investigated for wet-rub resistance, as well as printing quality, colour density, and colour uniformity.

5.2.4.1 Printing quality, colour density and uniformity

Formulations with PVOH

Formulations 1 to 5 contained PVOH. When these samples were compared with respect to printing quality, colour density and colour uniformity it was found that the paper coated with formulation 2 gave the best results in all three categories.

Formulation 2 contained 0.1% crosslinked polyamide particles and 4.9% silica (see Table 4.2).

Formulations without PVOH

Formulations 6 to 10 were those formulations that did not contain PVOH. Upon comparison of the printed paper samples of these five formulations, it was found that the paper sample coated with Formulation 6 was the best in all three areas of printing quality, colour density, and colour uniformity.

Formulation 6 contained 5% silica, with none of the crosslinked polyamide sample added (see Table 4.2).

Comparison of Formulations 2 and 6

Upon comparison of the two best formulations identified above, it was found that neither of the formulations gave superior performance in all three categories.

Formulation 6 was found to be superior with regards to printing quality, while Formulation 2 was found to be superior in colour density and colour uniformity.

Figure 5.10 shows part of a printed image on a paper sample coated with Formulation 2. Only half the image was printed on the coated part of the paper, with the top corner having been printed on an uncoated area. It is clear that the coated area shows increased colour density and uniformity.

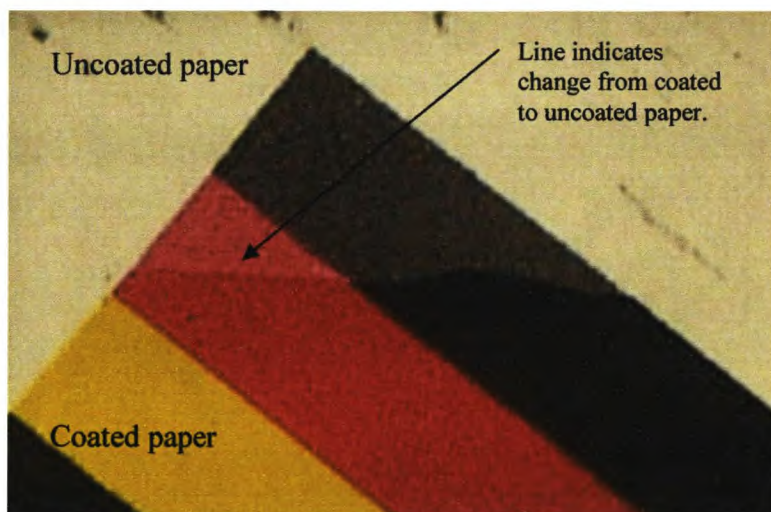


Figure 5.10: Image printed on a paper sample partially coated with Formulation 2.

5.2.4.2 Wet-rub test

The wet-rub test showed that the formulations without PVOH showed the least resistance to rubbing. However, the wet-rub resistance of the paper samples improved as higher percentages of the polyamide particles were present in the coating.

The formulations that contained PVOH also showed improved wet-rub resistance with increased percentages of crosslinked polyamide.

The crosslinked polyamide was therefore shown to act successfully as a binder between the paper surface and the silica pigment.

5.2.4.3 Summary

The comparisons of the different formulations with regards to printing quality and colour density and uniformity led to the identification of two of the formulations as giving excellent results. These formulations were Formulations 2 and 6.

However, when the results of the wet-rub test were taken into account, it was found that Formulation 6 had very little wet-rub resistance. Formulation 2, which is given in Table 5.14, was thus identified as the sample which gave the best overall performance, both in terms of wet-rub resistance and printing performance.

Table 5.14: Ingredients of Formulation 2, as given in parts per hundred.

Ingredient	Parts per hundred
Crosslinked polyamide (N200-H)	0.1
Silica HP39	4.9
Water	17
PVOH (10% solution)	50
BYK 333	0.2
Laponite JS (18% dispersion)	27.8

Chapter 6:

Method considered for the quantitative determination of printing quality

6.1 Introduction

The printing quality of a specific paper product is one of the important factors that consumers consider when faced with the choice of various paper products. Determination of printing quality is currently based on only a visual comparison of printed paper samples. There is as yet no quantitative method for determining printing quality, and no absolute standard is available. Consumers thus have to rely on subjective opinions when comparing the performance of different products.

For the purposes of scientific study the absence of a quantitative method which measures printing quality is also a distinct disadvantage. The development of a technique whereby printing quality may be measured, and standardized, has therefore become a necessity.

6.2 Geographical Imaging Systems technology

Geographical Imaging Systems (GIS) technology has been developed in the past 10 years as a research, analysis, and management tool in the geographical sciences. The technology consists of a computer system which is used specifically for the assembly, storage and manipulation of geographical information, often received in photographic form. The software used in GIS is ArcView GIS 3.2, and has been specifically designed to separate, store, and analyse various layers from photographic and other sources.

GIS technology makes it possible to separate different colour layers in a photographic or other image, enabling the user to:

- Determine relative image sizes.
- Determine the percentage colour visible in blends of different colours.
- Study colour transitions areas where different colours meet and blend.

6.3 Paper Application

By making use of the latter application, I thought it would be possible to apply the GIS technology for the very first time to an investigation of the ink colour boundaries of a printed image. This would enable a quantitative determination of the printing quality by an investigation of the degree of ink bleeding and the sharpness of the transition from one colour to the next.

In this chapter I describe attempts made to create a method whereby printing quality may be determined as a quantitative value, by investigating the boundary area where two different ink colours meet in a printed image.

6.4 Method

- 1) A test pattern containing the primary printing colours magenta, cyan, yellow, and black, was printed on a coated paper sample with a desk-top ink jet printer.
- 2) The printed test image was scanned into a computer using a desk-top electronic scanner. The pages were flattened against the scanner surface to achieve the maximum contact area, which minimized interference from folds and other physical characteristics of the paper surface.
- 3) A boundary area between two different colours was selected and saved as a BITMAP image in Microsoft Photo Editor, after which Corel Photo Paint 9 was used to separate the saved image into layers of cyan, magenta, yellow, and black. These layers were then saved as BITMAP images.
- 4) The GIS software was used to create fine grids on the saved BITMAP images. The image layers were now composites of small cells. Each cell was assigned a numerical value according to its colour intensity, and the combined values made up the value range of each image layer.
- 5) The value ranges of the layers were subtracted from each other, and the resultant range stored in an Excel spreadsheet. The Excel file contained two columns which were

labelled “value” and “count”. The “value” column indicated the colour intensity assigned to a specific cell, and the “count” column gave the number of cells present with the same assigned “value” (or colour intensity).

6) The negative values were chosen to represent one of the two colours, and the positive values thus represented the second colour. The assignment was made on an arbitrary base, but to ensure consistency the order of subtraction in the previous step was always the same. As the two ink colours bled into each other in the printed image, it was found that the sum of the resultant value range, as created in step 5, approached zero. This made it possible to identify the area which was made up of a mixture of the two colours.

7) The values in the Excel sheet could now be used to draw a graph which gave information as to the actual breadth of the boundary between the two ink colours, and the sharpness of the change from one colour to the next.

Figure 6.1 shows a typical graph obtained by the above method for the boundary area of two colours, called colour 1 and colour 2.

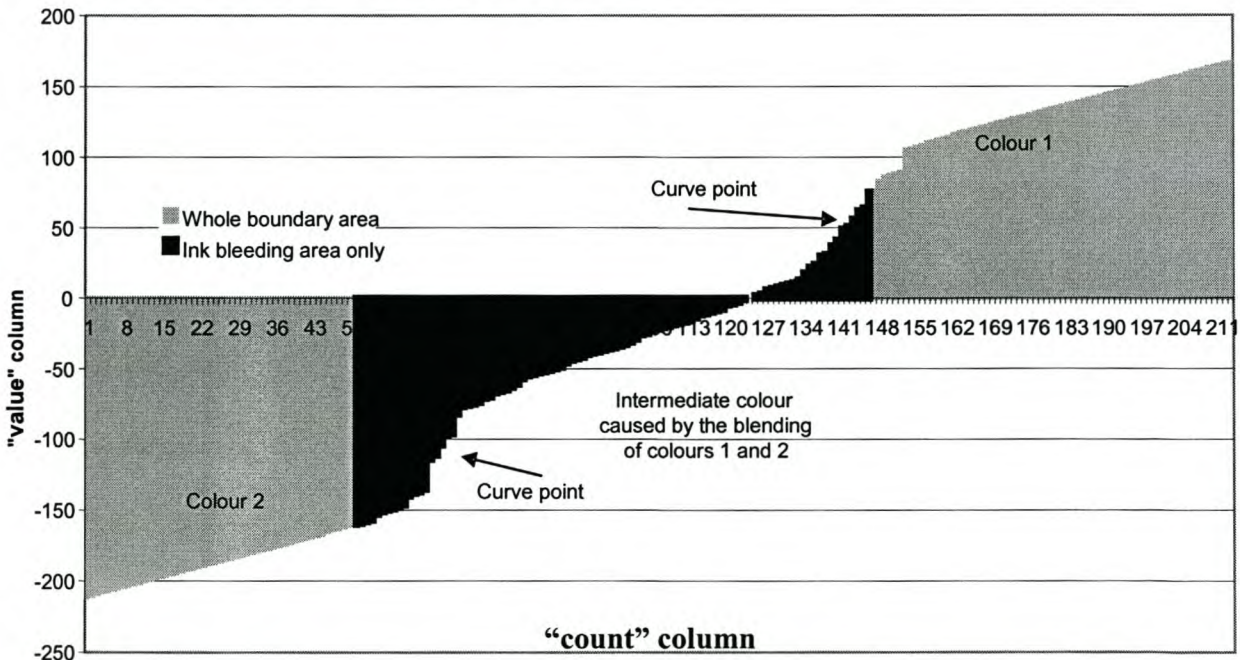


Figure 6.1: Graph of the “value” column containing the values assigned to the cells of the boundary area between two colours in a printed image, as printed on a standard paper sample.

If there is a lot of bleeding between the two ink colours, the boundary area will be very large and undefined. The gradient of the graph will be slight and the curve points will not be sharp. The distance between the curve points indicate the relative size of the area in which ink bleeding occurred.

If there is very little bleeding between the two ink colours the boundary area will be sharp and well defined. The graph of the gradient will be steep, and the curve points will be sharp, indicating abrupt colour changes. The distance between the two curve points will be less compared to a sample with more ink bleeding.

6.5 Experimental work

This work was done in collaboration with the GIS Lab at the Department of Geography and Environmental studies at the University of Stellenbosch. All computer work was performed by a GIS specialist.

In order to investigate the above method, a number of different coating formulations containing Laponite JS and Kaolin in different concentrations were prepared (see Table 6.1).

Table 6.1: Coating formulations prepared during development of GIS method.

Formulation	Laponite JS (%)	Kaolin (%)	PVOH* (%)	Water (%)
Kaolin1%_Lap1%	1	1	50	48
Kaolin1%_Lap2%	2	1	50	47
Kaolin1%_Lap3%	3	1	50	46
Kaolin2%_Lap1%	1	2	50	47
Kaolin3%_Lap1%	1	3	50	46

* 10% solution

The prepared formulations were coated onto standard printing paper with a laboratory draw-down coating machine. A 24 μm wire bar was used, and the coater was set at a

speed setting of 6. The coating formulation was applied to the coating bar manually, using a plastic pipette.

After the samples had been allowed to dry for 24 hours a test image was printed on the coated paper samples with a colour, desk-top ink-jet printer. The samples were then analyzed with the GIS software. An uncoated paper sample, named Rota-trim, was also printed and analyzed for comparative purposes.

6.6 Results

6.6.1 Ink-boundary between magenta and yellow ink colours

Figure 6.2 shows the graphs that were drawn with Excel from the information of the magenta/ yellow ink colour boundaries of the five different coated paper samples analyzed with the GIS technique, including the standard, uncoated sample.

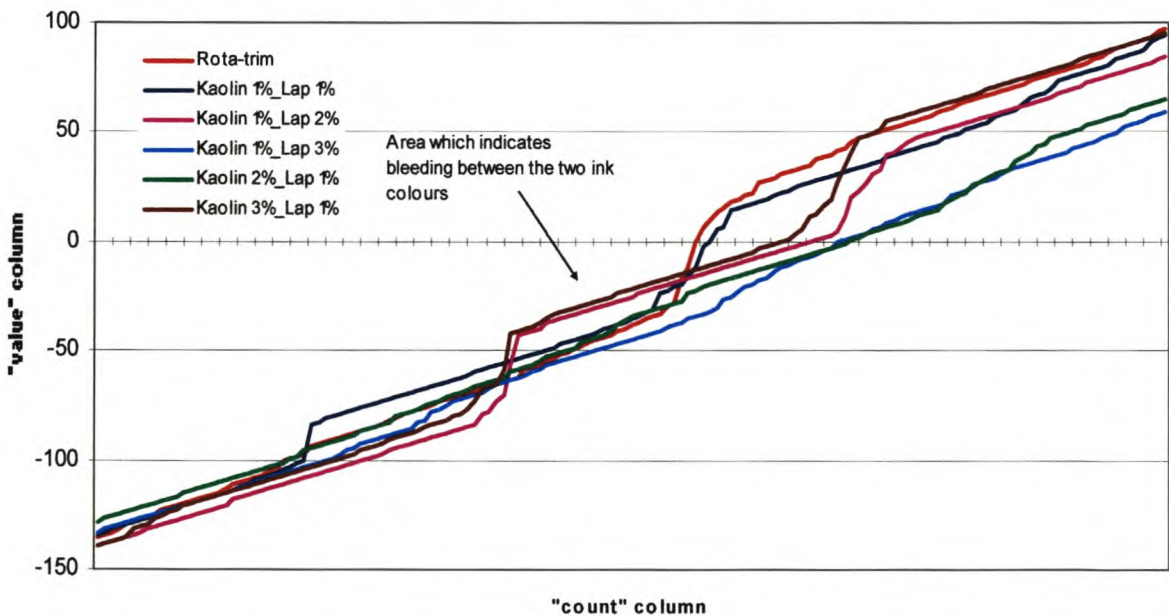


Figure 6.2: Magenta/ yellow ink colour boundaries for different coated paper samples that were analyzed.

The uncoated sample (red graph) showed a single sharp curve point (or gradient change), indicating a sharp and well-defined boundary between the two ink colours.

The Kaolin1%_Lap1% sample (dark blue graph) appeared to show a sharp curve point, but on closer examination a second curve point was located below the x-axis. The graph

of the sample thus showed two curve points, indicating the presence of three colours (or two colour boundaries). On visual inspection the third colour was found to be the intermediate colour created by the bleeding and blending of the yellow and magenta inks.

The distance between the curve points gave an indication of the size of the boundary area, which was relatively large when compared with the graphs of the other samples.

The samples Kaolin1%_Lap2% (pink graph) and Kaolin3%_Lap1% (brown graph) both showed two sharp curve points, indicating that three colours were present in these two samples. This was confirmed through visual observation. The three colours were identified as yellow, magenta, and an intermediate colour caused by the blending of the two inks at the boundary area. The sharpness of the gradient changes indicated well-defined boundaries.

The distances between the curve points were less than for the Kaolin 1%_Lap 1% sample, indicating that the boundary areas were relatively smaller than in this sample.

The two samples Kaolin1%_Lap3% (light blue graph) and Kaolin2%_Lap1% (green graph) did not show any curve points. This indicated that the two ink colours in these samples had bled so much that the software did not recognize the presence of different colours; it only recognized a single intermediate colour. These results correlated very well with a visual inspection of the samples.

6.6.2 Comparison with Visual Observation

Using the GIS technique, sample Kaolin1%_Lap2% was identified as having the sharpest and smallest ink boundary of the samples that were analyzed. This compared excellently with visual observation, which identified the above-mentioned sample as being one of the top three samples. The other two samples that were considered satisfactory, as determined by visual observation, were Kaolin1%_Lap1% and Kaolin3%_Lap1%. These were also identified by GIS as being good samples due to the distinct curve points.

These results indicated that there had definitely been a degree of success with the method development. However, as mentioned before the work was done in collaboration with a

GIS specialist at the Department of Geography and Environmental studies at the University of Stellenbosch. Unfortunately this person finished their period of employment before the method could be developed further, and no suitable replacement operator could be found to continue the work that had been started.

6.7 Disadvantages

The GIS ArcView software is complex, and intensive training is needed to operate the program correctly. The assistance of a suitably trained and dedicated operator is therefore a necessity.

The application is novel and unknown, and thus the operator would need to understand the work required and have insight into the software challenges and requirements of the application in order to address any needs or problems that may arise.

6.8 Conclusion

A method was developed by which it was possible to assign numerical values to printed images, and use these to draw graphs which give information on the sharpness of the transition between ink colours.

Unfortunately the software is complicated and not suitable for use by an untrained person and an operator is needed for the analyses. The knowledge and initiative of the operator is important for the successful development and utilization of the technique, making the technique operator dependent. The identification and determination of the necessary requirements for such an operator fell outside the scope of this research study.

Chapter 7: Conclusions and Recommendations

7.1 Conclusions of this study

1) For the purpose of this study, the unsaturated linear 2,6-polyamide was identified as a suitable organic, hydrophilic polymer, containing cationic functionality and unsaturation. It was later crosslinked with a vinyl monomer, either HEMA or 4-VP, to produce hydrophilic, water swellable particles.

The material had the following characteristics and advantages:

- The amide group which imparts hydrogen bonding sites and subsequent hydrophilicity.
- The amide group which provides anionic bonding sites.
- It offered the possibility of synthesizing controlled molecular weight, unsaturated, linear polymers.
- There is a wide range of vinyl monomers available that could be used to crosslink this unsaturated linear polyamide by free-radical polymerization, to form particles.

2) Linear pre-polymer chains of the 2,6-polyamide were successfully synthesized by a phosphorylation condensation reaction involving the difunctional monomers 1,6-hexanediamine and fumaric acid. The polymer was characterized in terms of structure and molecular weight by means of ^{13}C NMR and ESMS techniques, respectively, providing proof of the success of the polymerization reactions.

3) Successful crosslinking of the 2,6-polyamide was achieved by the use of a free radical reaction involving the unsaturation in the linear polyamide backbone and one of two vinyl monomers, namely HEMA or 4-VP. The presence of the successfully crosslinked polyamide was confirmed structurally with ^{13}C NMR, and an increase in the molecular weights from the linear to the crosslinked polyamide product was observed with ESMS.

SEM and light scattering experiments proved that the crosslinked polyamide samples formed swollen particles when dispersed in water. The diameters of the particles were found to be in the nanometer range.

4) Formulations were prepared from one of the crosslinked polyamide samples, and coated onto starch-sized base paper. The polyamide chosen showed uniform particle size, and did not form conglomerates. Formulations were prepared with, and without, PVOH, and the silica pigment was replaced with the crosslinked particles.

The coated paper samples were printed with a desk-top ink-jet printer.

5) The coated, printed paper samples were tested for wet-rub resistance and compared in terms of printing quality, colour density, and colour uniformity.

Wet-rub resistance was shown to improve with increasing percentages of the crosslinked polyamide present in the formulations for the crosslinked polyamide sample N200-H. The crosslinked polyamide was thus capable of acting as a binder in the coating formulations.

Formulation 2, containing 0.1% crosslinked polyamide N200-H, was identified as the best sample in terms of colour density and colour uniformity. The printing quality of this product was equal to that of the product with no crosslinked polyamide polymer added. The crosslinked polyamide N200-H was thus found to:

- Improve wet-rub resistance
- Improve colour density
- Improve colour intensity
- Equal printing quality

7.2 Recommendations for future work

The crosslinked polyamide products were shown to have the ability to act as binders between the pigment and the paper surface. Further investigation into the binding strength and ability of these crosslinked polyamide polymers are therefore warranted.

The effect of the crosslinked polyamide product N200-H on the colour density and colour uniformity of a printed paper sample is good cause for further investigation of this product as a partial replacement for silica in ink-jet printing applications.

A last recommendation is the further investigation into the development of GIS technology, which may be used as a quantitative measure of printing quality.

Chapter 8:

References

- (1) Glittenberg, D.; Voight, A. 11 March 2004. *Printing and Coating: How to improve ink-jet papers*. Accessed 11 March 2004. Website. Available from http://www.paperloop.com/db_area/archive/ppi_mag/2004/01/05.html.
- (2) Lyne, M. B.; Aspler, J. S. *TAPPI* 1985, 68, 106-110.
- (3) Yamazaki, N.; Higashi, F. *Advances in Polymer Science* 1981, 38, 1-25.
- (4) Donigian, D. W.; Wernett, P. C.; McFadden, M. G.; McKay, J. J. *TAPPI* 1999, 82, 175-182.
- (5) Becker, D.; Kasper, K. *Rundbrief Fotografie* 1998, 3, 10-14.
- (6) Ryu, R. Y.; Gilbert, R. D.; Khan, S. A. *TAPPI* 1999, 82, 128-134.
- (7) Oliver, J. F. *TAPPI* 1984, 67, 90-94.
- (8) Hladnik, A.; Muck, T. *Dyes and Pigments* 2002, 54, 253-263.
- (9) Harper, D. T. *Paper Coatings*; Noyes Data Corporation: Park Ridge, 1976; Vol. 1.
- (10) Boylan, J. R. *TAPPI* 1997, 80, 68-70.
- (11) Becker, D.; Dransmann, G.; Kasper, K.; Quarts, W.; William, D. R. 1995. *DE Patent No. A 4322178*
- (12) Kijimuta, H.; Suzuki, S. 1995. *EP Patent No. A 0634287*

- (13) Dransmann, G.; Juenger, C.; Westval, H. 1997. *DE Patent No. A 0806299*
- (14) Sato, H.; Suzuki, S. 1996. *JP Patent No. 8282088*
- (15) Sumita, K. 1990. *JP Patent No. 2276670*
- (16) Kote, K. 2000. *JP Patent No. 2000-108501*
- (17) Sumita, K.; Suzuki, S. 1993. *JP Patent No. 5024336*
- (18) Kinoshita, S.; Miyaji, N.; Tokunaga, Y. 2003. *JP Patent No. 2003-48639*
- (19) Ferrar, W. T.; Bugner, D. E.; Romano, C. E. 1997. *US Patent No. A 5605760*
- (20) Hetzler, K. G.; McCormack, A. L. 1996. *US Patent No. WO-A 9619346*
- (21) Schreader, L. R.; Warner, D. 1999. *US Patent No. WO-A 9907588*
- (22) Hill Jr, C. T.; Pekala, R. W. 2000. *US Patent No. A 6020058*
- (23) Dubouchet, C.; Benassi, G.; Gillet, M.; Pinchard, G. 2000. *BE Patent No. A 1012087*
- (24) Burns, E. G.; Dicillo, J.; Shaw-Klein, L. J. 2000. *US Patent No. A 0995611*
- (25) van der Velden-Schuermans, B.; De Vries, I. 2002. *USA Patent No. WO 02/053391 A1*
- (26) Sheth, P. J. 1988. *US Patent No. A 0283200*
- (27) Leatherman, D. D.; Young, J. 1989. *US Patent No. A 4861644*
- (28) Hoge, W. H. 1982. *US Patent No. A 4350655*

- (29) Leatherman, D. D.; Schwarz, R. A.; Leigh, T. H. 1989. *US Patent No. A 4833172*
- (30) Silenius, P. 1999. *EP Patent No. 09609130 A2*
- (31) Conley, D. P.; Looock, G. W.; Preston, B. W.; Withiam, M. C. 1999. *USA Patent No. WO 9957059 A1*
- (32) Chen, T.; Chu, L.; Sasasivan, S.; Gallo, E. A.; Wang, X. 2002. *USA Patent No. 2002155260 A1*
- (33) Sharma, K.; Bermel, A. D.; Bringly, J. F.; Landry-Coltrain, C. 2004. *USA Patent No. 2004001925 A1*
- (34) Wexler, A. 2002. *EP Patent No. 1184195 A2*
- (35) Wexler, A. 2002. *EP Patent No. 1184194 A2*
- (36) Chu, L.; Chen, T. 2001. *US Patent No. 1132217 A1*
- (37) Reiko, K.; Masanori, N.; Toyoaki, S.; Nishishinjuku, A. J. 1995. *EP Patent No. 0659779 A2*
- (38) Asao, K.; Morita, H.; Onishi, H.; Kimoto, M.; Yoshioka, Y.; Saito, H. 2002. *EP Patent No. 1182229 A1*
- (39) Craun, G. P.; Kaminski, V. V. 1996. *USA Patent No. 5576360*
- (40) Braun, D.; Cherdron, H.; Kern, W. *Section 4.1 Polycondensation, In Techniques of Polymer Syntheses and Characterization; Wiley-Interscience Vol. 1, pp 197-240.*

- (41) Imohl, W. *Section 3.3 Polyamide Resins*, In *Ullmann's Encyclopaedia of Industrial Chemistry*; Elvers, B.; Hawkins, S.; Schulz, G., Eds.; VCH Publishers, 1992; Vol. A23, pp 105-110.
- (42) Kohan, M. I. *Polyamides*, In *Ullmann's Encyclopaedia of Industrial Chemistry*; Elvers, B.; Hawkins, S.; Schulz, G., Eds.; VCH Publishers, 1992; Vol. A21, pp 179-205.
- (43) Stofberg, D. L., 1995. Synthesis of polyamides from monomers derived from Furfural. M.Science Thesis, University of Stellenbosch, Stellenbosch.
- (44) Sachindrapal, P.; Nanjan, M. *Journal of Polymer Science: Polymer Chemistry Edition* 1983, 21, 2301-2309.
- (45) Sachindrapal, P.; Nanjan, M. *Journal of Polymer Science: Polymer Chemistry Edition* 1984, 3705-3713.
- (46) Ozawa, M.; Li, J.; Nakahara, K.; Xiao, L.; Sugawara, H.; Kitazawa, K.; Kinbara, K.; Saigo, K. *Journal of Polymer Science: Part A: Polymer Chemistry* 1998, 36, 3139-3146.
- (47) Diakoumakos, C. D.; Mikroyannidis, J. A. *European Polymer Journal* 1995, 31, 761-767.
- (48) Bottino, F.; Di Pasquale, G.; Scalia, L.; Pollicino, A. *Polymer* 2001, 42, 3323-3332.
- (49) Hsiao, S.-H.; Yang, C.-P. *Journal of Polymer Science: Part A: Polymer Chemistry* 1990, 28, 1149-1159.
- (50) Simionescu, M.; Marcu, M.; Cazacu, M. *European Polymer Journal* 2003, 39, 777-784.

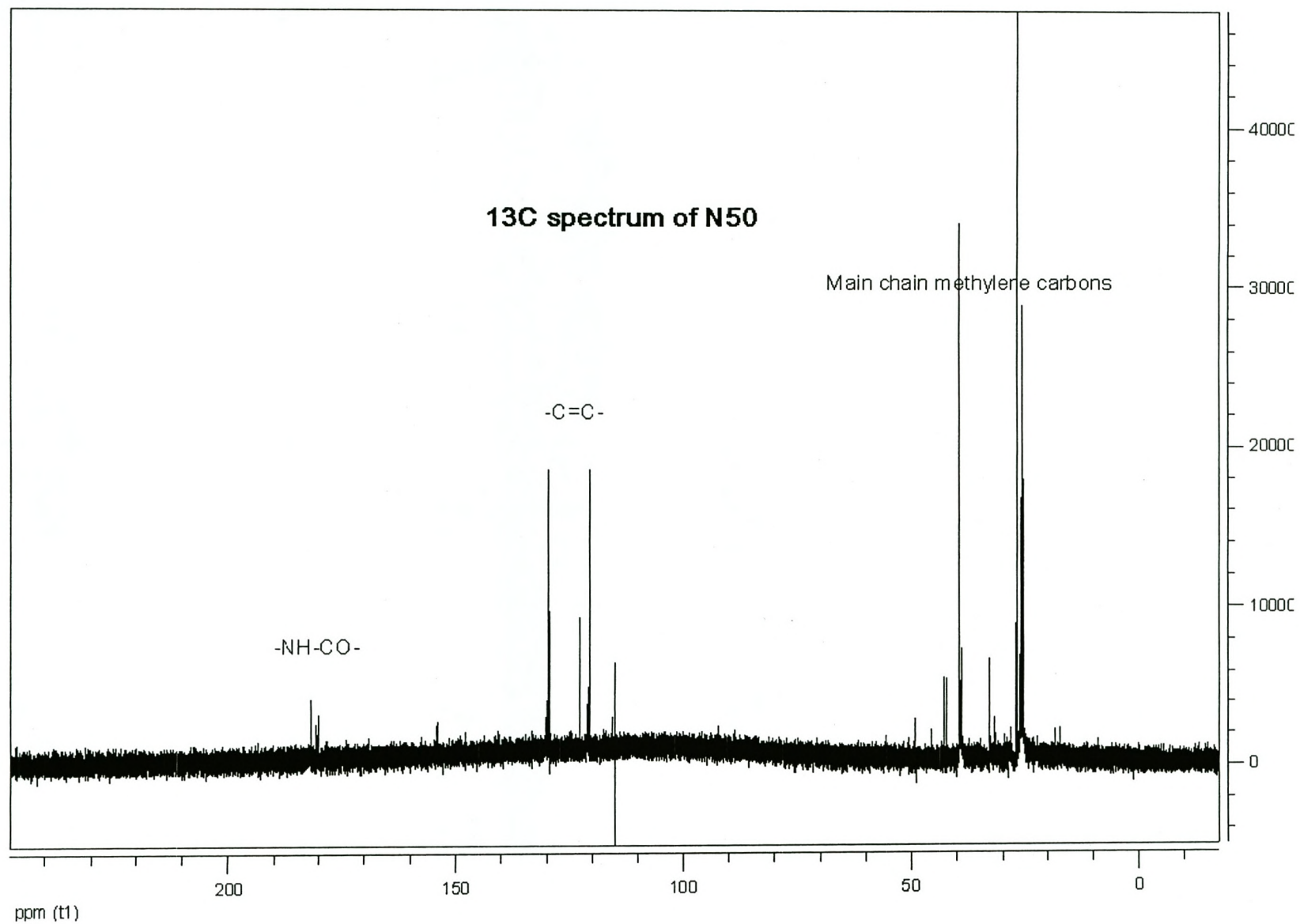
- (51) <http://www.glymes.com/proglyme.php>. Accessed 14 June 2004. Website.
- (52) You, Y.-C.; Jiao, J.-l.; Li, Z.; Zhu, C.-Y. *Journal of Applied Polymer Science* 2003, 88, 2725-2731.
- (53) Ni, C.; Wang, Z.; Zhu, X. X. *Journal of Applied Polymer Science* 2004, 91, 1792-1797.
- (54) McEwan, C. N.; Simonsick Jr, W. J.; Larse, B. S.; Ute, K.; Hatada, K. *Journal of the American Society for Mass Spectrometry* 1995, 6, 906-911.

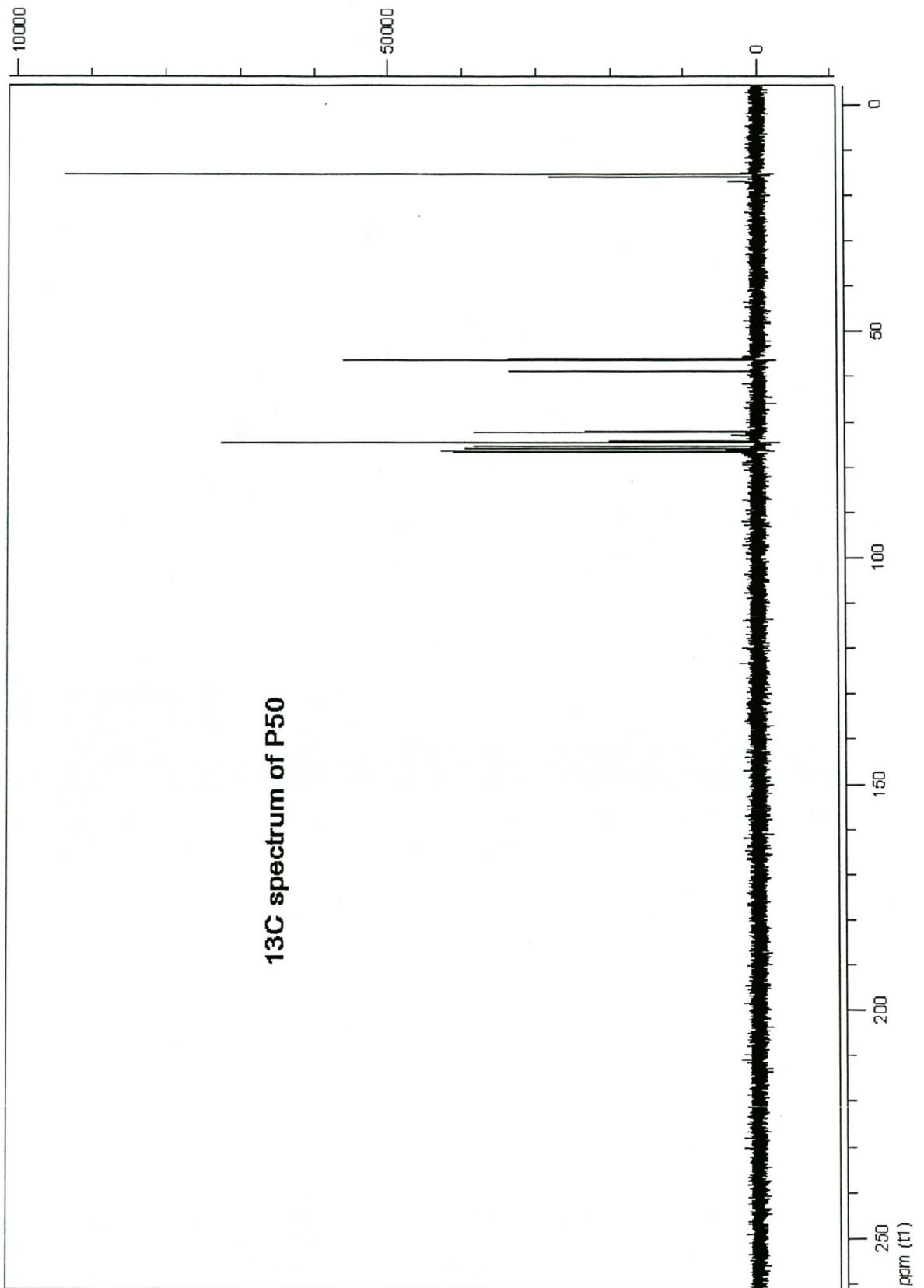
Appendix 1: ^{13}C NMR Spectra of polymers produced

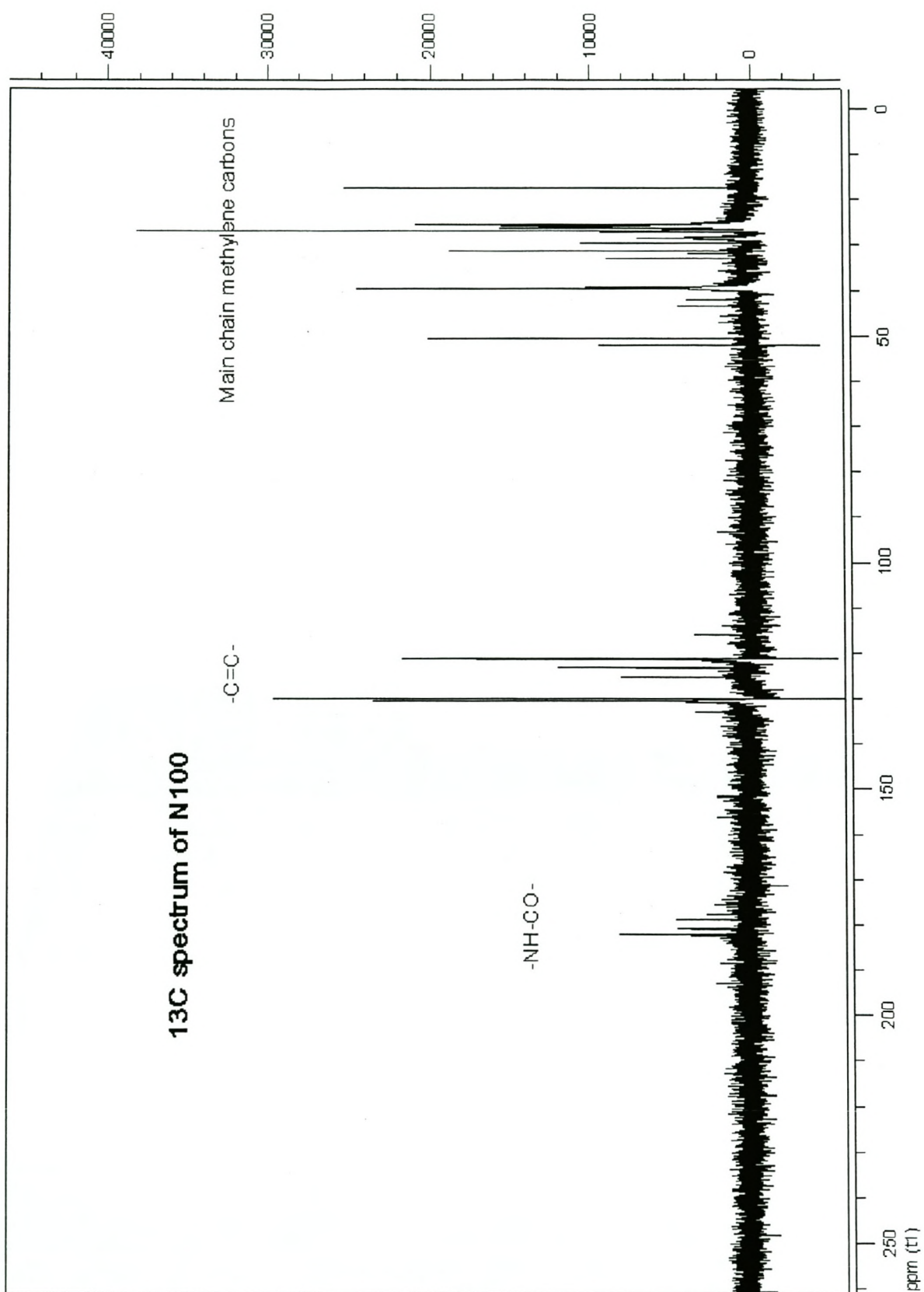
Table of Contents

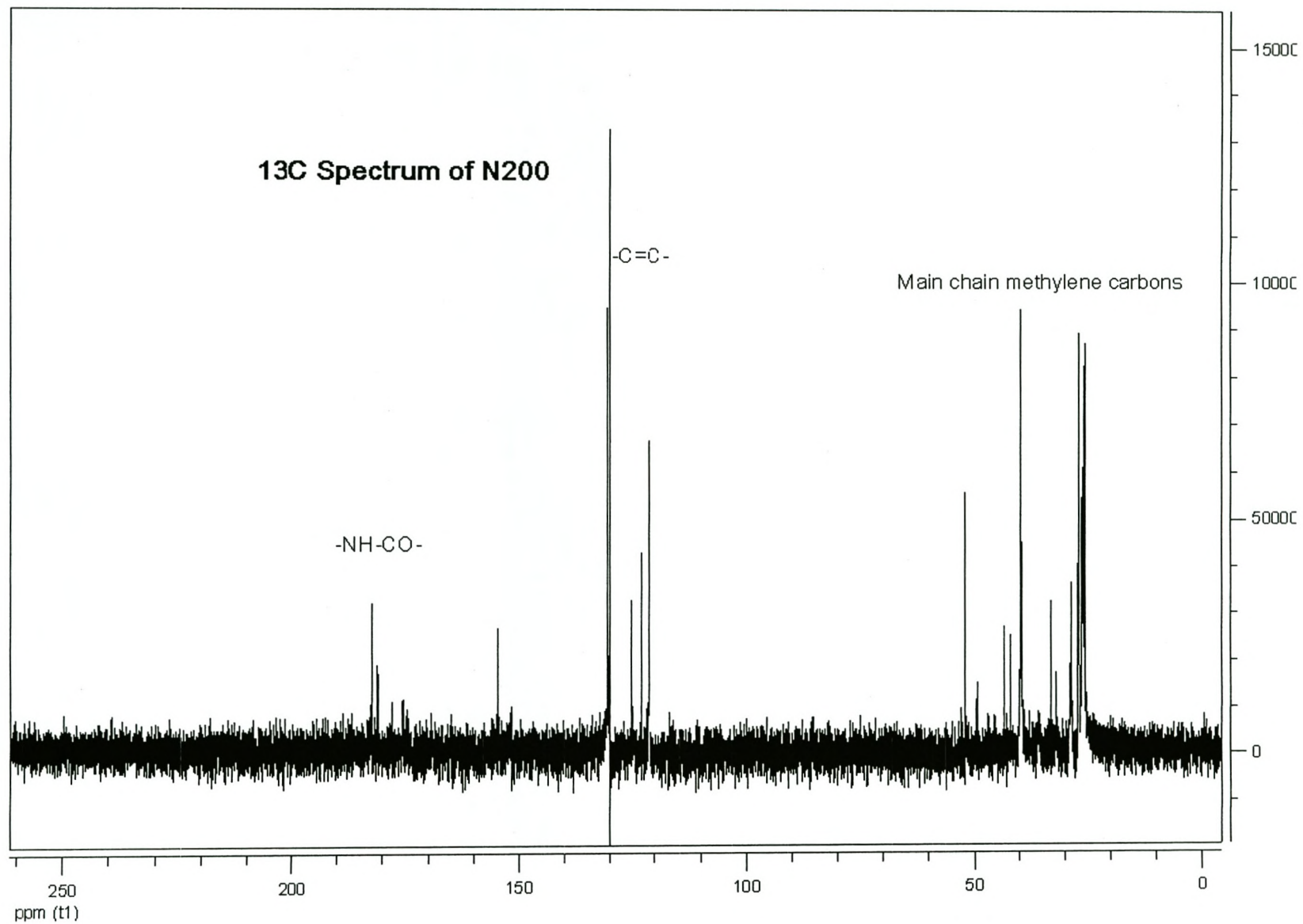
^{13}C spectrum of N50	80
^{13}C spectrum of P50	81
^{13}C spectrum of N100	82
^{13}C spectrum of N200	83
^{13}C spectrum of N50-H	84
^{13}C spectrum of N50-VP	85
^{13}C spectrum of N100-H	86
^{13}C spectrum of N100-VP	87
^{13}C spectrum of N200-H	88
^{13}C spectrum of N200-VP	89

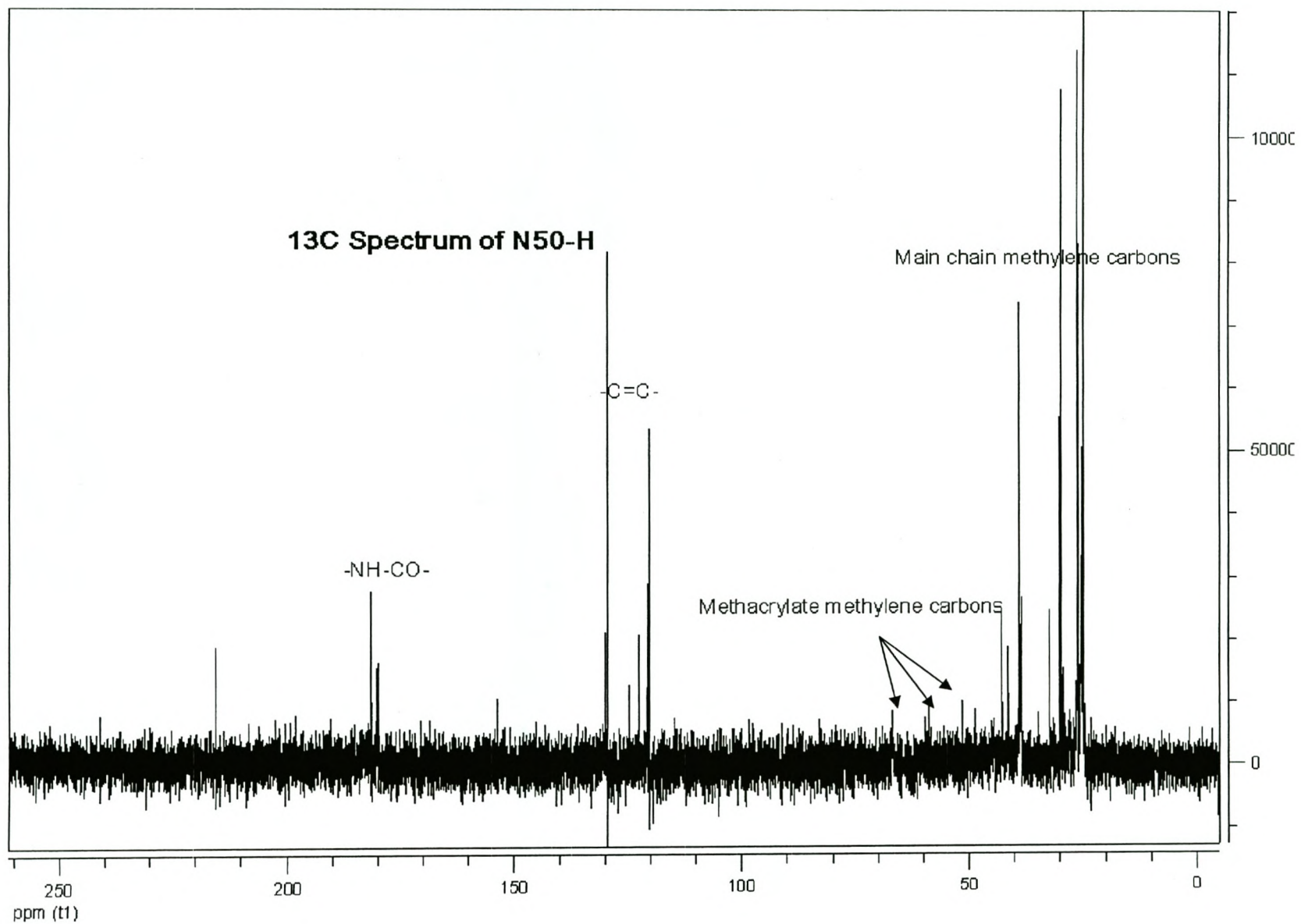
- 80 -

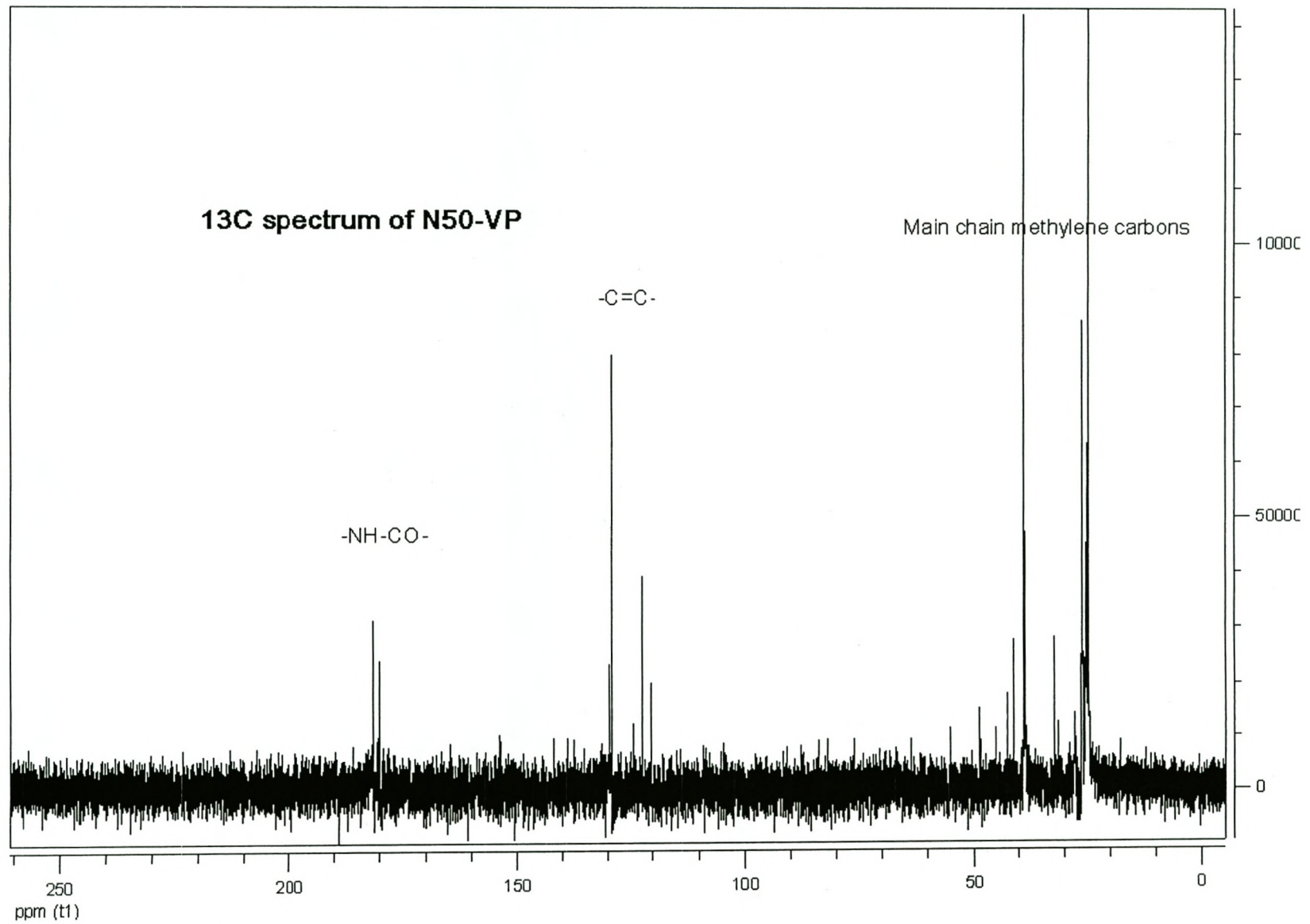




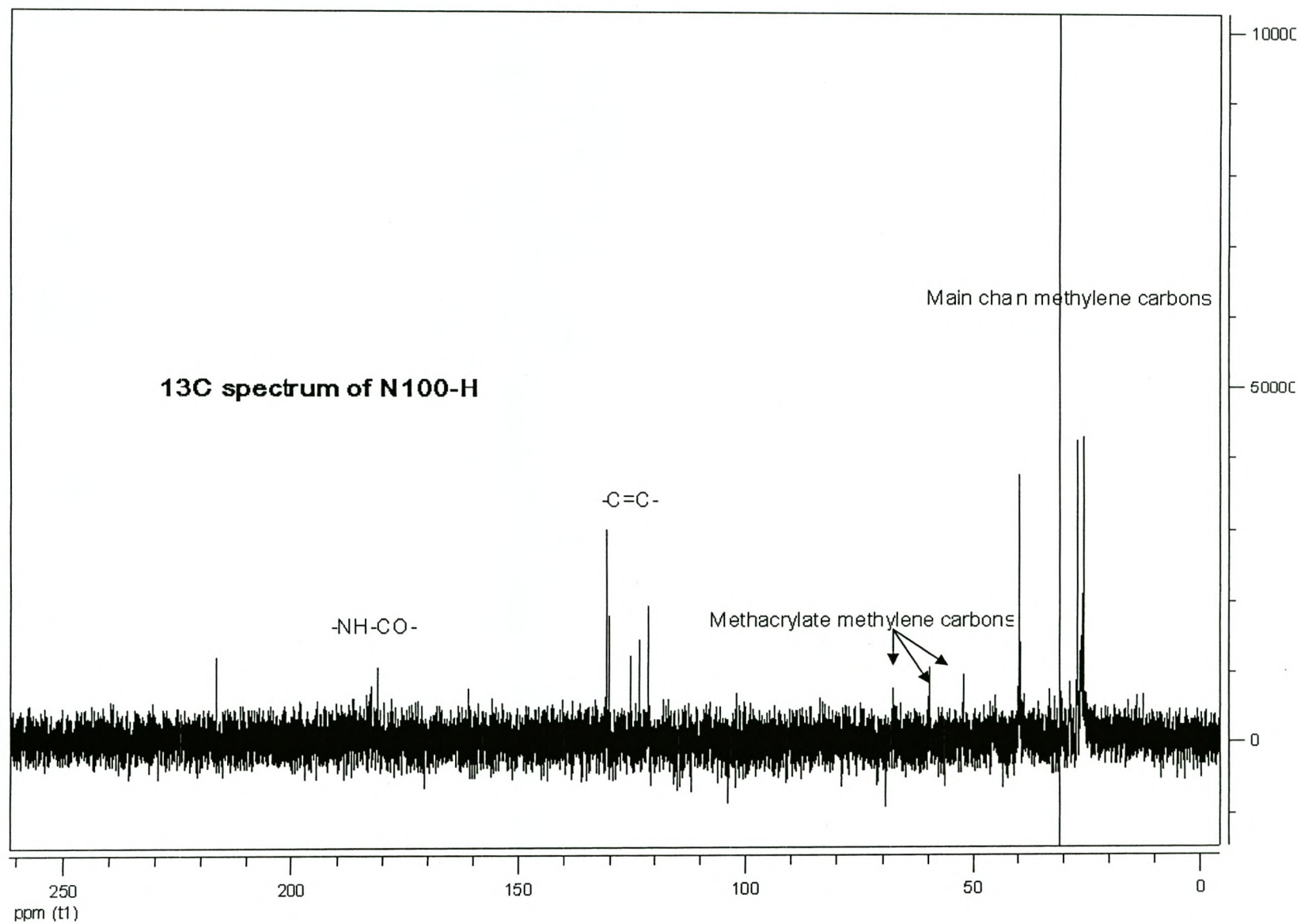


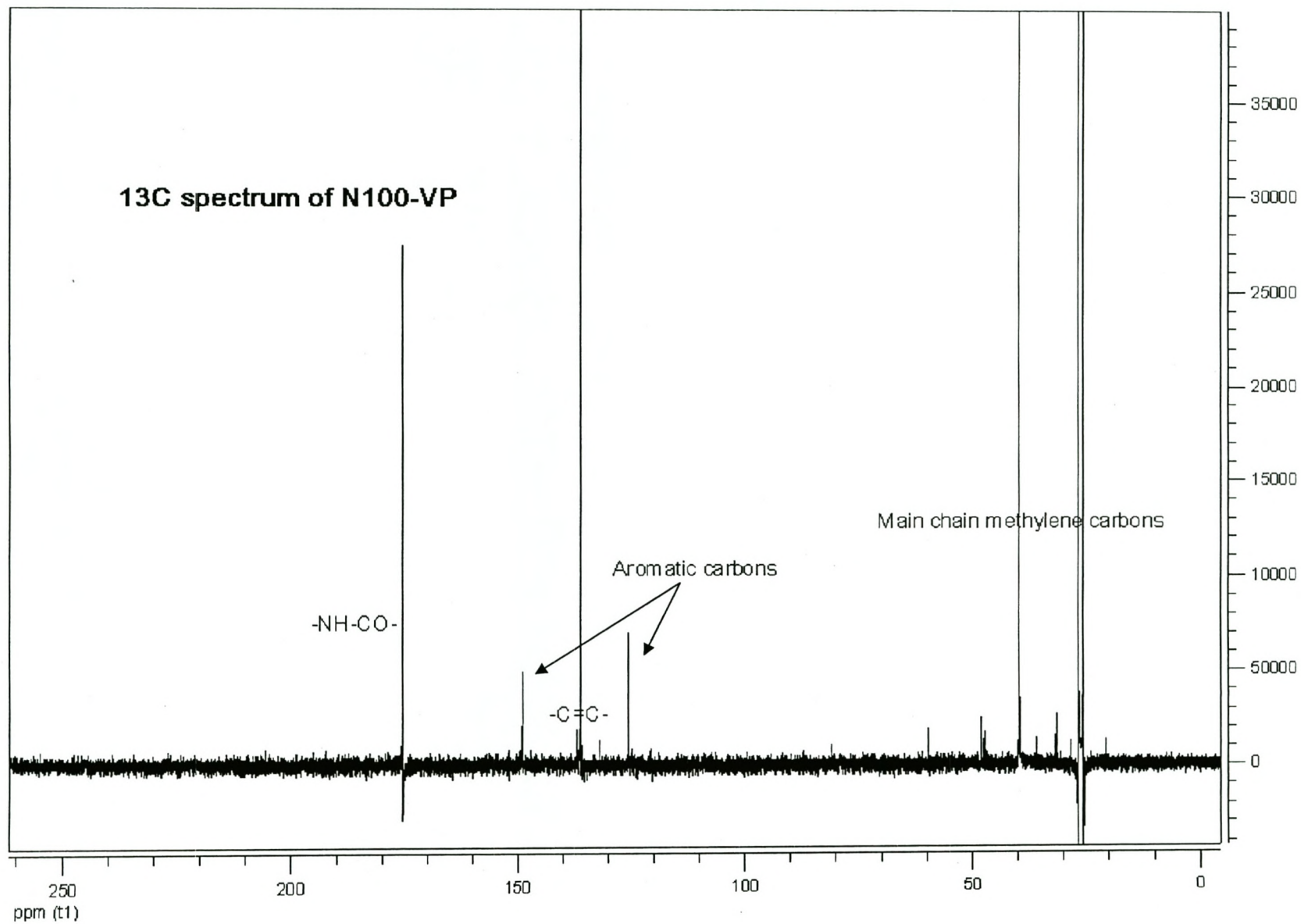


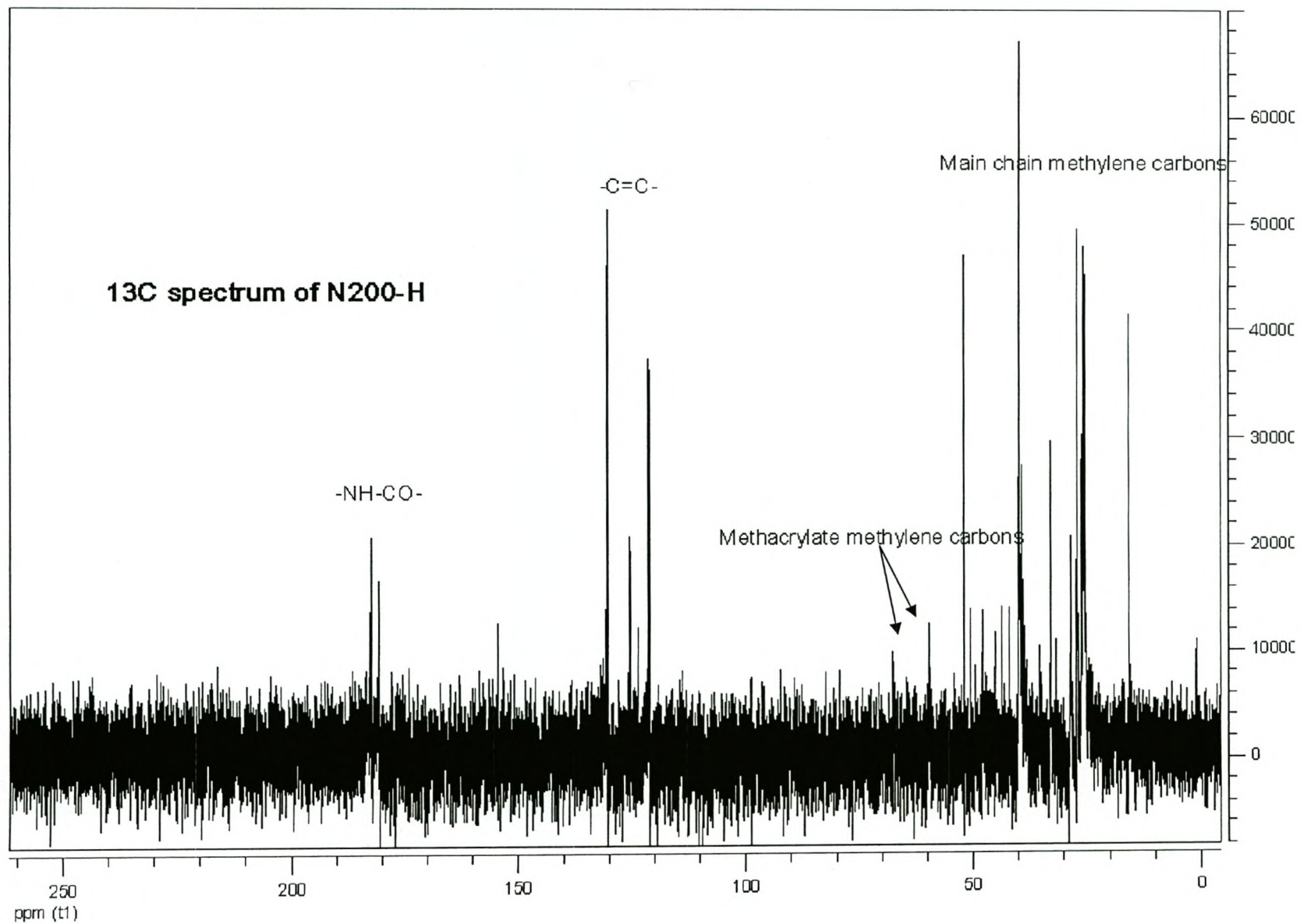


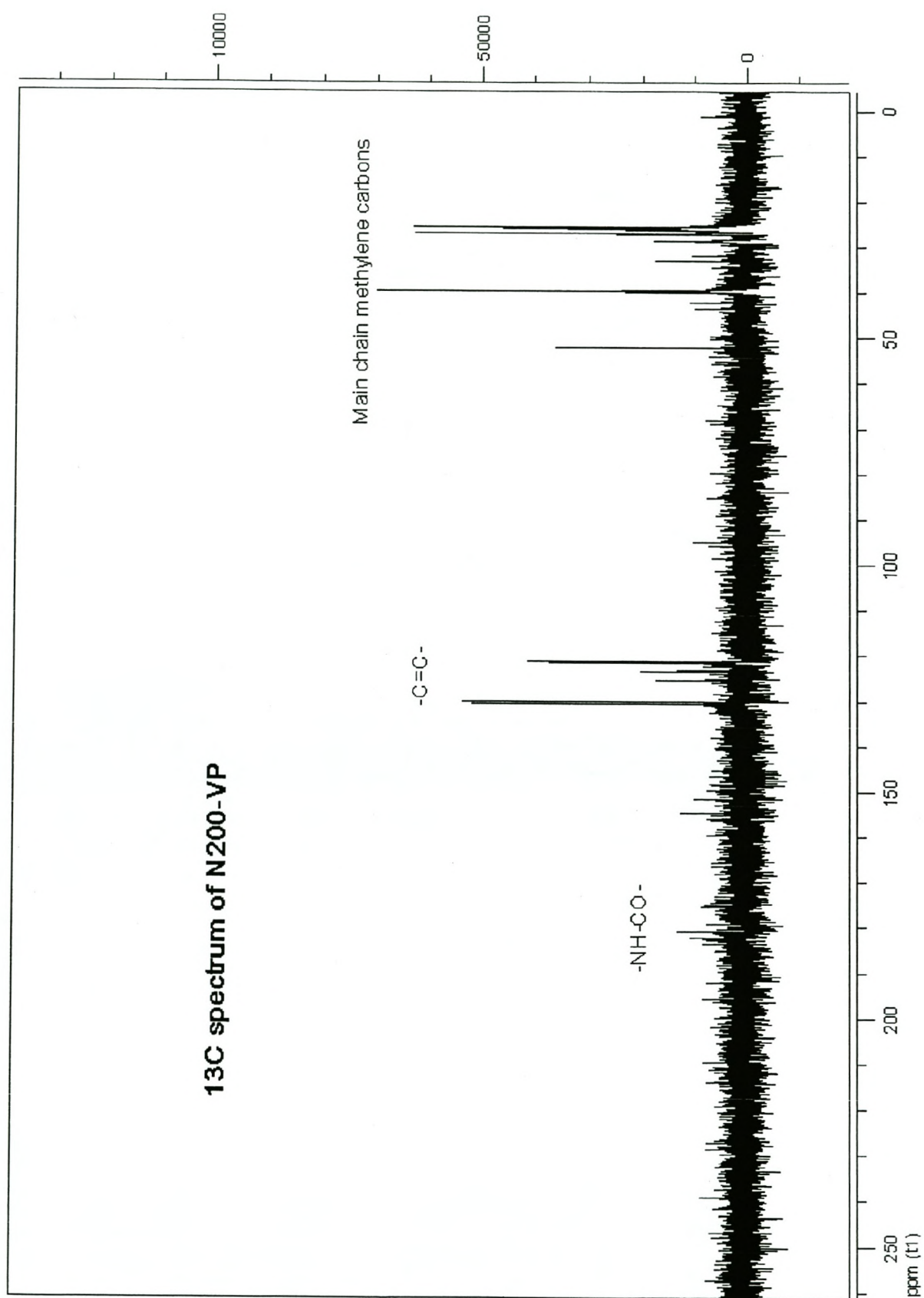


- 98 -







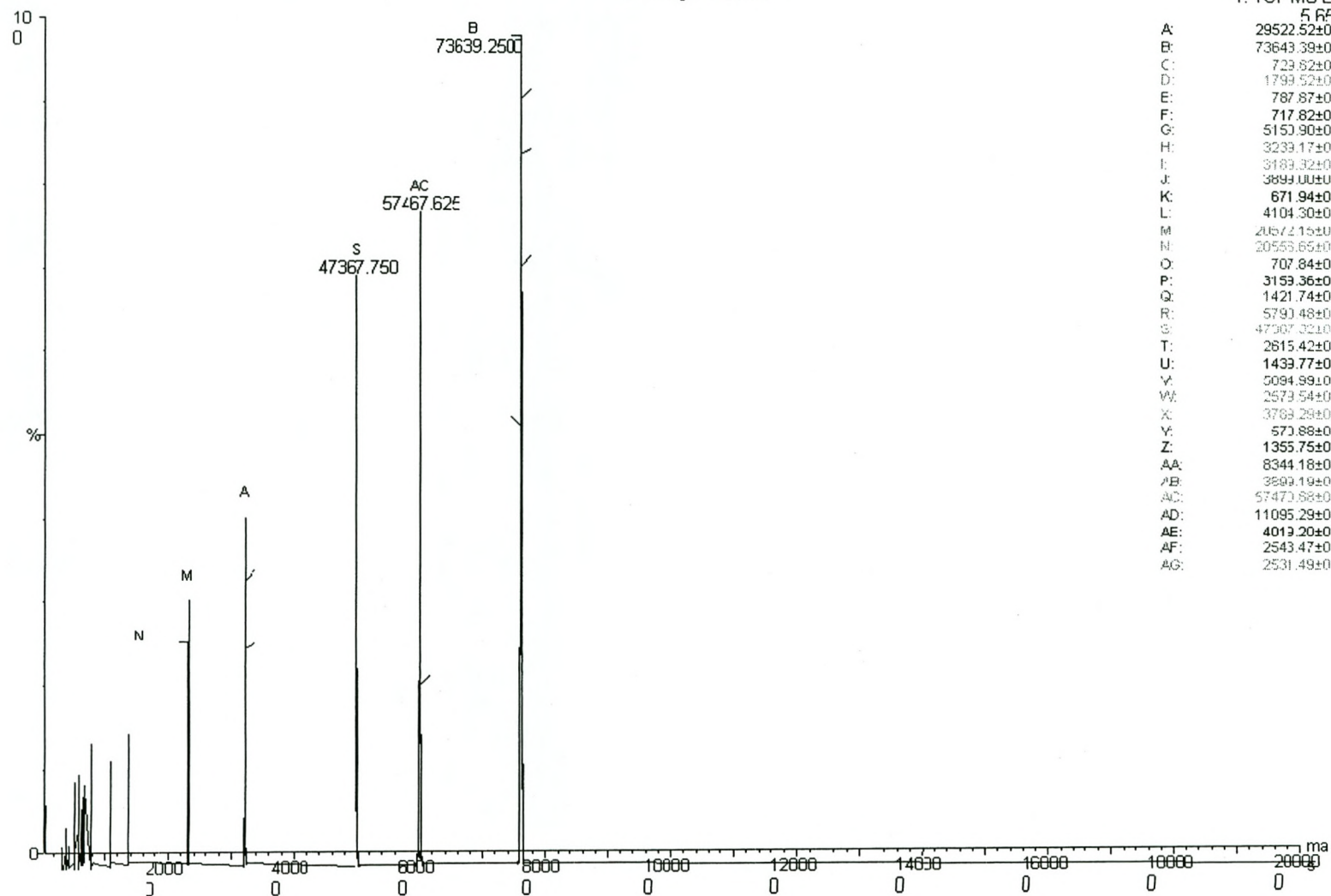


Appendix 2: ESMS spectra of polymer samples produced

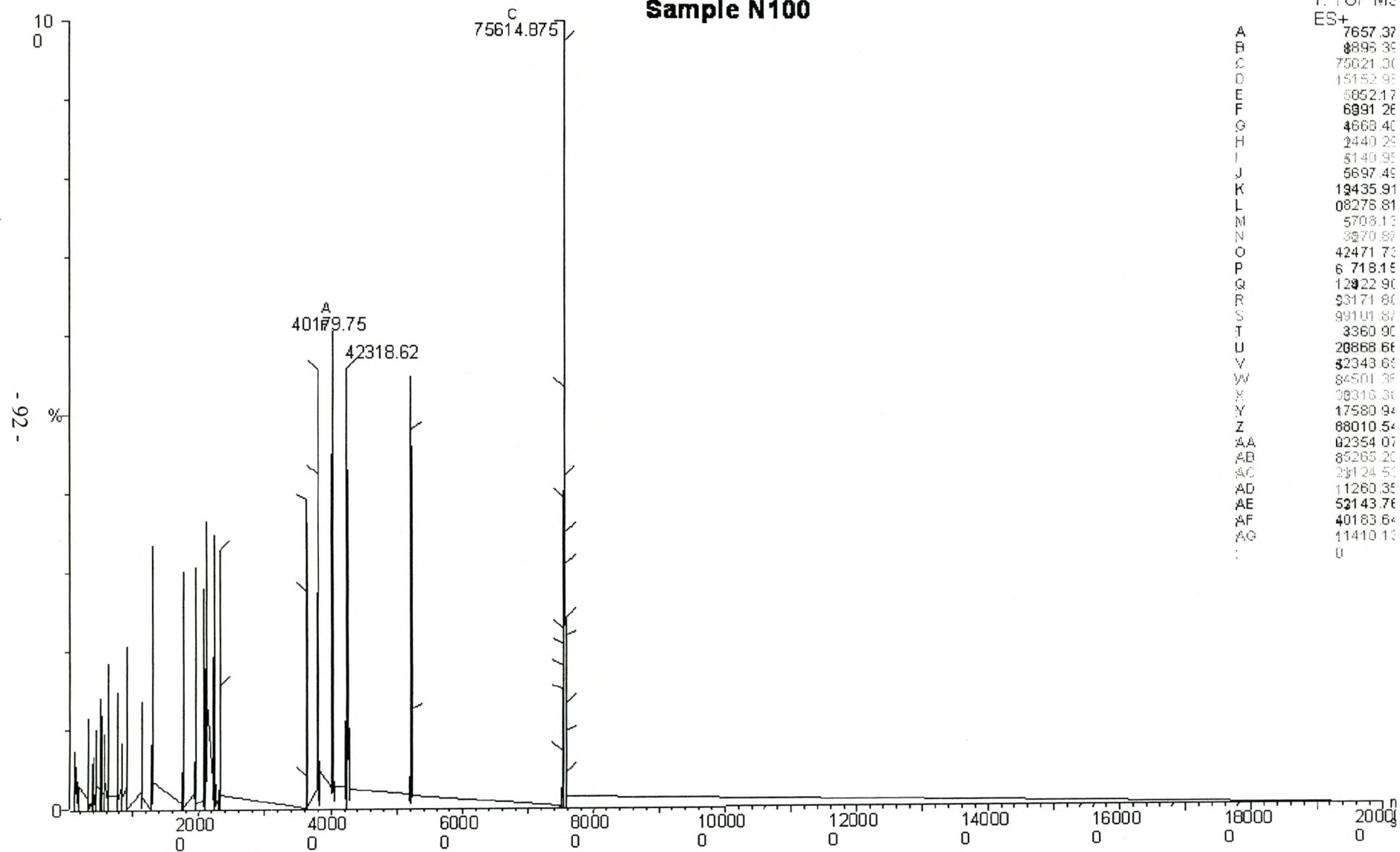
Table of Contents

ESMS spectrum of polymer sample N50	91
ESMS spectrum of polymer sample N100	92
ESMS spectrum of polymer sample N200	93
ESMS spectrum of polymer sample P50	94
ESMS spectrum of polymer sample P100	95
ESMS spectrum of polymer sample P200	96
ESMS spectrum of polymer sample N50-H	97
ESMS spectrum of polymer sample N50-VP	98
ESMS spectrum of polymer sample N100-H	99
ESMS spectrum of polymer sample N100-VP	100
ESMS spectrum of polymer sample N200-H	101
ESMS spectrum of polymer sample N200-VP	102

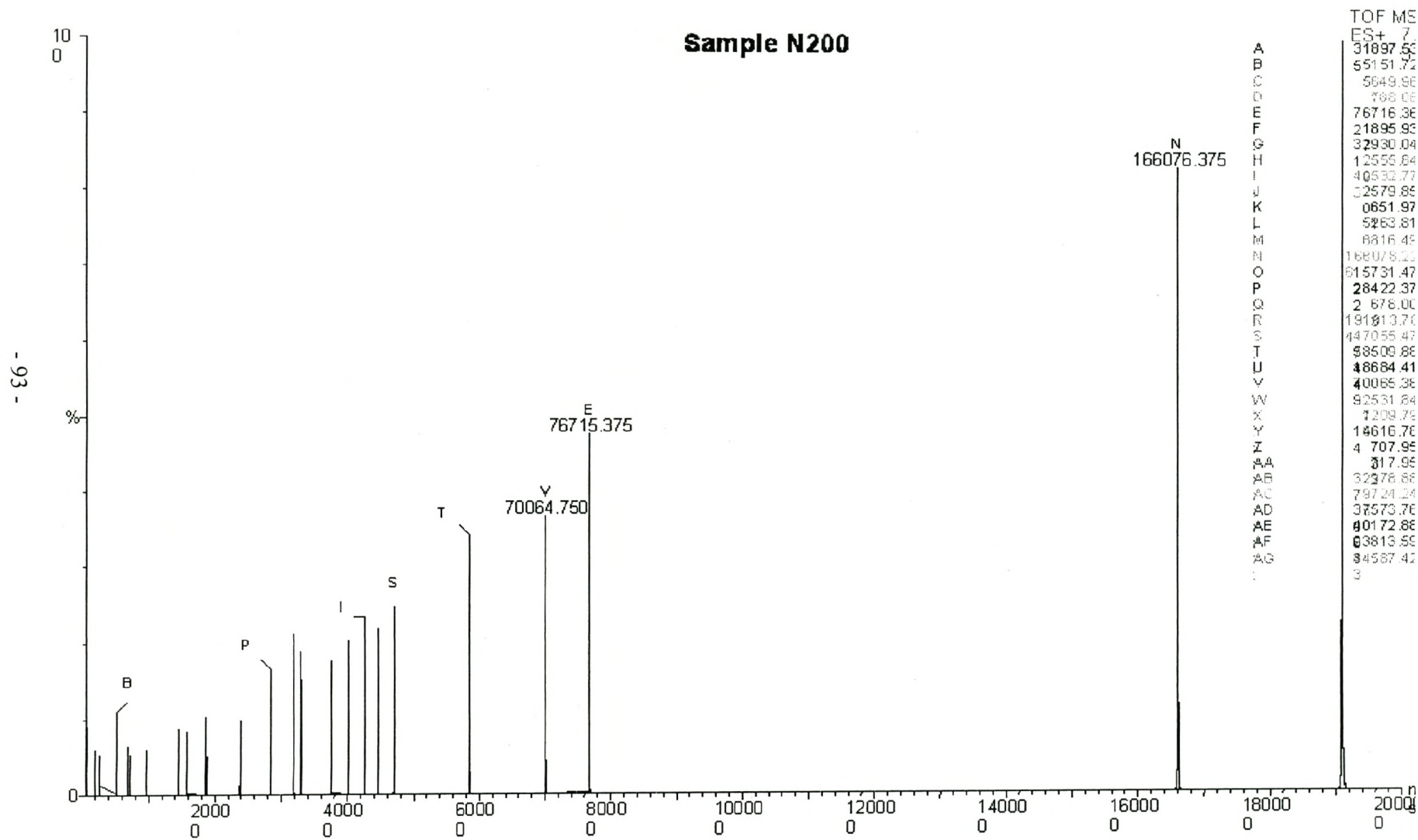
Sample N50



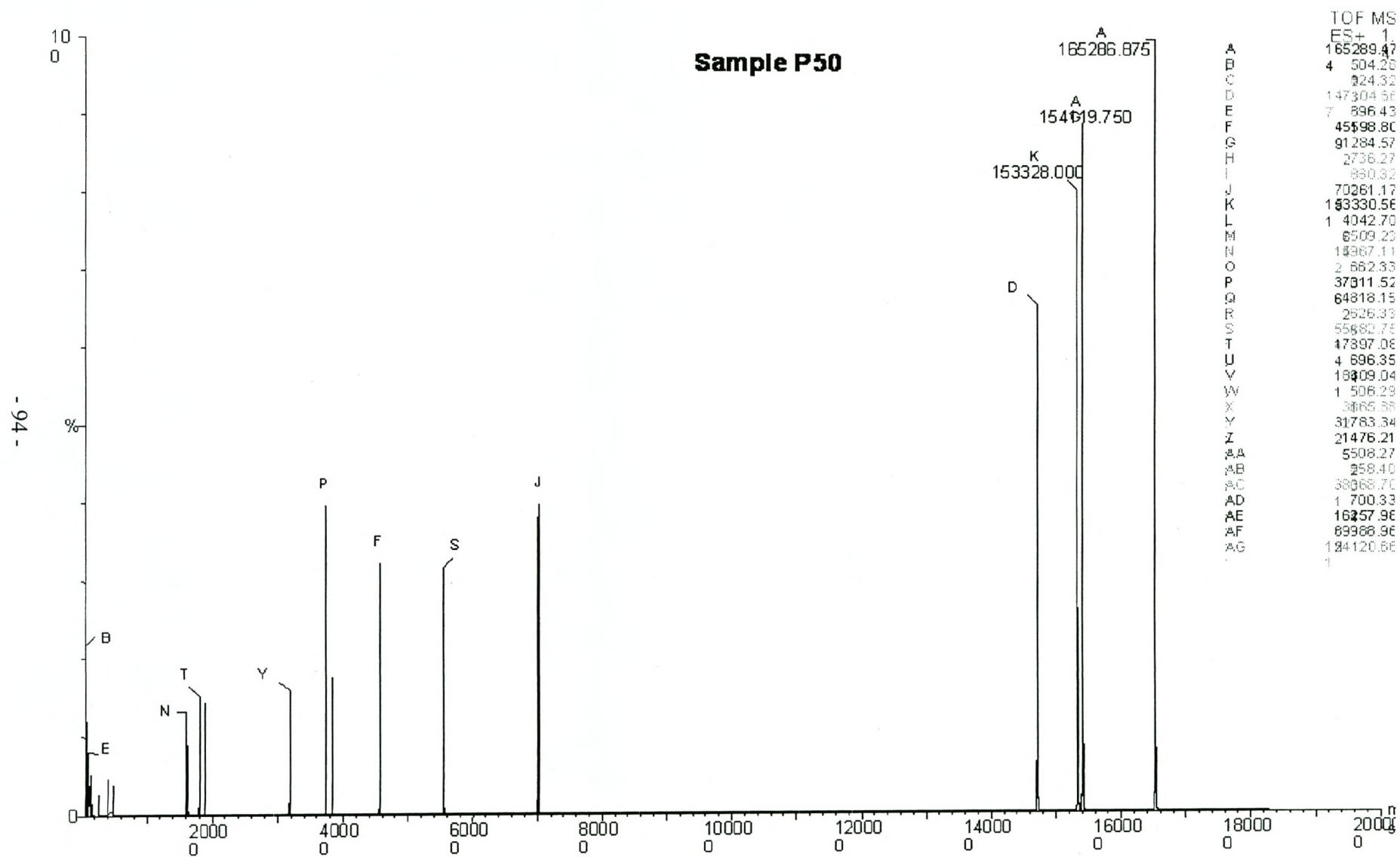
Sample N100

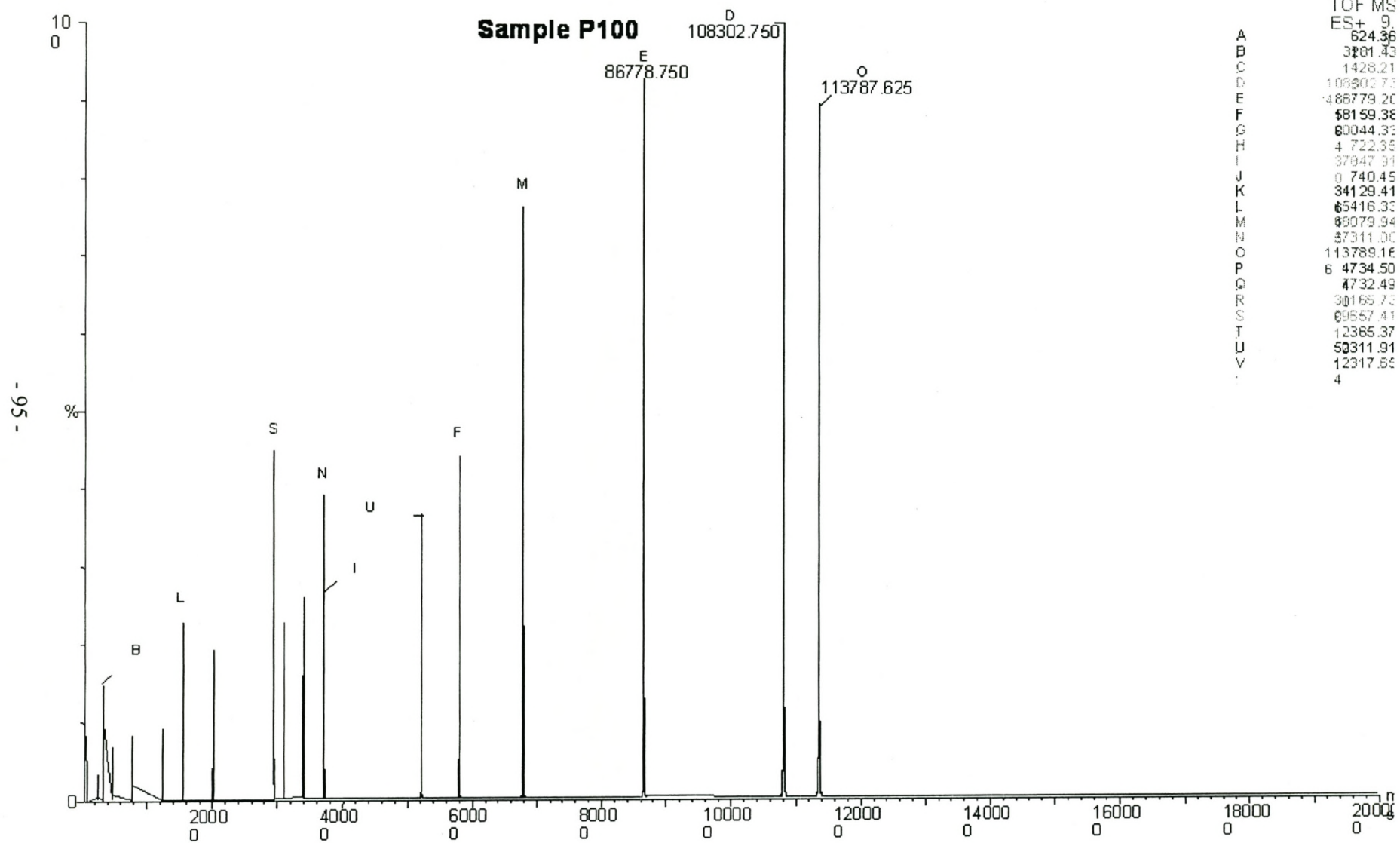


Sample N200



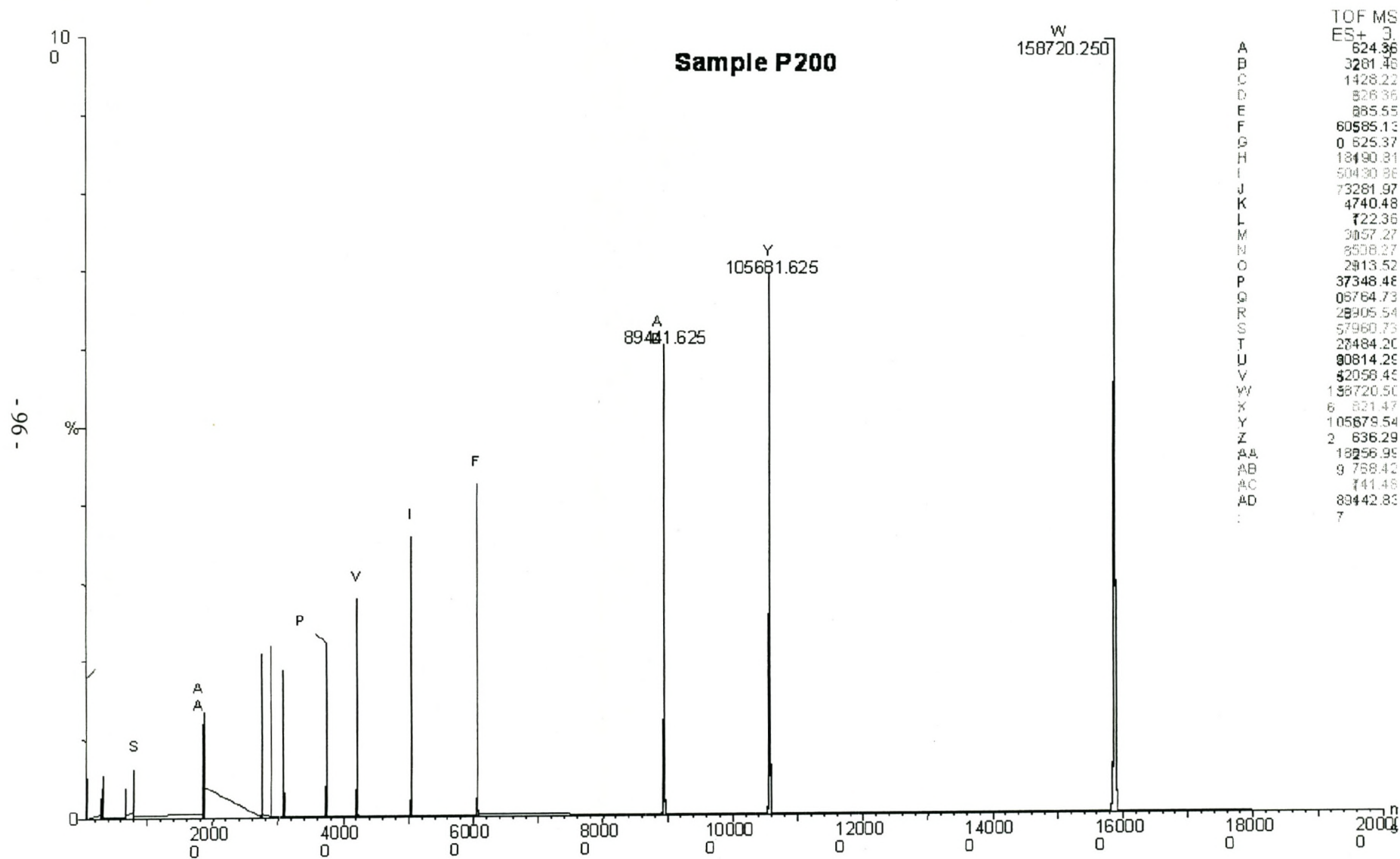
- 93 -

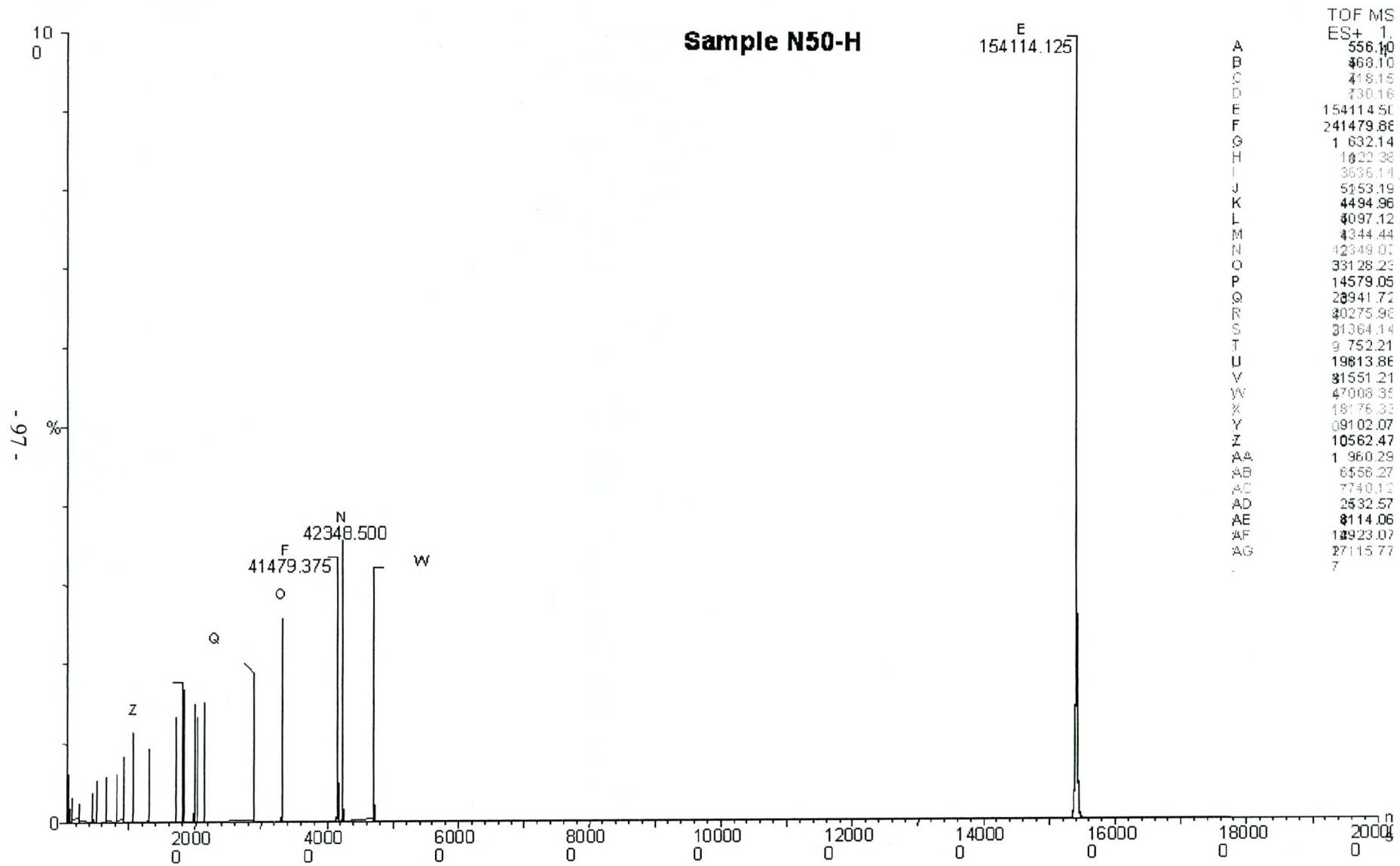




TOF MS

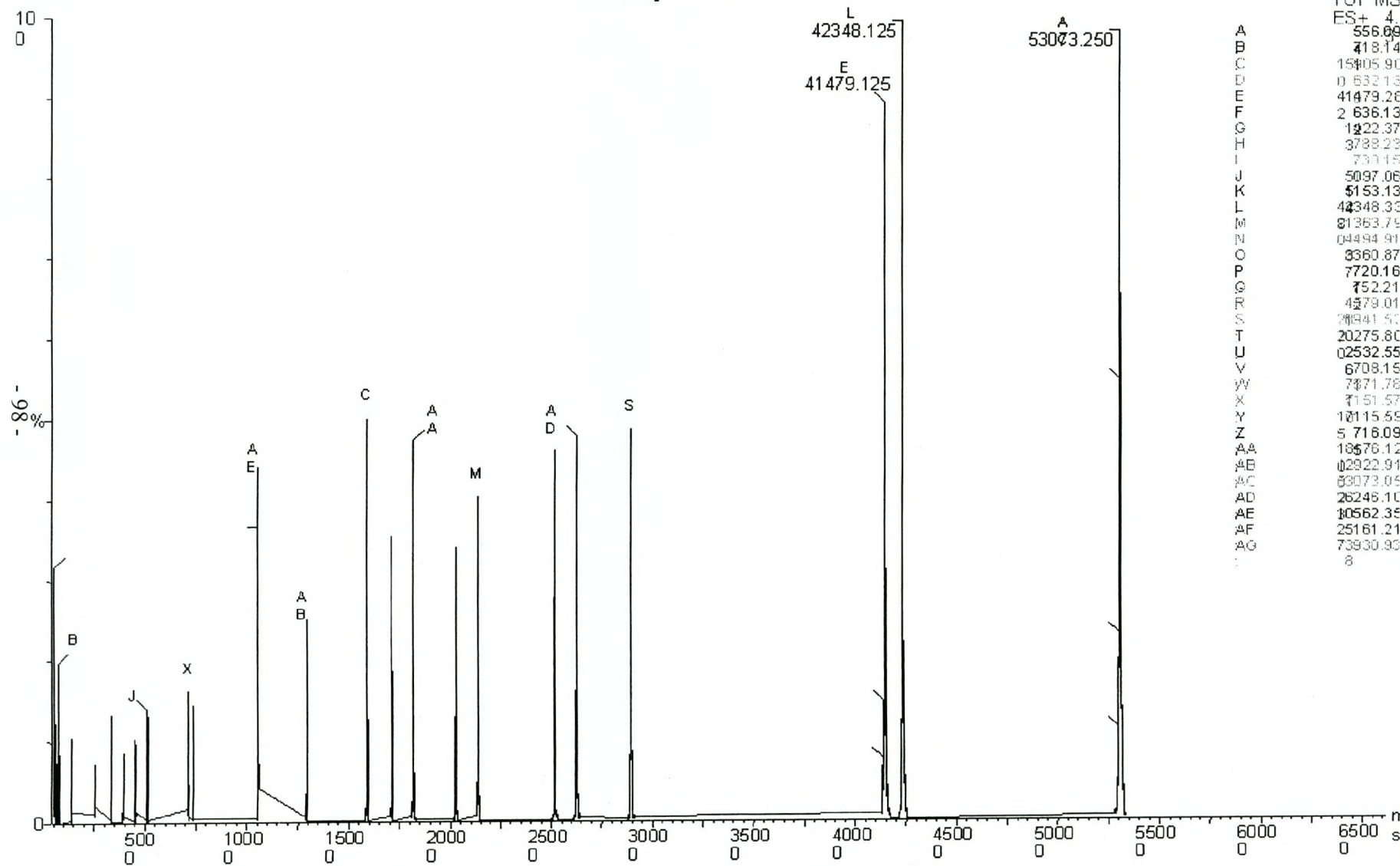
A	624.36
B	3281.43
C	1428.21
D	108302.75
E	86779.20
F	58159.38
G	60044.33
H	4722.35
I	37947.31
J	0740.45
K	34129.41
L	65416.30
M	85079.94
N	113789.16
O	113789.16
P	64734.50
Q	4732.49
R	30165.73
S	69557.41
T	12365.37
U	50311.91
V	12317.65
W	4

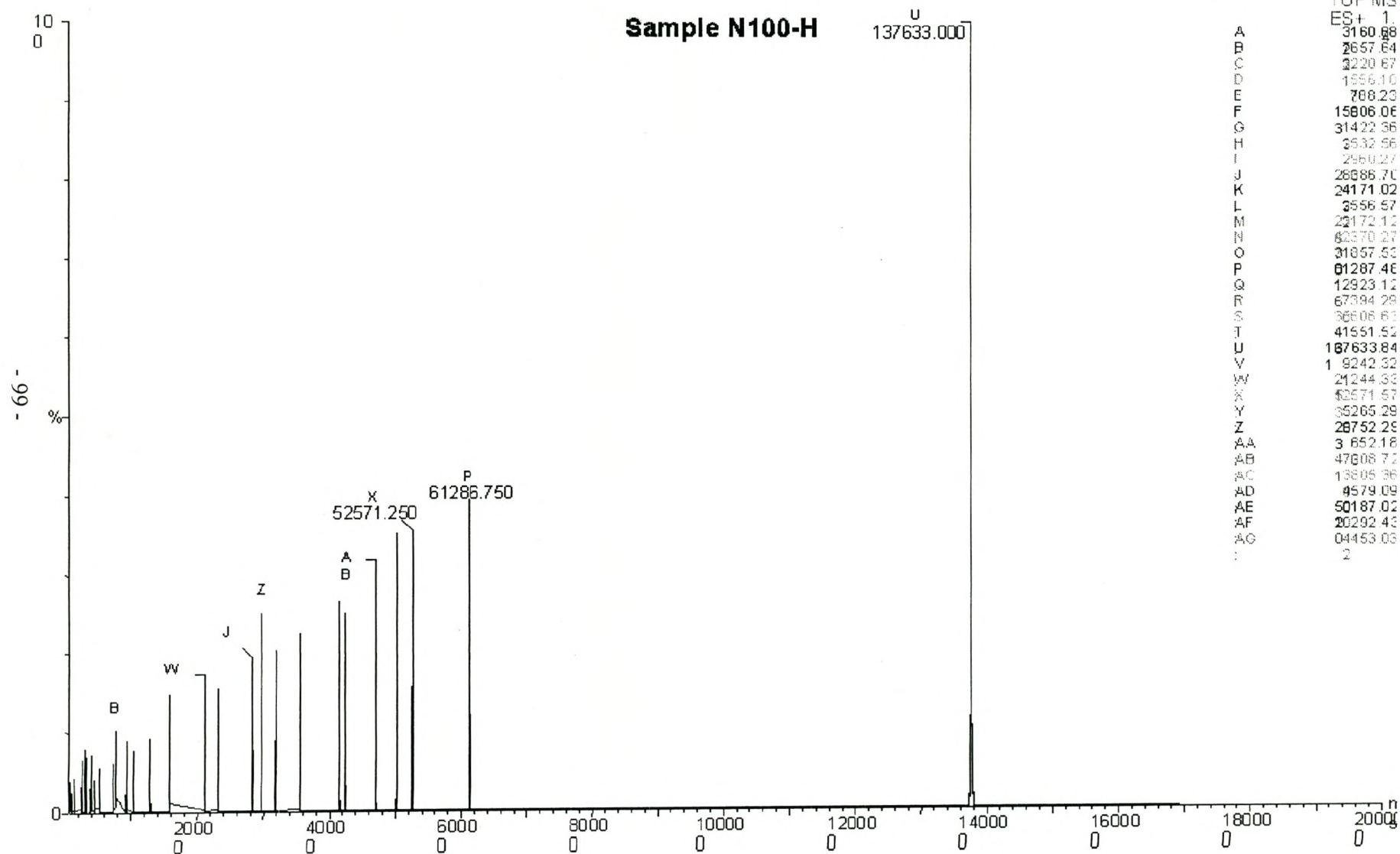




Label	m/z
A	556.10
B	468.10
C	418.15
D	730.16
E	154114.50
F	241479.86
G	1632.14
H	1022.38
I	3536.14
J	5153.19
K	4494.96
L	4097.12
M	4344.44
N	42348.01
O	33128.23
P	14579.05
Q	28941.72
R	40275.96
S	21064.14
T	9752.21
U	19813.86
V	31551.21
W	47008.35
X	18176.33
Y	109102.07
Z	10562.47
AA	1960.29
AB	6556.27
AC	7740.12
AD	2532.57
AE	8114.06
AF	10923.07
AG	27115.77
7	

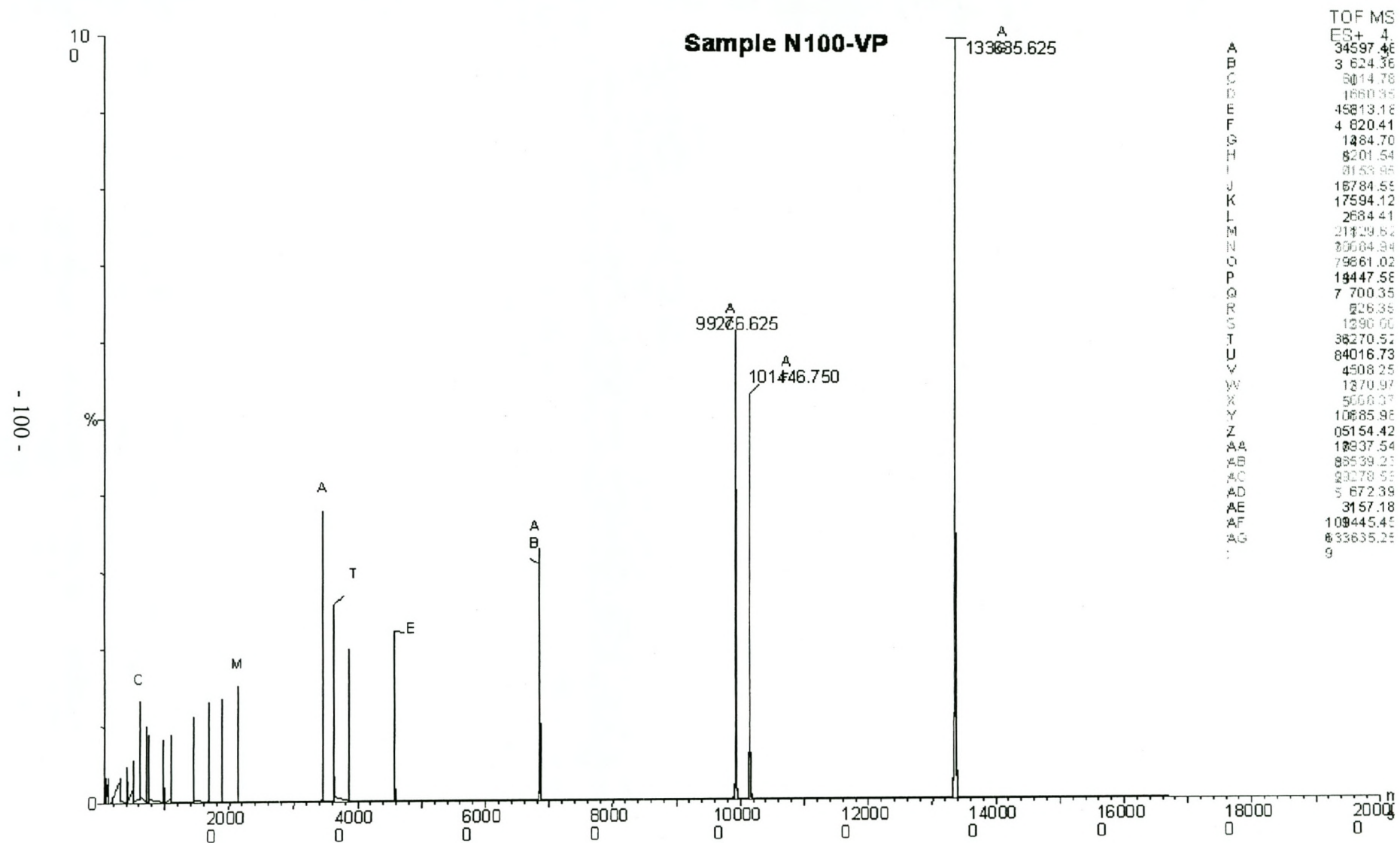
Sample N50-VP



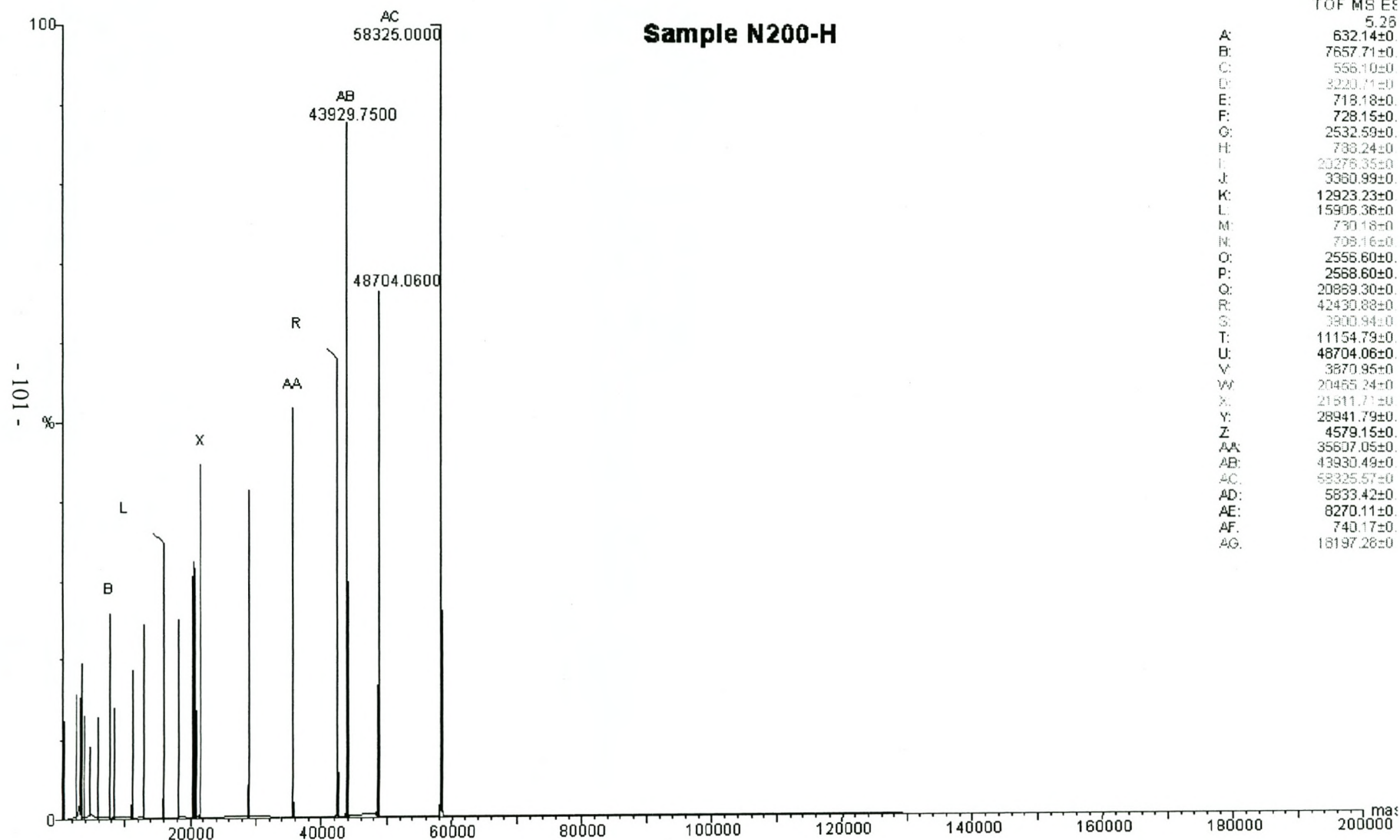


TOF MS

ES+ 1.	3160.68
A	2657.64
B	3220.67
C	1556.10
D	708.23
E	15606.06
F	31422.36
G	3532.56
H	2960.27
I	26886.70
J	24171.02
K	3556.57
L	22172.12
M	62370.27
N	31857.53
O	61267.46
P	12923.12
Q	67394.28
R	36806.61
S	41551.52
T	187633.84
U	19242.32
V	21244.33
W	42571.57
X	35265.29
Y	26752.28
Z	3652.16
AA	47608.72
AB	13806.36
AC	4579.09
AD	50187.02
AE	20292.43
AF	04453.03
AG	2



Sample N200-H



TOF MS ES

A:	632.14±0
B:	7657.71±0
C:	556.10±0
D:	3220.71±0
E:	719.18±0
F:	728.15±0
G:	2532.59±0
H:	788.24±0
I:	20276.35±0
J:	3360.99±0
K:	12923.23±0
L:	15906.36±0
M:	730.18±0
N:	709.16±0
O:	2556.60±0
P:	2568.60±0
Q:	20869.30±0
R:	42430.88±0
S:	3900.94±0
T:	11154.79±0
U:	48704.06±0
V:	3870.95±0
W:	20465.24±0
X:	21511.71±0
Y:	28941.79±0
Z:	4579.15±0
AA:	35607.05±0
AB:	43930.49±0
AC:	58325.57±0
AD:	5833.42±0
AE:	8270.11±0
AF:	740.17±0
AG:	18197.28±0

Sample N200-VP

